Environmental Photoinduced Toxicity of Polycyclic Aromatic Hydrocarbons: Occurrence and Toxicity of Photomodified PAHs and Predictive Modeling of Photoinduced Toxicity

by

Mark Allan Lampi

A thesis
presented to the University of Waterloo
in fulfillment of the
thesis requirement for the degree of
Doctor of Philosophy
in
Biology

Waterloo, Ontario, Canada, 2005

I hereby declare that I am the sole author of this thesis. This is a true copy of the thesis, including any required final revisions, as accepted by my examiners.

I understand that my thesis may be made electronically available to the public.

Abstract

Polycyclic aromatic hydrocarbons (PAHs) are ubiquitous environmental contaminants known for their photoinduced toxicity. There are two mechanisms through which this may occur: photosensitization and photomodification. Photosensitization generally leads to the production of singlet oxygen, a reactive oxygen species (ROS), which is highly damaging to biological molecules. Photomodification of PAHs, usually via oxygenation, results in the formation of new compounds (oxyPAHs), and can occur under environmentally relevant levels of actinic radiation.

PAHs and oxyPAHs readily adsorb to the organic phase of particulate matter in the environment such as sediments. It is logical to conclude that sediment transport will also facilitate the transport of these contaminants, and it has been shown that in the course of transport, degradative processes evoke a change in the profile of the PAHs present. Sediment samples taken along a transect from Hamilton Harbour were fractionated, and analyzed using a 2D HPLC method. All sediments contained intact and modified PAHs, although a marked change was noted in the profile of compounds present in the samples, which differ in distance from shore. Fractions of sediment extract were tested for toxicity using a bacterial respiration assay. Toxicity was observed in fractions containing modified PAHs, and was similar to that of intact PAH-containing fractions.

Subsequently, the toxicities of 16 intact PAHs were assessed to *Daphnia magna* under two ultraviolet radiation (UV) conditions. The toxicity of intact PAHs generally increased in the presence of full spectrum simulated solar radiation (SSR), relative to visible light plus UVA only. To expand the existing data on the effects of PAH photoproducts to animals, fourteen oxyPAHs were also assayed with *D. magna*, most of

which were highly toxic without further photomodification. The data presented highlight the effects of UV radiation on mediating PAH toxicity. The importance of the role of photomodification is also stressed, as several oxyPAHs were highly toxic to *D. magna*, a key bioindicator species in aquatic ecosystems.

A QSAR model previously developed for *Lemna gibba* showed that a photosensitization factor (PSF) and a photomodification factor (PMF) could be combined to describe toxicity. To determine whether it was predictive for *D. magna*, toxicity was assessed as both EC50 and ET50. As with *L. gibba* and *Vibrio fischeri*, neither the PSF nor the PMF alone correlated to *D. magna* toxicity. However, a PSF modified for *D. magna* did in fact exhibit correlation with toxicity, which was further improved when summed with a modified PMF. The greatest correlation was observed with EC50 toxicity data. This research provides further evidence that models that include factors for photosensitization and photomodification will likely be applicable across a broad range of species. To gain further knowledge of the roles that the variables contributing to the photosensitization and photomodification, a structural equation model was constructed based on the *D. magna* QSAR. This model accounted for a high amount of variance in six sets of toxicity data, as well as insight into the mechanisms of phototoxicity affecting different aquatic organisms.

Acknowledgements

It is hard to find the words to express my gratitude to the many people who have helped me along my journey through graduate school. The process, though highly demanding, was equally rewarding for me, as both a scientist, and a person.

First of all (and not the least), I would like to thank my supervisor, Dr. Bruce Greenberg, for his constant support and encouragement, a vast degree of academic freedom, and for always having a kind word. Thanks also to my committee members, Dr. George Dixon and Dr. Matt Vijayan, for their input along the way, which was really appreciated.

I would like to thank the Canadian Natural Sciences and Engineering Research Council (NSERC), and the Canadian Network of Toxicology Centres (CNTC) for providing a substantial source of income, as well as the University of Waterloo Graduate Scholarship and Teaching Assistantship programs.

Many thanks go to the friends and colleagues both in and out of the lab that I have met along the way, as I couldn't have done it without you. You know who you are, and I wish you all the best.

To my wife Yulia, thank you for your all of your support through this, and your tolerance for my many extracurricular activities and shenanigans, and for Maya.

Finally, to my family: Mom, Dad and Dana. Thank you for everything. You have kept me going through thick and thin, and I couldn't have done it without you.

Dedication

To my parents, for everything.

Table of Contents

List of Figures

xi

List of Tables

Chapter 1
Introduction

The science of toxicology dates to the earliest humans, who used various natural toxins for hunting, warfare and poisoning/assassination (Klaassen et al. 1996). Environmental toxicology (or ecotoxicology), derived from the terms "ecology" and "toxicology", is the study of the effects of pollutants on the environment, whether at the organismal, population or ecosystem level. The field of ecotoxicology, and indeed the field of toxicology in general, has grown from an amalgamation of individual sciences, including chemistry, biology, ecology, and pharmacology among others (Oehme 1979). The necessity of the field was born as a result of an unprecedented influx of pollutants to the environment brought on by the Industrial Age from widespread use of fossil fuels in heating, industry, and later on with the use of the internal combustion engine. Indeed, the majority of pollutants currently present in our environment are largely of anthropogenic origin. Thus, as a society, we are largely responsible for the state of the world that we currently inhabit.

Increasing public awareness regarding environmental issues has led to the rapid expansion and development of the field of ecotoxicology. There have been several (ill)defining moments that have contributed to the public perception of this field, including widespread mercury poisoning in Japan, through ingestion of tainted seafood, and the realization of the indirect effects on wildlife of the extensive use of DDT as a pesticide. The release of crude oil from the Exxon Valdez is fresh in our memories, as are the effects this had on species of high societal value, as was portrayed extensively by the media. Currently, major areas of investigation include the study of the environmental

transport of contaminants to pristine environments. For example, brominated flame retardants, and polychlorinated biphenyls are exerting negative effects in Arctic environments, despite a lack of local contaminant release. Pharmaceutical chemicals have also been found almost ubiquitously in watersheds surrounding areas of urban and agricultural development. One cannot help but notice that our concern regarding the effect we, as a species, have on the environment is generally in hindsight, rather than foresight. The exchange of the position of these two views is one of critical importance if the protection of natural resources is to be a mandate.

The central theme of this thesis involves a common class of environmental pollutants: polycyclic aromatic hydrocarbons (PAHs). These compounds are found widely throughout the environment, associated with urban centres, and industrialized regions. Exposure of PAHs to UV radiation can result in photoinduced toxicity whereby a non- or weakly toxic compound can have significant biological effects, generally via one of two mechanisms: photomodification or photosensitization. The occurrence and toxicity of photomodified PAHs are addressed in this thesis, as are methods of predictive modeling of PAH phototoxicity based on theories encompassing both photomodification and photosensitization.

> On Earth, the problem had been with cars. The disadvantages involved in pulling lots of black sticky slime from out of the ground where it had been safely hidden out of harm's way, turning it into tar to cover the land with, smoke to fill the air with, and pouring the rest into the sea, all seemed to outweigh the advantages of being able to get more quickly from one place to another – particularly when the place you arrived at had probably become, as a result of this, very similar to the place you had left, i.e. covered with tar, full of smoke and short of fish.
>
> --Douglas Adams

1.1 Occurrence and Properties of Polycyclic Aromatic Hydrocarbons

Polycyclic aromatic hydrocarbons (PAHs) are ubiquitous environmental pollutants, with well-documented toxic, mutagenic, and carcinogenic properties. These compounds are produced by natural sources including forest and grass fires, volcanoes, and seepage of oil into the environment (Neff 1985; Eisler 1987). However, the majority of PAHs are released into the environment from a wide variety of anthropogenic sources, including petroleum spills, the incomplete combustion of fossil fuels in electric power generation, refuse incineration, home heating, internal combustion engines, as well as the production of coke, carbon black, coal tar and asphalt (Neff 1985; Eisler 1987; Burgess et al. 2003). PAHs are released at high levels in the environment; the Canadian National Pollutant Release Inventory (NPRI) (Environment Canada 2005) reported 2.6 metric tonnes of PAHs released as waste in Canada in 2002, and for the same year, the USEPA reported 1,480 metric tonnes of PAHs released in the US (US EPA 2004). Because of the large quantity of PAHs produced by human activities, these contaminants are found in most industrialized regions worldwide.

Environmentally relevant PAHs range between two to seven conjugated rings, and are not limited to homocyclic rings. The US EPA has designated sixteen of these as priority pollutants due to their adverse effects (US EPA 2002b) (Figure 1.1). PAHs are highly hydrophobic compounds, with physicochemical properties that generally favour association with particulate matter. These compounds are usually associated with airborne particulate matter (Fox and Olive 1979; Legzdins et al. 1995; Oda 1998), soil (Chen et al. 2004; Lors and Mossmann 2005), sediments in the water column (Marvin 1994; Boese 1999; Marvin et al. 2000; Lampi et al. 2001; White 2002; Kilemade et al.
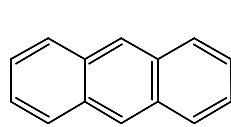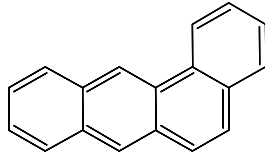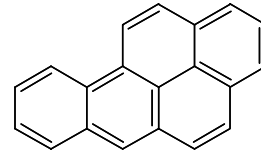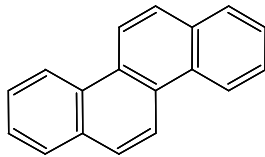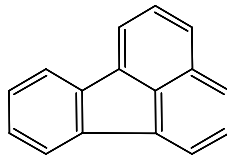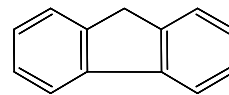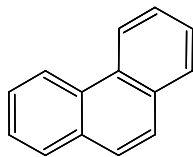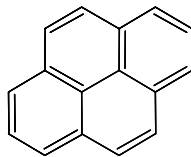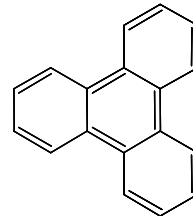
Figure 1.1. Structures of several common PAHs.
Abbreviations as follows: ANT, anthracene; BAA, benz[a]anthracene; BAP,
benzo[a]pyrene; CHR, chrysene; FLA, fluoranthene; FLU, fluorene; PHE, phenanthrene;
PYR, pyrene; TRI, triphenylene.

2004; Olajire et al. 2005), as well as organic surface films in urban environments (Gingrich et al. 2001; Butt et al. 2004). PAHs are detectable in the water column (Papadoyannis et al. 2002; Kurihara et al. 2005), and despite their low volatility are capable of undergoing atmospheric transport (Baker and Eisenreich 1990). The hydrophobic nature of these compounds results in their partitioning into organisms residing in contaminated environments, particularly aquatic systems. For instance, PAHs have been detected in fish (White and Triplett 2002; Hornung et al. 2004), zooplankton (Trucco et al. 1983; Gewurtz et al. 2000), mussels (Gewurtz et al. 2003), as well as several other species used in laboratory studies (Newsted and Giesy 1987; Warshawsky et al. 1995; Duxbury 1997).

The structure of PAHs includes conjugated π-bonding orbitals, which results in the absorption of light in the UV/far blue region of the spectrum that is present in solar radiation (Nikolaou 1984; Newsted and Giesy 1987; Larson and Berenbaum 1988; Krylov et al. 1997). Absorption of light energy can alter the toxicity of these compounds through two different mechanisms: photosensitization and photomodification (Krylov et al. 1997). Photosensitization generally leads to the production of singlet oxygen, and other reactive oxygen species (ROS), which are capable of damaging biological molecules (Foote 1991). Photomodification of PAHs is defined here as photooxidation and photolysis, and results in the formation of new compounds with increased polarity, and in many cases, increased toxicity (Zhu et al. 1995; Duxbury 1997; Mallakin et al. 2000; Brack et al. 2003; Shimada et al. 2004; Lampi et al. 2005).

1.2 Photosensitization and Singlet Oxygen

Inherently, environmental pollutants will also be exposed to ultraviolet (UV) radiation in the form of sunlight, leading to a myriad of possible photochemical reactions. The mechanisms of photoinduced toxicity are described in Figure 1.2, and are highly dependent on the physicochemical properties of the absorbing compound. The first law of photochemistry states that for a photochemical event to occur, a photon must be absorbed (Kohen et al. 1995). Thus, the absorption spectrum of the compound must overlap with the spectrum of the radiation source (e.g. sunlight).

PAHs exist in the ground state with two electrons residing in the outer shell in what is known as the highest occupied molecular orbital (HOMO). These electrons are pictorially described as ↑, and assigned a spin number of +½, or ↓, and a spin number -½. Absorption of a photon excites one of the two electrons to the excited singlet state (ESS, Figure 1.2). The ESS nomenclature reflects the 2S + 1 rule, where S is the sum of the spin numbers of the electrons (Kohen et al. 1995). When the electrons have opposite spins, their sum is zero and 2S + 1 = 1, hence the term singlet state. From the ESS, the electron can emit a photon through fluorescence, returning to the ground state, directly interact with other molecules, or relax to the ground state through internal conversion.

Importantly, in a process called intersystem crossing, a transition can be made by the ESS electron to the excited triplet state (ETS). Electrons with the same spin number sum to one, and 2n + 1 = 3, hence the term triplet state. The ETS is a key factor in environmental photochemistry. In undergoing intersystem crossing, the electron

6
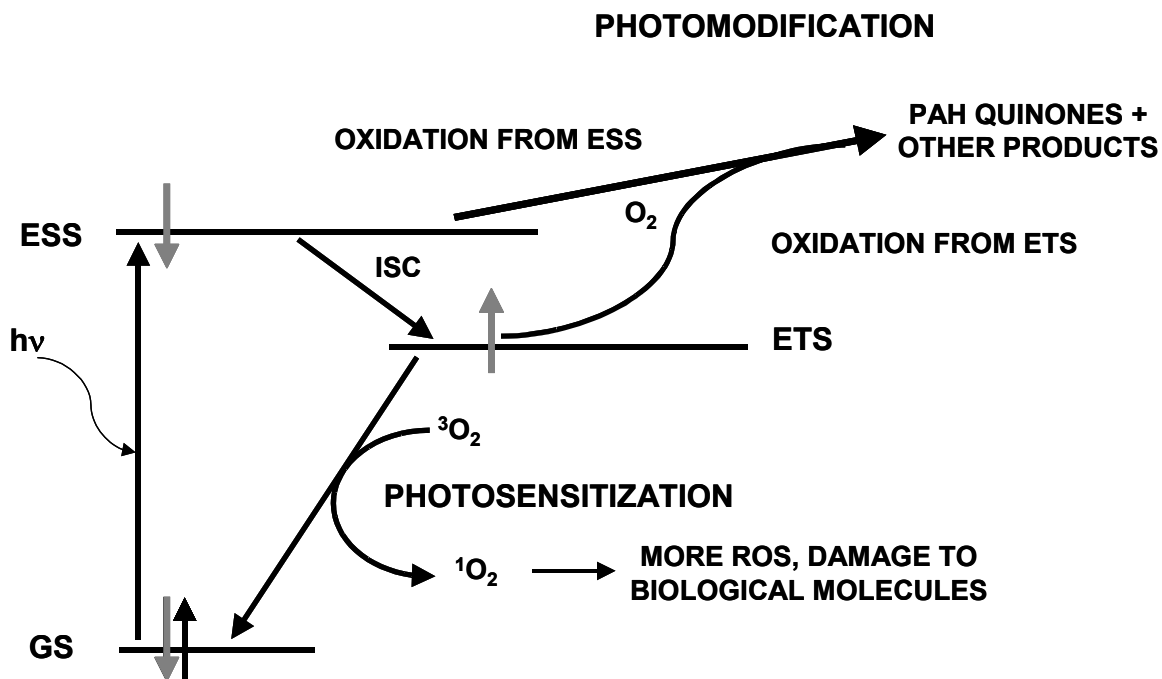
Figure 1.2. Jablonski diagram illustrating the mechanisms of photoinduced toxicity of PAHs.
Abbreviations: GS, ground state molecule (PAH); ESS, excited singlet state; ISC, intersystem crossing; ETS, excited triplet state, $^3O_2$, triplet (ground) state oxygen; $^1O_2$, singlet state oxygen. Short arrows represent electrons with opposite spin numbers (grey: $+\frac{1}{2}$, black: $-\frac{1}{2}$).

undergoes a spin transition, resulting in the excited electron attaining the same spin number as the remaining ground state electron. Similar to the ESS, a photon can be emitted through phosphorescence returning the electron to the ground state. However, Pauli's exclusion principal states that two electrons with the same spin number cannot exist in the same state. Thus, transition of the ETS electron to the ground state is quantum mechanically forbidden, and a compound in the ETS is extremely long-lived compared to the ESS ($\sim 10^{-1}$ -10^{-4} sec vs. $\sim 10^{-9}$ sec) (Foote 1976). This is a reason that phosphorescence is a phenomenon of long duration, and an important factor in why the ETS is a critical state in photochemistry; the longevity provides a greater chance for photochemical reactions to occur. For a compound to exhibit phototoxicity, it must also have high triplet state quantum efficiency; a high fraction of the photons absorbed must lead to the formation of the ETS. This will further increase the probability of the occurrence of a photochemical reaction, many of which involve the ETS, as described below.

Photosensitization is a common occurrence, with human health implications both positive and negative in nature, and widespread environmental ramifications. In this process, the photosensitizing molecule, which is the ground state molecule in Figure 1.2, absorbs a photon, and ultimately achieves the ETS. From this point, rather than undergoing internal conversion, or phosphorescing to the ground state, the molecule can interact with molecular oxygen. An important point is that the ground state of molecular oxygen is the triplet state. In fact, diatomic oxygen (O_2) qualifies as a free radical, as it possesses two unpaired electrons (Halliwell and Gutteridge 1999). Hund's rule states that every orbital in the subshell of a molecule must be occupied by a single electron before any orbital can be doubly occupied. Further, that electrons in singly

8

occupied orbitals usually have the same spin number, which is lower in energy

(Solomons 1996). Thus, the two unpaired electrons of molecular oxygen occupy

different orbitals, and have the same spin number. The consequence of this is that

ground state molecular oxygen exists in the triplet state. While this may seem

inconsequential, it is important, since oxygen, which should be highly reactive, is not.

The Pauli Exclusion principal forbids singlet-triplet reactions, and all molecules of

biological interest exist in the ground state as singlets (Kohen et al. 1995). However, a

compound in the ETS may interact with triplet state oxygen, and during this interaction,

energy is exchanged between the two molecules. The triplet molecule loses energy via

Type II photosensitization (Figure 1.3), and returns to the ground singlet state, while

oxygen gains energy, and is elevated to the singlet state. This singlet oxygen species

($^1O_2$) is highly reactive and biologically damaging; it will generally react with the first

molecule with which it comes into contact. Alternatively, and a process that has been

shown to be important in photochemical reactions on airborne particulate matter, is Type

I photosensitization (Figure 1.3). In this reaction, the triplet state molecule can directly

interact with another molecule, and transfer a proton or electron, resulting in a radical

that can then further react with oxygen, or other molecules (Foote 1968). Indeed, certain

constituents of atmospheric particulate organic matter, which interestingly include

photomodified PAHs such as anthraquinone, phenanthrenequinone, and benzanthrone,

are known to enhance photochemical reactions of other PAHs in this manner (Jang and

McDow 1995; Feilberg 2000).
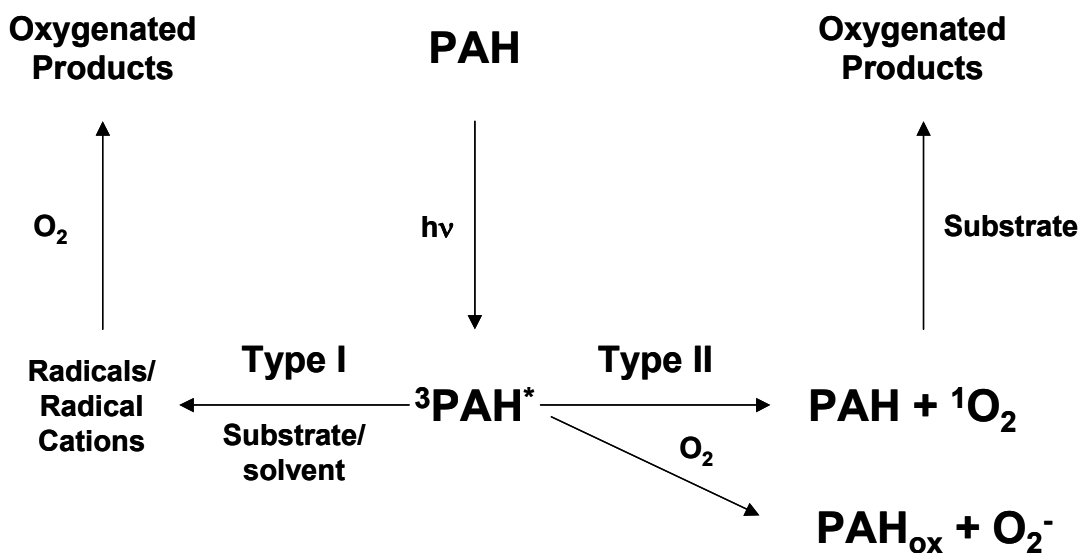
Figure 1.3. Type I and II mechanisms of photosensitization.
Adapted from Foote (1968; 1976). ^{3}PAH* represents a PAH in the excited triplet state; hν: photon of light; $^1O_2$: singlet oxygen; O_2^-: superoxide anion.

1.3 Environmental Relevance of PAH Photosensitization

Photosensitization has been widely documented in environmental toxicology, particularly with respect to homo- and heterocyclic PAHs (Kagan 1985; Gala and Giesy 1992; Mekenyan et al. 1994b; Mekenyan et al. 1994a; Huang et al. 1997a; Wiegman et al. 2002). These compounds are ideal photosensitizers, as they are conjugated aromatic systems, with an abundance of π electrons, and are able to absorb environmentally relevant wavelengths of radiation (Krylov et al. 1997). Indeed, the photosensitized production of highly reactive, and biologically damaging singlet oxygen is an important, and well-studied aspect of PAH phototoxicity (Larson and Berenbaum 1988).

Photosensitization generally leads to the production of singlet oxygen, which is capable of damaging biological molecules (Foote 1968; Halliwell and Gutteridge 1999). This phenomenon is known to affect a wide variety of aquatic organisms including those living within the water column, such as fish (Oris and Giesy 1985), zooplankton (Newsted and Giesy 1987; Nikkila et al. 1999; Diamond et al. 2000), algae and phytoplankton (Gala and Giesy 1992; Wiegman et al. 2002; Marwood et al. 2003), and bacteria (El-Alawi et al. 2001). Sediment-associated organisms including benthic anthropods (Ankley et al. 1994) and bivalves (Weinstein and Polk 2001; Ahrens et al. 2002) are also affected, as well as aquatic vegetation (Huang et al. 1997a; Huang et al. 1997b). Indeed, photosensitization has generally been considered the major mechanism of PAH phototoxicity (Ankley et al. 2003), although the role of environmental photomodification of PAHs has also been recognized as an important mode of PAH phototoxicity (Huang et al. 1997a; McConkey et al. 1997; Mallakin et al. 1999; Marwood

et al. 1999; Blaha et al. 2001; Machala et al. 2001; Brack et al. 2003; Kurihara et al. 2005).

The importance of environmental photosensitization as a mechanism of PAH photoinduced toxicity was extensively studied during the 1980s (Bowling et al. 1983; Cody et al. 1984; Allred and Giesy 1985; Kagan 1985; Oris and Giesy 1985; Newsted and Giesy 1987; Oris and Giesy 1987), although the role of UV radiation in enhancing biological effects of PAHs was recognized previously (Tso and Lu 1964; Morgan et al. 1977). The concern was that PAHs, which do not generally exhibit toxicity at levels below their aqueous solubilities, could be toxic at levels previously thought to be safe. Thus, photoinduced toxicity presented an alarming issue due to the ubiquity of this class of contaminants in aquatic environments where sunlight is a factor. PAHs are also generally highly hydrophobic, with high octanol-water partition coefficients (K_{OW}) and bioconcentration factors (Newsted and Giesy 1987; Mackay et al. 1992; de Maagd et al. 1998), and thus they easily partition from the aqueous phase into organic matter or organisms. If an organism that has a high body concentration of a PAH is exposed to UV, the potential for toxicity is evident, and has been demonstrated by many investigators (Newsted and Giesy 1987; Wernersson 1997; Nikkila et al. 1999; Choi and Oris 2000; Ahrens et al. 2002; Kummerová and Kmentová 2004).

1.4 Environmental Photomodification of PAHs

The role of singlet oxygen in environmental toxicology is not strictly limited to biological damage caused by photosensitization. Relatively speaking, a more recent area in the ecotoxicology of PAHs involves the production of photomodified compounds, generally via oxygenation (oxyPAHs). As discussed in the previous section, PAHs are

generally good photosensitizers via Type II reactions creating $^1O_2$. However, $^1O_2$-induced biological damage is not the only mechanism of PAH phototoxicity. Many PAHs can undergo subsequent reactions with ground state $^3O_2$ from the ETS (Figure 1.2), or with $^1O_2$ (Greenstock and Wiebe 1978; Mallakin et al. 2000; Fasnacht and Blough 2003), forming new compounds that are often more toxic and/or mutagenic than the parent PAH (McCoy et al. 1979; Nikolaou 1984; Huang et al. 1995; Huang et al. 1997a; McConkey et al. 1997; Brack et al. 2003; Lampi et al. 2005).

Photodegradation via photolysis is a major source of elimination of PAHs from various environmental compartments (Nikolaou 1984), however this is not the only pathway that occurs. Indeed, the aromaticity of several PAHs leads to electron densities that favour reaction with $^1O_2$ (Wiberg 1997). For instance, ANT, which is a known photosensitizer is able to form an endoperoxide via 1,4-cycloaddition of molecular oxygen across its central ring (Figure 1.4) (Fox and Olive 1979). This endoperoxide subsequently splits, resulting in the primary ANT photoproduct 9,10-anthraquinone (ATQ) (Fox and Olive 1979; Nikolaou 1984; Mallakin et al. 2000). Several other PAH-quinones are formed in this manner, including benz[a]anthraquinone, benz[b]anthraquinone, and dibenz[a,h]anthraquinone (Malkin 1992; Wiberg 1997). This can occur via reaction of $^1O_2$ with ground state PAH, as well as triplet PAH with $^3O_2$ (Fox and Olive 1979; Fasnacht and Blough 2003). There are a wide variety of other oxyPAHs that are formed via PAH photomodification. Some of these include phenanthrenequinone (McConkey et al. 1997), many hydroxylated anthraquinones (Mallakin et al. 2000; Brack et al. 2003), benzo[a]pyrenequinones and benzo[e]pyrenequinones (Surowiec and Bartos 2002;
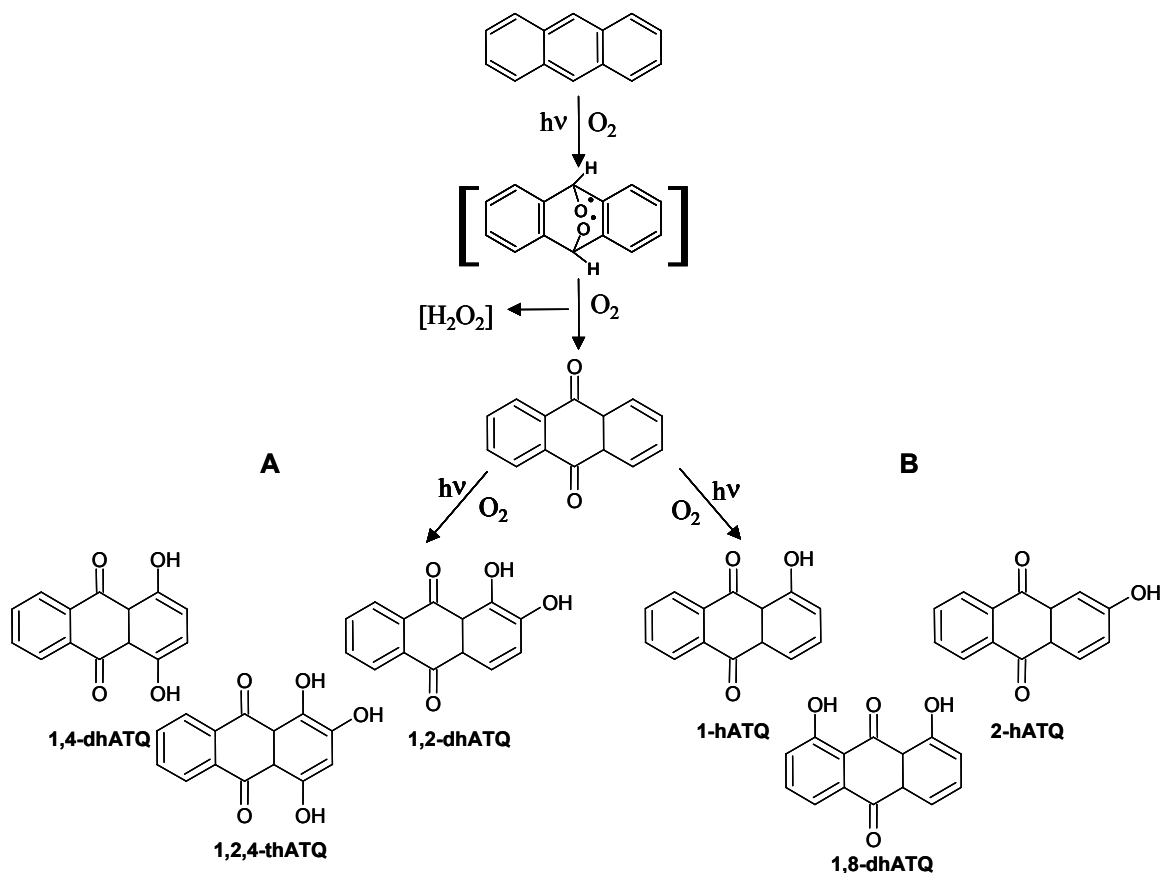
Figure 1.4. Reaction mechanism for photooxidation of anthracene (ANT).
A. Photolabile oxyPAHs; B. Photostable oxyPAHs. 1,4dhATQ: 1,4-dihydroxyanthraquinone; 1,2,4-thATQ: 1,2,4-trihydroxyanthraquinone; 1,2-dhATQ: 1,2-dihydroxyanthraquinone; 1-hATQ: 1-hydroxyanthraquinone, 1,8-dhATQ: 1,8-dihydroxyanthraquinone; 2-hATQ: 2-hydroxyanthraquinoneAdapted from Mallakin et al. (2000).

Reed et al. 2003; Fioressi and Arce 2005), and a host of other unidentified compounds, resulting from the photomodification of a variety of PAHs (Huang et al. 1995; Huang et al. 1997a).

OxyPAHs are less hydrophobic than the parent PAHs, although some hydrophobicity remains, thereby facilitating accumulation in biological membranes (Huang et al. 1993; Ren 1996; Krylov et al. 1997; McConkey et al. 1997). They can then manifest toxicity to a variety of organisms through specific mechanisms (Chesis et al. 1984; Bondy et al. 1994; Zhu et al. 1995; Huang et al. 1997b; Li et al. 2000; Kumagai et al. 2002; Yu et al. 2002; Briggs et al. 2003; Kepley et al. 2003; Shimada et al. 2004). The photomodification process occurs under environmentally relevant levels of actinic radiation (Katz et al. 1979; Huang et al. 1993; McConkey et al. 1997; Mallakin et al. 2000). This fact combined with the ubiquitous presence of PAHs in the environment leads to the hypothesis that the contribution of modified PAHs to environmental toxicant loads is significant.

1.5 Occurrence of Photomodified PAHs in the Environment

The presence of modified PAHs (oxyPAHs) in the environment is now recognized, and a thorough assessment of loads of these contaminants is currently underway. This class of contaminants is not solely restricted to oxygen-containing compounds. Indeed, photomodification of PAHs resulting in nitro-PAHs has been reported extensively, although it appears that this photoreaction is largely limited to airborne particulate matter, likely due to the availability of hydroxyl- and nitrate- radicals as a co-reactants and co-pollutants (Arey and Atkinson 2003). There is concern regarding the formation of nitro-PAHs due to high increases in mutagenicity, compared to the parent compounds

(Pitts et al. 1978; Durant et al. 1996; Enya et al. 1997; Durant et al. 1998; Hannigan 1998). Further, since they are often associated with airborne particulate matter, they are cause for human health concerns due to inhalation of particulate matter.

Modified PAHs have been detected widely throughout the environment, in a variety of compartments including soil, airborne particulate matter, sediments and pore water, and within the water column (Legzdins et al. 1995; Enya et al. 1997; Kosian et al. 1998; Lampi et al. 2001; Papadoyannis et al. 2002). Legzdins et al. (1995) fractionated air samples collected from Hamilton, Ontario, a highly industrialized city, and found that the samples contained many modified PAHs. Several other groups report similar findings, with a broad range of compounds including ATQ, benz[a]anthraquinone (BAQ), benzanthrone (BAT), benzo[b]anthraquinone (BBQ), benzo[a]pyrenequinones (BPQs), and phenanthrenequinone (PHQ) (Konig et al. 1983; Allen et al. 1997; Durant et al. 1998; Hannigan 1998; Oda 1998; Koeber et al. 1999; Nicol et al. 2001; Kishikawa et al. 2004). The occurrence of mutagenic nitro-PAHs has also been widely documented (Enya et al. 1997; Durant et al. 1998; Hannigan 1998; Yaffe et al. 2001; Feilberg et al. 2002). Clearly, the presence of modified PAHs in airborne aerosols is a widespread phenomenon, and it is likely that there is a risk associated with these compounds. Indeed, several of these constituents have been shown to be mutagens in human cells (Durant et al. 1996; Hannigan et al. 1997; Durant et al. 1998; Hannigan 1998; Reed et al. 2003; Lamy et al. 2004), and a recent laboratory study associates lower risk of mutation with reduced exposure to airborne particulate matter (Somers et al. 2004). Although modified PAHs were not causally associated with this decrease in risk of mutations, one cannot help but notice the correlation.

Photomodified PAHs are also commonly found in the aquatic environment. High levels of ATQ were detected in sediments collected from a series of sites in the Gulf of Saudi Arabia, which were contaminated through spills resulting from the 1991 Gulf War (Ehrhardt and Burns 1993). ATQ, methylated-ATQs, BAQ and 9-fluoreneone were observed using GC/MS and GC/MS/MS in sediments contaminated by an aluminum smelter (Mosi et al. 1997). This study illustrated the importance of sensitive analytical methods, in the analysis of oxyPAHs in complex environmental matrices, as BAQ, which has a range of biological effects (Blaha et al. 2001; Machala et al. 2001; Lampi et al. 2005) was only detectable using the latter technique. OxyPAHs have been detected by McCarthy et al. (2004) and Lampi et al. (2001) in sediment extracts from Hamilton Harbour, Hamilton, Canada, a site highly contaminated with PAHs. Machala et al. (2001) identified ATQ, BAT and BAQ in contaminated river sediments from the Czech Republic, all at levels within an order of magnitude of the parent PAHs. OxyPAHs have also been detected in marine sediments, implying that this phenomenon is not limited to freshwater systems (McKinney et al. 1999). ATQ, BAT and anthrone (ATO) have also been found in mutagenic estuarine sediment extracts in the UK (Thomas et al. 2001). Kosian et al. (1998) reported that a number of modified PAHs, including BAT and 1-hydroxyATQ, were present in sediment pore water samples collected from a contaminated stream in close proximity to an oil refinery. OxyPAHs have also been detected within the water column (Papadoyannis et al. 2002; Kurihara et al. 2005). This is not surprising as these compounds are less hydrophobic than the parent PAHs. The presence of oxyPAHs within aquatic systems is unequivocal, and there is a potential risk to benthic organisms, as well as those residing in the water column.

1.6 Influence of Spectral Quality on Photoinduced Toxicity of PAHs

A mitigating factor in the photoinduced toxicity of PAHs is spectral quality. Similar to the direct effects of UV on aquatic organisms, the spectral distribution and penetration into the water column must be taken into account in the consideration of photoinduced toxicity (Hader et al. 1995). That is to say, the correct wavelengths of radiation must be present in the exposure spectrum to facilitate the process. There are several issues that affect spectral quality, including attenuation of UV radiation in aqueous systems, time of day, season, optical properties of the water, as well as presence of the compound of concern (Hader et al. 1995). Some specific examples are the concentration of dissolved organic matter (DOM), scattering by particulate matter, as well as depth, since water alone attenuates UV radiation (Smith et al. 2004). However, photoactive wavelengths have been shown to penetrate several meters into the water column (Holst and Giesy 1989; Smith et al. 2004), indicating there is a basis of concern for photoinduced effects.

Several studies have indicated the importance of spectral quality in the study of PAH photoinduced toxicity (Fernandez and L'Haridon 1992; Spehar et al. 1999; Diamond et al. 2000; Diamond et al. 2003; Lampi et al. 2005), and it is generally recognized that photoinduced toxicity is a function of spectral quality, intensity and chemical dose (Oris and Giesy 1986; Ankley et al. 1995; Marwood et al. 2003). The importance of spectral quality mentioned above would appear to mandate the necessity of site-specific spectral analyses in the risk assessment of contaminated sites (Diamond et al. 2000; McDonald and Chapman 2002).

1.7 Predictive Modeling of Photoinduced Toxicity of PAHs

An important aspect of environmental risk assessment is the ability to predict toxicity of chemicals not previously investigated. One manner of achieving this goal is through the use of quantitative structure-activity relationships (QSARs). This is a type of mathematical modeling that strives to relate the physicochemical properties of a class of compounds to their associated biological effects. Predictive modeling is attractive as it can reduce the costs associated with testing of new and existing chemicals. Inception of this idea occurred more than a century ago; early studies correlated an increase in narcosis with increased oil/water partition coefficients (Nendza 1998). Indeed, QSAR modeling has been widely applied in toxicology.

Quantitative structure-activity relationships (QSARs) in environmental toxicology are designed to accurately predict ecotoxicological impacts of a chemical or class of chemicals. They must correctly account for environmental modifying factors, and ultimately, attain this for a variety of species. There have been several models presented that account for the modifying effect of UV light on PAHs, which has been shown to increase PAH toxicity and mutagenicity (Arfsten et al. 1996; Yu 2002). Attempts at correlating biological effects with photophysical properties began as early as 1964, when Epstein et al. (1964) noted that PAHs with high photodynamic activity were more carcinogenic than compounds with low activity. This trend of investigating photoinduced mutagenicity/carcinogenicity continued with Morgan et al. (1977), who was able to correlate several photochemical parameters, including singlet and triplet energies, with carcinogenic activity in a wide variety of PAHs. Newsted and Giesy (1987) developed one of the first QSARs for photoinduced toxicity of PAHs. They

discovered a hyperbolic relationship between lowest triplet state energy and both LT50, as well as LT50 adjusted for PAH concentration. Mekenyan et al. (1994b), using data from Newsted and Giesy, showed that toxicity was hyperbolically related to the HOMO-LUMO gap energy (HOMO: highest occupied molecular orbital; LUMO: lowest unoccupied molecular orbital). They attributed this to internal and external factors that all contributed to the formation of this hyperbola. Other studies have made use of the data of Newsted and Giesy (Mekenyan et al. 1994a; Betowski et al. 2002), although these generally served to evaluate different computational methods for estimating some of the photochemical parameters involved. However, there are factors that some of these models have overlooked. Generally, they do not account for photomodification of PAHs, despite the presence of toxic photoproducts in the environment (Swartz et al. 1997; Lampi et al. 2001). Another concern is the fact that the spectra generated by many commercial solar simulating light sources do not encompass the full range of UV wavelengths that contribute to toxicity under environmentally relevant conditions (Wiegman et al. 2002). This could result in the underestimation of toxicity.

Some of the concerns noted above have been addressed in research that is more current. Krylov et al. (1997) and Huang et al. (1997a) presented a model that expressed PAH phototoxicity as a bipartite mechanism, encompassing both photosensitization and photomodification. This model was found to be highly predictive of photoinduced toxicity in both *Lemna gibba* (Huang et al. 1997a) and *Vibrio fischeri* (El-Alawi et al. 2002). In a susequent study, Estrada and Patlewicz (2004) were critical of methods employing exclusive parameters, such as the sole use triplet state energy, or the HOMO-LUMO gap. They hypothesize that photoactivation via photosensitization is not the sole contributor to toxicity. Interestingly, Estrada and Patlewicz (2004) attribute metabolic

activation, rather than photomodification as the other contributor to toxicity. Nevertheless, their hypothesis substantiates the bipartite mechanism for toxicity, if one simply considers chemical modification as the additional factor contributing to toxicity.

Recent advances in the technological fields related to computing have led to a large increase in the use of sophisticated modeling techniques. Ecotoxicology is no different, and indeed there has been wide application of such technology. A recent introduction to the field has been the use of complex methods, particularly neural network models (Kaiser 2003; He and Jurs 2005). A complementary technique that is not widely employed in ecotoxicology is structural equation modeling (SEM) (Reckhow et al. 2005). This method encompasses many statistical techniques including regression, factor and path analysis (Bollen 1989). Structural equation modeling allows for testing of hypotheses regarding relationships between observed and latent (unobserved) variables. Latent variables are theoretical concepts that unite phenomena under a single term, and are expressed in terms of directly measured variables (Loehlin 2004). The use of SEM enables the weighting of these properties, and their contribution to each latent variable individually, as well as the contribution of the latent variables to toxicity. This type of modeling shows promise for application to ecotoxicology. Potential future uses include assessment of synergism, and for development and evaluation of predictive models developed for diverse contaminants.

1.8 Use of *Daphnia magna* in Ecotoxicology

Daphnia magna (Crustacea: Cladocera) is an organism routinely used in toxicity testing in Canadian laboratories (Environment Canada 1990). This freshwater microcrustacean, commonly known as the water flea, can be found in lakes and ponds

in northern and western North America (Pennak 1989). Feeding mainly on plankton, daphnids can reach 5-6 mm in size, and reproduce by cyclic parthenogenesis (US EPA 2002a). Their life cycle consists of four periods: egg, juvenile, adolescent and adult, and the average lifespan of *D. magna* is approximately 56 days at 20°C (Pennak 1989; US EPA 2002a).

There are several reasons for the suitability of *D. magna* as a test organism. Daphnids are broadly distributed across a wide range of habitats in the northern hemisphere, and serve an important role in aquatic food chains as an energy source for many fish species (Environment Canada 1990). Their short life cycle is conducive to chronic and reproductive toxicity testing. As well, daphnids exhibit high sensitivity to pollutants, and ease of culture and assay. They are small in size, and require small volumes of test solution (Environment Canada 1990), resulting in less overall toxicant required for assays, and thus, less contaminated waste solution.

1.9 Project Objectives

The initial research objective was first, to characterize the occurrence of oxyPAHs in sediment collected along a transect from a contaminated site. Sediment extracts were fractionated to separate intact- from oxy-PAHs. Subsequently, the fractions were assayed to determine the contribution of fractional constituents to toxicity. Relative changes in ratios of intact and oxyPAHs were also investigated to assess the likelihood of photomodification within the water column during sediment transport processes.

It is clear that there exists a wide range of effects of photoinduced toxicity of PAHs. This was further investigated in this thesis through the assessment of PAH phototoxicity to *D. magna* under different irradiance spectra, to contribute to the knowledge of the

22

effects of spectral quality on toxicity. The presence of a large variety of oxyPAHs resultant from photochemical reactions in the environment is acknowledged. However, very little is known about the biological effects of this class of contaminants, particularly from an ecotoxicological viewpoint. This was addressed in this thesis through an assessment of toxicity of a variety of oxyPAHs to *D. magna*. To complement these studies, and the existing status of QSAR modeling of photoinduced toxicity, interspecies applicability of an existing QSAR model was examined. Finally, structural equation modeling, an innovative statistical method, was applied to further substantiate the QSAR model, and to gain insight into the mechanisms of the photoinduced toxicity of PAHs.

This thesis is divided into chapters for each of the aforementioned studies. Chapter 2 discusses the occurrence and toxicity of oxyPAHs from contaminated sediments. Chapter 3 discusses the effects of spectral quality on PAH photoinduced toxicity, in addition to the toxicity of a host of relevant oxyPAHs. In Chapter 4, the adequacy of an existing QSAR model that encompasses both photomodification as well as photosensitization, in predicting interspecies photoinduced toxicity is discussed. Chapter 5 introduces the method and applicability of structural equation modeling to environmental phototoxicity of PAHs.

Chapter 2

Occurrence and Toxicity of Photomodified PAHs in Contaminated Sediments

2.1 Introduction

Polycyclic aromatic hydrocarbons (PAHs) are commonly found in contaminated environments, and can be toxic, mutagenic, and carcinogenic. The majority of PAHs are released into the environment through anthropogenic activities, including petroleum spills, electric power generation, refuse incineration, home heating, internal combustion engines, and the production of coke, carbon black, coal tar and asphalt (Nikolaou 1984; Neff 1985; Eisler 1987). Because of the large volume of PAHs produced by human activities, these contaminants are found in most industrialized regions.

The photoinduced toxicity of PAHs manifests via two different mechanisms: photosensitization and photomodification (Krylov et al. 1997). The production of singlet oxygen via photosensitization can result in ROS-induced damage to biological molecules (Foote 1976; Girotti 1983). Photomodification of PAHs via photooxidation and photolysis results in the formation of new compounds with increased polarity. They still possess some hydrophobicity, and thus the ability to accumulate in biological membranes (Huang et al. 1993; Ren 1996; Krylov et al. 1997; McConkey et al. 1997). Photomodification is rapid under environmentally relevant levels of actinic radiation (Katz et al. 1979; Huang et al. 1993; McConkey et al. 1997; Mallakin et al. 2000), from which it may be hypothesized that the contribution of modified PAHs to the environmental load of PAHs is significant.

The presence of modified PAHs in the environment is now recognized, and a thorough investigation of these contaminants is currently underway. Hazard assessment of these compounds is also ongoing, and recently some groups have reported that modified PAHs (including oxy- and nitro- derivatives) are widely distributed throughout the environment (Legzdins et al. 1995; Enya et al. 1997; Kosian et al. 1998; Machala et al. 2001; Papadoyannis et al. 2002; Kurihara et al. 2005). Legzdins et al. (1995) found that air samples collected from Hamilton, Ontario, contained many forms of modified PAHs. Included were anthraquinone (ATQ), benzanthrone (BAT), benz[a]anthraquinone (BAQ), 9-nitroanthracene, and 2-nitrofluoranthene, all in comparable concentrations with intact PAHs. Enya et al. (1997) found the modified PAHs 3-nitrobenzanthrone, 3,9-dinitrobenzanthrone, and 1,8-dinitropyrene in diesel engine exhaust and air samples collected in Tokyo. All were produced by the combustion of diesel fuel, photooxidation, or a combination of both. Kosian et al. (1998) reported that a number of modified PAHs, including BAT, and 1-hydroxyATQ were present in sediment pore water samples collected from a contaminated stream in close proximity to an oil refinery.

Photomodification can significantly alter the bioactivity of a compound, and many of the photooxidation products of PAHs (oxyPAHs) exhibit greater toxicity than the parent compounds. Oris and Giesy (1985) demonstrated that the LT50 decreased when juvenile sunfish were exposed to ultraviolet light and anthracene (ANT) simultaneously. Newsted and Giesy (1987) showed that a number of PAHs, including ANT, were phototoxic to the cladoceran, *Daphnia magna*. However, these studies attributed the observed phototoxicity to the photosensitization mechanism described above.

Evidence exists that modified PAHs are equally, or more toxic, mutagenic and/or carcinogenic than the parent compounds (Gibson 1978; Legzdins et al. 1995; Enya et al.

1997; McConkey et al. 1997; Lampi et al. 2001). It is well established that PAHs become more toxic and mutagenic following cytochrome P450-catalyzed oxidation (Sims et al. 1974; Huberman et al. 1976; Yang et al. 1977). It is not surprising then, that PAHs modified by alternative means (e.g. photomodification) are more hazardous as well. In fact, one of the highest reported scores in an Ames test was produced by the modified PAH 3-nitrobenzanthrone (Enya et al. 1997). They also found 1,8-dinitropyrene to be a powerful mutagen. Furthermore, oxy- and nitro-PAH-containing fractions have been found to exhibit greater direct mutagenicity than fractions containing intact PAHs (Legzdins et al. 1995). Fractions of samples of sediment pore water collected from a contaminated stream were found to be toxic, despite a lack of intact PAHs (Kosian et al. 1998). These fractions did contain modified PAHs, although other compounds were present that may have contributed to toxicity. In another study, the toxicity of 14 of 16 PAHs increased upon photomodification (Krylov et al. 1997). It is important to note that modified PAHs require neither biological activation, nor UV radiation to exhibit toxicity and mutagenicity (Gibson 1978; Legzdins et al. 1995; Enya et al. 1997; McConkey et al. 1997). However, toxicity and mutagenicity may be further increased in the presence of UV radiation (Oris and Giesy 1985; Newsted and Giesy 1987; Huang et al. 1993; Ankley et al. 1994).

It is hypothesized that environmental photomodification of PAHs will contribute significantly to the environmental load of toxic contaminants. Further, this class of compounds is overlooked by current regulations in the US and Canada, and might pose a risk of unknown magnitude, if undetected amounts of toxic compounds are indeed present. Therefore, one objective of the study was to identify photomodified PAHs in contaminated environments, particularly aquatic environments. Another objective was to

determine whether PAH photomodification could occur during sediment transport processes in the water column. In this chapter, a two-dimensional HPLC method to fractionate and identify PAHs and oxyPAHs in sediment samples was used. The sediment samples were taken along a transect in Hamilton Harbour and changes in the contaminant profiles, with respect to ratios of intact and oxyPAHs, are described. To assess the toxicity of the fractions, and determine the contribution of oxyPAHs to the toxicant load, a novel microbial assay used to assess toxicity of sediment fractions.

2.2 Materials and Methods

2.2.1 Sediment Collection and Extraction

Sediment samples were taken along a transect in 100 m intervals, starting 100 m from shore at a docking port near Randle Reef in Hamilton Harbour, Hamilton, Ontario, Canada (Figure 2.1), July 7, 2000. This site is contaminated with PAHs from the high concentration of industry surrounding the harbour, as well as from a spill of coke at this particular location. A ponar was used to make surface sediment grabs of approximately 1 kg. These samples were extracted using a modification of US EPA method 3550B for ultrasonic extraction of sediments (US EPA 1998). Briefly, sediment was air dried in the dark. 4 g of dry sediment was then suspended in 10 mL of hexane:acetone (1:1, v/v), and ultrasonicated for 20 minutes at room temperature using a Branson Model 450 Sonifier (Branson Ultrasonics Corporation, Danbury, CT). The sonifier was set at a duty cycle of 50%, with an output of approximately 25 Watts, and a frequency of 20 kHz. Particulate matter was removed by centrifugation and the extract was concentrated to 2 mL with a gentle stream of N_2.
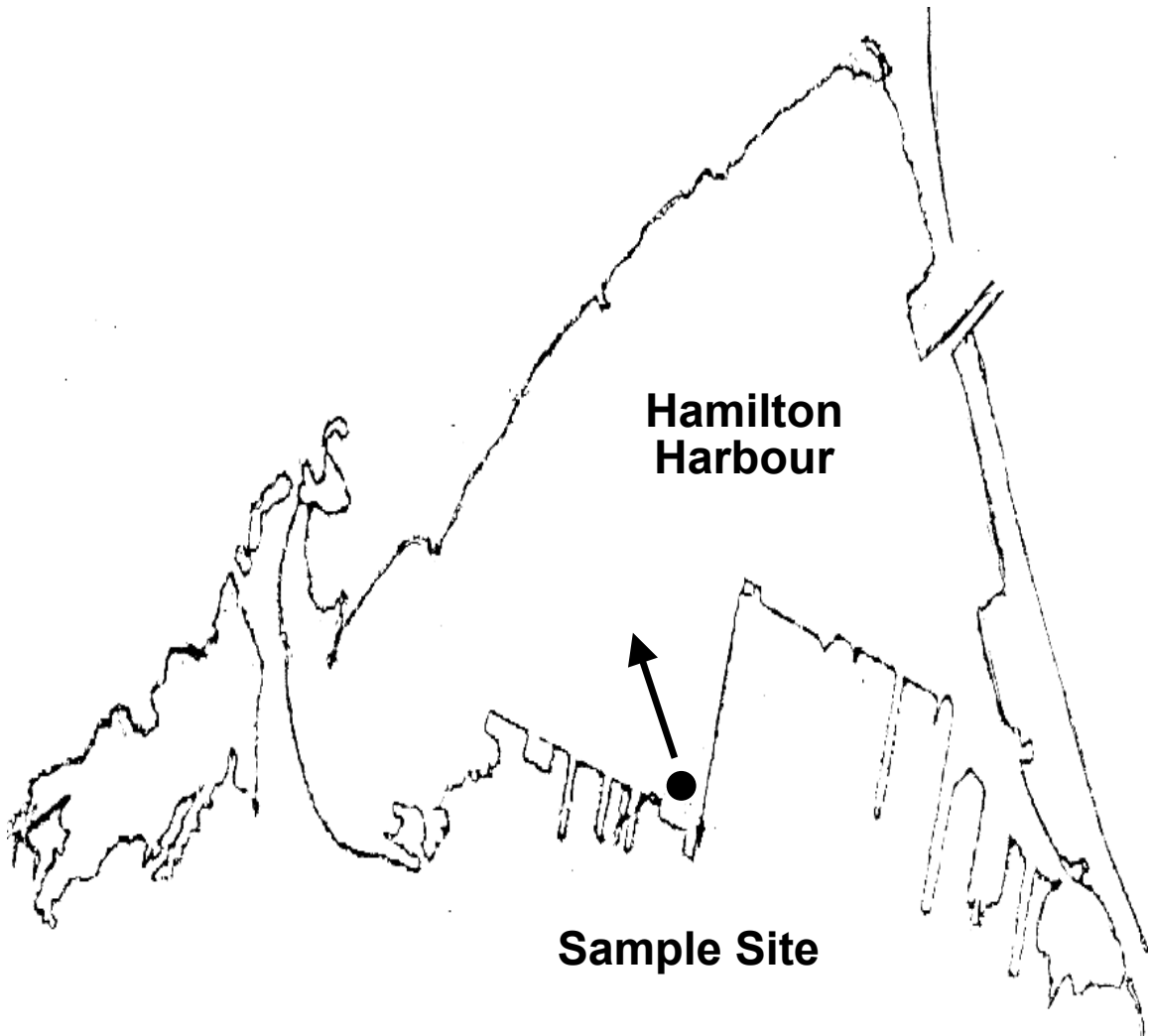
Figure 2.1. Map of Hamilton Harbour, Hamilton, Ontario, Canada, and sample site for sediment collection.

2.2.2 Two-Dimensional HPLC Fractionation of Sediment Extracts

2.2.2.1 Normal Phase HPLC Fractionation of Sediment Extracts

Extracts were fractionated using a normal phase high performance liquid chromatography (NP-HPLC) method developed for this study. A Beckman HPLC system comprised of a System Gold 126 Programmable Solvent Module, and 169 Photodiode Array Detector, using System Gold software (Beckman Coulter Canada Ltd., Mississauga, ON, Canada) was used for the normal phase fractionation. Samples were eluted through a Waters 10×250 mm Partisil polar amino-cyano (PAC, 10 μm) semi-preparative column (Waters, Mississauga, ON, Canada). 250 μL aliquots of extract were injected onto the column via a 2 mL manual injection loop. The flow rate was 2 mL/min, using a step gradient of hexane:tetrahydrofuran (THF) (95:5, v/v, Solvent A) and methanol:THF (80:20, v/v, Solvent B). The gradient used was as follows: 0-5 min, 100% Solvent A; 5-10 min, 90% Solvent A; 10-15 min, 80% Solvent A; 15-30 min, 100% Solvent B (Figure 2.2). Eluent was collected in a total of six fractions: fraction 3, 10-15 min; fraction 4a, 15-17.5 min; fraction 4b, 17.5-20 min, fraction 5a, 20-22.5 min, fraction 5b, 22.5-25 min, fraction 6, 25-30 min. Fractions were collected during the initial 10 min, although subsequent analysis revealed a lack of PAHs present. With this method, polarity increases as a function of retention time, thus fractions collected earlier will contain non-polar compounds, including intact PAHs. Fractions collected later will contain more polar compounds, including modified PAHs. The fractions were dried under a gentle stream of N_2, and resuspended in acetonitrile for subsequent chemical analysis, or DMSO for toxicity assays.
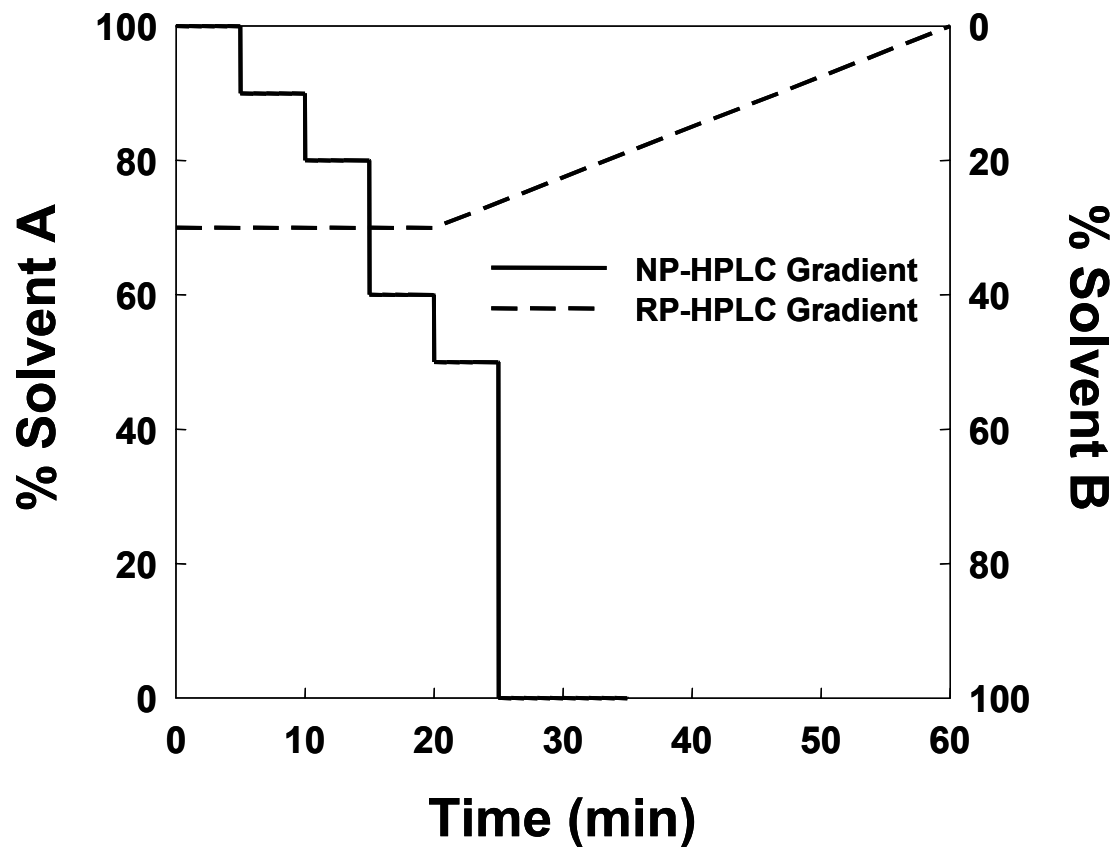
Figure 2.2. Solvent gradients for normal phase, and reverse phase HPLC fractionation and analysis of contaminated sediment extracts.
Solvents used were as follows: Normal Phase Solvent A, 95:5 (v/v) hexane:tetrahydrofuran (THF), Normal Phase Solvent B: 80:20 (v/v) methanol:THF; Reverse Phase Solvent A, acetonitrile, Reverse Phase Solvent B, pH 3.0 H_2O.

2.2.2.2 Reverse Phase HPLC –PDA Analysis of Sediment Fractions

Reverse phase HPLC analysis was performed with a Shimadzu HPLC system comprised of an SCL-10A system controller, two LC-10AD dual pumps, an SCL-10A photodiode array detector, and an SIL-10A autoinjector, with the Class-VP 4.3 software package (Shimadzu Scientific Instruments Inc., Columbia, MD, USA). Samples of fractions were eluted through a 4.6 × 250 mm, 5 μm Supelcosil LC-18 analytical column (Sigma-Aldrich Canada Ltd., Oakville, ON, Canada). A gradient at a flow rate of 1.0 mL/min was used, beginning with 70:30 acetonitrile:pH 3.0 water (v/v) for 20 min, and subsequently ramping to 100% acetonitrile from 20-60 min (Figure 2.2). The photodiode array detector was set to scan 210 nm to 400 nm to create absorbance spectra of components eluting off the column. Spectra and retention times were then compared with existing compounds in a library previously created, enabling identification of the components.

2.2.3 Culture of *Vibrio fischeri* for Toxicity Assays

Whole sediment extract and fractions from sediment extract were tested for toxicity using a bacterial respiration assay. *Vibrio fischeri* (strain NRRL B-11177) was grown as described by El-Alawi et al. (2001). Briefly, bacteria were cultured in a complex medium using the following formulation: KH_2PO_4, 18.4 mM; NaCl, 0.5 M; $MgSO_4 \cdot 7\ H_2O$, 4.1 mM; glycerol, 54.3 mM; yeast extract 1 gL^{-1}; peptone, 5 gL^{-1}; bactopeptamin, 1 gL^{-1}; agar, 15 gL^{-1} (when required). The final pH of the medium was adjusted to 7.2 ± 0.1 with 10 M NaOH. Peptone and yeast extract were obtained from BDH Inc. (Toronto, ON, Canada), and bactopeptamin was obtained from Difco Laboratories (Detroit, MI, USA). A minimal

medium was also used, which was identical to the complex medium, without glycerol, yeast extract, peptone, and bactopeptamin.

Stock cultures of *V. fischeri* grown on agar plates were used for primary inoculation of 100 mL complex medium in Erlenmeyer flasks. After inoculation, bacteria were grown for 18 h at room temperature (20°C ± 1), with shaking. Two 15 mL aliquots of culture were centrifuged for 10 min at 12 000 rpm. The supernatant was aspirated off, and the remaining pellet was resuspended in 1 mL minimal medium. To determine the working bacterial concentration, 10 μL of bacterial suspension was added to 1 mL 0.9% NaCl, and the OD was measured at 650 nm in a spectrophotometer (Perkin-Elmer, Mississauga, ON, Canada). An OD of 0.9 was desired, and if the original 10 μL aliquot of bacterial suspension was too dense, further dilution of the stock suspension was made with 0.9% NaCl.

2.2.4 Assessment of O_2 Consumption in *V. fischeri*

The inhibition of O_2 consumption of *V. fischeri* subsequent to exposure of Hamilton Harbour sediment extract fractions was assessed. Aerated 0.9% NaCl was added to the chamber of a Hansatech Respire 1 Clark-type O_2 electrode (PP Systems Inc. Amesbury, MA, USA) to a final volume of 1 mL. The instrument was allowed to stabilize, after which 10 μL of DMSO (control) or DMSO-suspended fraction was added. The instrument was again allowed to stabilize, after which 10 μL of bacterial suspension was added. Consumption of O_2 was monitored for 15 min. Slopes were calculated, and compared to control.

2.3 Results

2.3.1 Normal Phase HPLC of Hamilton Harbour Sediment Extracts

The initial part of this study used a 2D HPLC method to fractionate and identify PAHs and oxyPAHs in sediment samples taken along a transect in Hamilton Harbour (Figure 2.1). Modified PAHs were found in these contaminated sediment samples. Subsequent toxicity testing revealed the presence of modified PAHs that were toxic at levels comparable to intact PAHs. To create fractions of sediment extracts, a normal phase HPLC method that was designed to separate polar from non-polar compounds was employed. This method was used on three sediment samples taken 100 m (depth, 5 m), 200 m (depth, 10 m) and 300 m (depth, 9 m) from shore. These were labeled Sites 1, 2 and 3, respectively. Normal phase (NP) chromatograms are presented in Figure 2.3. It is evident from the chromatograms, that as distance increases from shore there is a decrease in extractable components eluting from the column. Site 3, had less material than Site 2, which in turn, had less material that Site 1.

2.3.2 Reverse Phase HPLC Analysis of Hamilton Harbour Fractions

Following the fractionation with NP HPLC, fractions were analyzed using reverse phase (RP) HPLC with diode array detection. It was the intent of this study to identify intact and modified PAHs in the various fractions collected. This was done by comparing eluent absorbance spectra to spectra of standard compounds previously identified. A representative trace is seen in Figure 2.4. As expected, there was a wide variety of PAHs identified. Further, the presence of oxyPAHs was also detected. Table 2.1 shows the different compounds identified in the fractions from Site 1, which was closest to

33
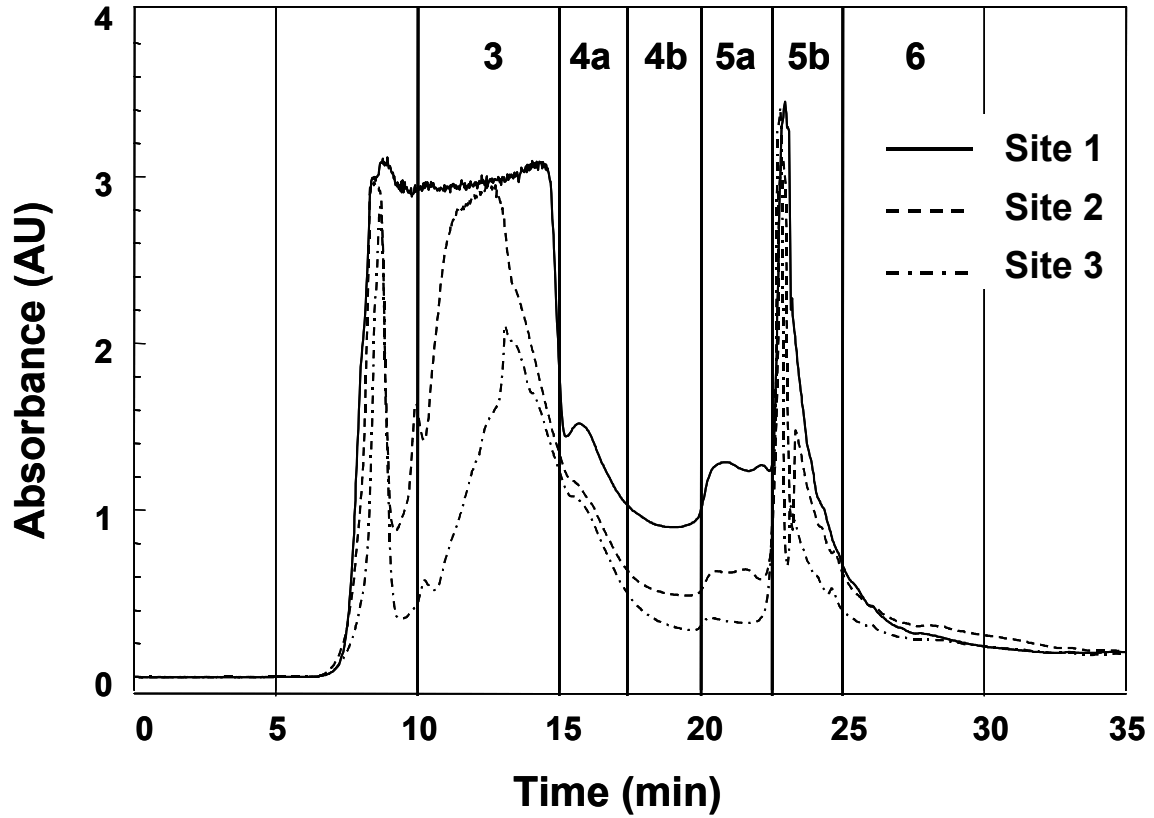
Figure 2.3. Normal phase HPLC chromatograms of extracts of Hamilton Harbour sediments collected at Sites 1, 2 and 3.
AU: absorbance units. Numbers refer to fractions collected.
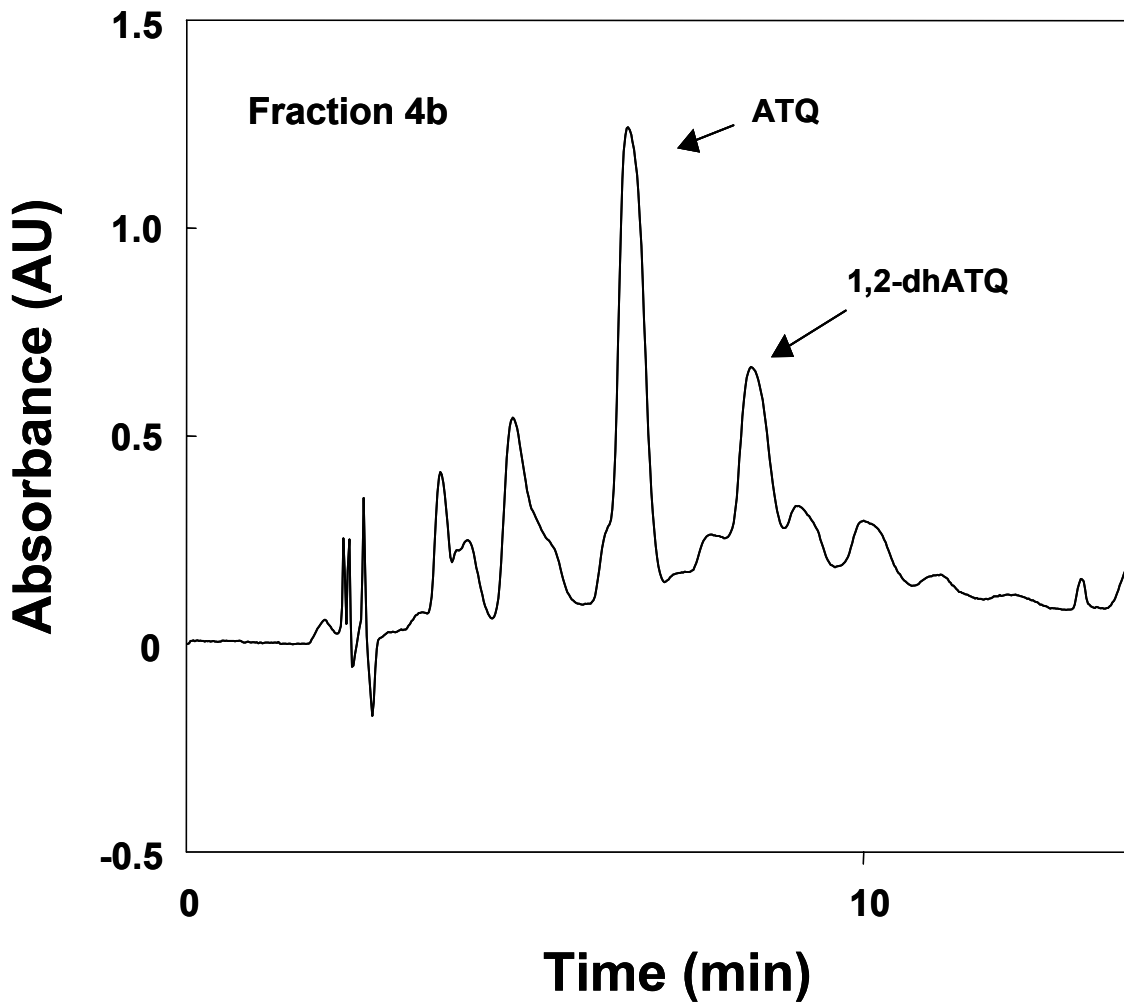
Figure 2.4. Representative reverse phase HPLC chromatogram of an oxyPAH-containing fraction of Hamilton Harbour sediment extract.
ATQ: anthraquinone; 1,2-dhATQ: 1,2-dihydroxyanthraquinone.

Compound	Fraction 3	Fraction 4a	Fraction 4b	Fraction 5a	Fraction 5b	Fraction 6
ANT	+++					
FLA	+++	+				
PHE	+++					
PYR	+++	+				
BAA/CHR		++	++	++		
TRI		+	+	+		
BBF/BKF				++	++	
BAP				+	++	
IPY				+	++	
BGP						
ATQ		+	++	+		
1,2-dhATQ		+	+	++		
Phenolic?						+++

Table 2.1. PAHs and oxyPAHs in fractions of Site 1 sediment.
Abbreviations: ANT, anthracene; FLA, fluoranthene; PHE, phenanthrene; PYR, pyrene; BAA, benz[a]anthracene; CHR, chrysene; TRI, triphenylene; BBF, benzo[b]fluoranthene; BKF, benzo[k]fluoranthene; BAP, benzo[a]pyrene; IPY, indeno[1,2,3-cd]pyrene; BGP, benzo[g,h,I]perylene; ATQ, anthraquinone; 1,2-dhATQ, putative hydroxyanthraquinone. +- arbitrary concentration unit based on relative absorbance of reverse phase HPLC. +- relative absorbance from 0-1; ++- rel. abs. from 1-2; +++- rel. abs. greater than 2.

shore, and the most contaminated site. Sites 2 and 3 were similarly analyzed, and contained a similar range of compounds, although at diminished levels. Fraction 3 contained high amounts of some of the smaller PAHs (e.g. naphthalene, anthracene, phenanthrene), while some of the larger intact PAHs (e.g. fluoranthene, benzo[a]pyrene) appeared in later fractions. Fractions 4a, 4b and 5a contained ATQ, and putatively, 1,2-dihydroxyATQ (1,2-dhATQ). In addition to the identified compounds in Figure 2.3, there were additional peaks that were not identifiable. Based on retention times of oxyPAH standards, and the complexity of photomodification (i.e. it is unlikely that only two photoproducts are formed) (Mallakin et al. 2000), it is possible that some of these were oxyPAHs. Fraction 5b contained large intact PAHs with 5 to 6 rings, as well as humic materials, while fraction 6 contained high amounts of putative phenolic substances. Some of these could include later PAH degradation products such as a variety of oxygenated benzene derivatives (Mallakin et al. 2000).

2.3.3 Changes in Contaminant Profile Along the Transect

One of the goals of this study was to determine whether PAH photomodification could occur during sediment transport processes in the water column. If this was the case, there should be a change in the ratio of oxy- to intact PAHs. Given that there was no additional source of PAHs, it was hypothesized that there would be a quantitative decrease in PAH levels, accompanied by a relative increase in oxyPAH levels in samples farther from the source of the PAHs. This is depicted in Figure 2.5, which displays hypothetical kinetics of a PAH and its primary photoproduct. As the distance from shore increases, the photoproduct would reach a peak and then decrease, while the intact, parent PAH would steadily decrease. This diagram is based on an
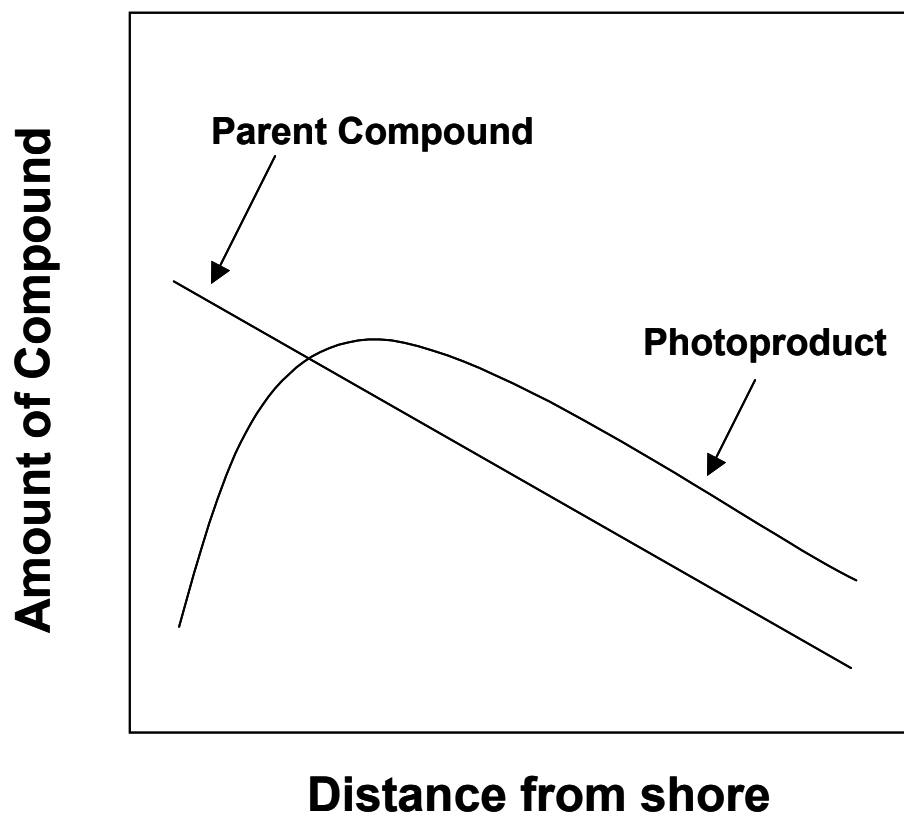
Figure 2.5. Hypothetical kinetics of photomodification of a parent compound forming a photoproduct during sediment transport.

assumption of zero-order kinetics. Two intact PAHs were chosen: ANT and FLA. ANT is the parent compound to the widely occurring oxyPAH, ATQ. ANT has very fast photooxidation kinetics in sunlight (Krylov et al. 1997). Fluoranthene is recognized as a relatively stable PAH, that does not undergo rapid photomodification (Krylov et al. 1997). It was chosen to represent a baseline chemical. Relative amounts of ANT, ATQ and FLA are presented in Figure 2.6. A decrease in relative amounts of all of these compounds was observed along the transect, although the primary photoproduct of ANT, ATQ decreased less than the other two compounds. Ratios of ATQ:FLA, and ATQ:ANT were also determined at each of the sites, and are plotted in Figure 2.7. The ATQ:FLA ratio increased initially between the samples collected at 100 and 200 m from shore, then decreased between the latter two points along the transect. The ATQ:ANT ratio displayed a similar change with distance from shore.

2.3.4 Application of a Microbial Bioassay to Assess Toxicity of Sediment Fractions

To assess whether oxyPAHs contribute to the toxicant load in contaminated sediments, a novel microbial bioassay was used. Inhibition of O_2 consumption in *V. fischeri* was determined with exposure to equivalent amounts of sediment extract. This is a direct measure of respiration (Tripuranthakam et al. 1999). The change in the concentration of O_2 was measured with an O_2 electrode, from which a slope was calculated and compared to control. Inhibition of O_2 consumption by *V. fischeri* exposed to the 6 NP fractions, as well as the whole extract is shown in Figure 2.8. The fraction with the greatest inhibition of respiration was fraction 4a, followed closely by 3, 5b, and 6. The effects caused by the oxyPAH fractions are on the order of toxicity of the intact PAH-containing fractions indicating that these compounds do contribute to toxicity.
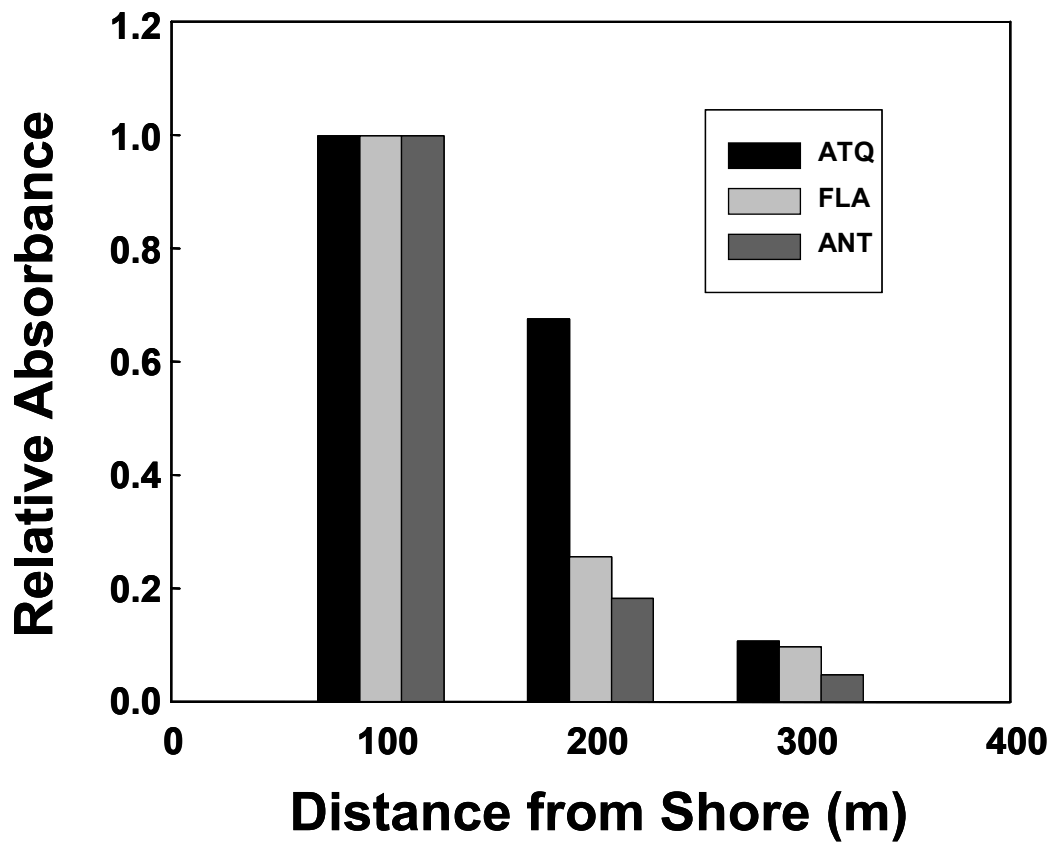
Figure 2.6. Relative amounts of three different toxicants at sites increasing in distance from shore.
ATQ: anthraquinone; ANT: anthracene; FLA: fluoranthene (n=3).
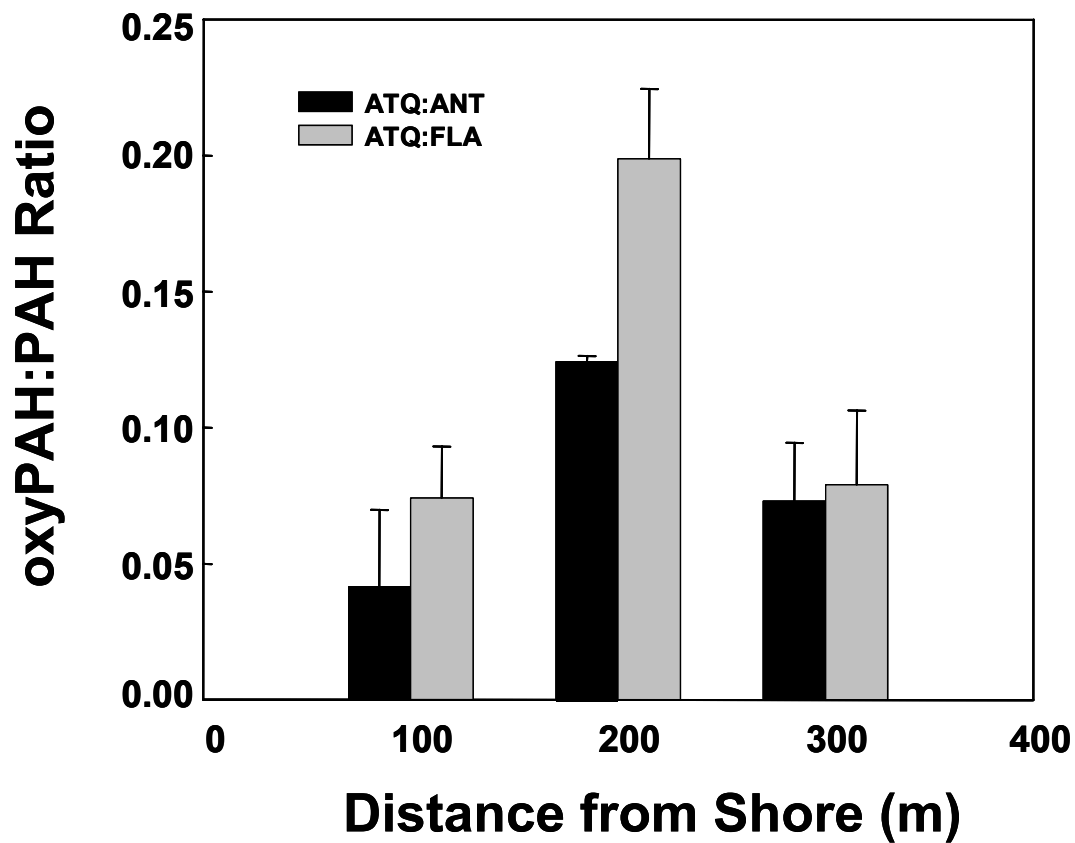
Figure 2.7. OxyPAH:PAH ratios at sites increasing in distance from shore.
ATQ: anthraquinone; ANT: anthracene; FLA: fluoranthene. Error bars: $\pm$ 1 SD (n=3).
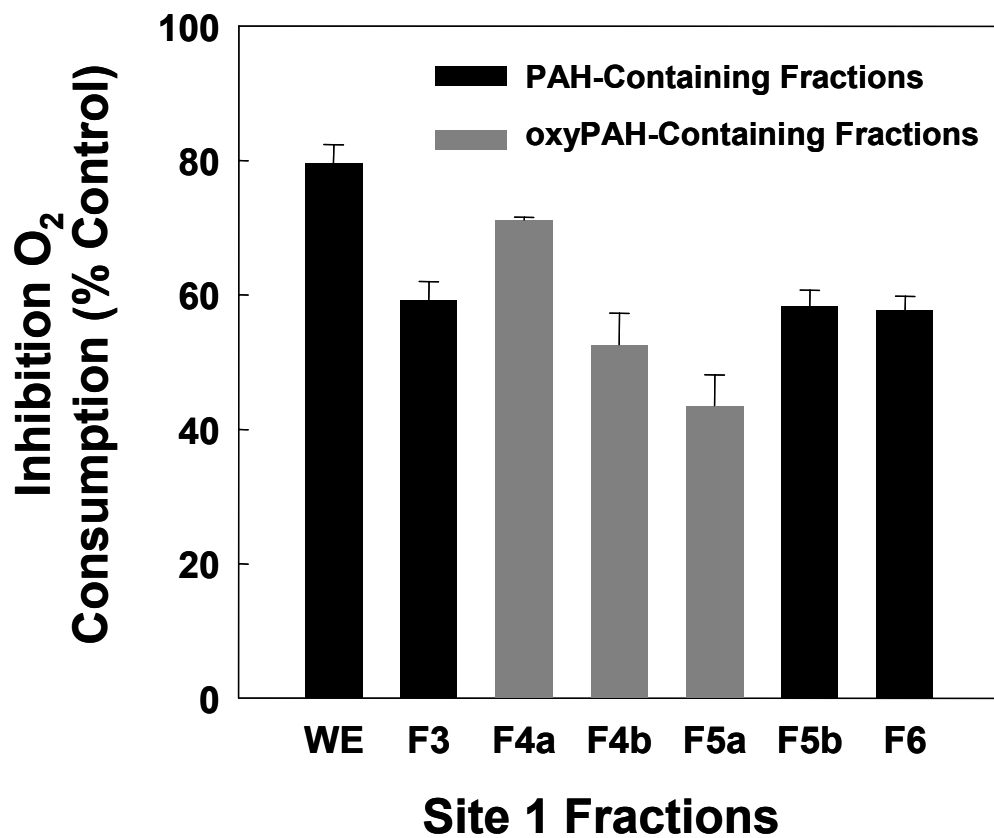
Figure 2.8. Inhibition of oxygen consumption of *V. fischeri* exposed to contaminated fractions.
Grey bars denote oxyPAH-containing fractions, while intact PAH-containing fractions are denoted by the black bars. WE: whole extract. Error bars: $\pm$ 1 SD (n = 3).

2.4 Discussion

Fractionation via normal phase HPLC and subsequent analysis has revealed modified PAHs in polar fractions of sediments collected from Hamilton Harbour. This site is located in a highly industrialized region involved in steel production. It is widely acknowledged that numerous byproducts of steel production contain high concentrations of PAHs (Nikolaou 1984; Lors and Mossmann 2005), which are likely to contribute greatly to the pollutants found in Hamilton Harbour sediments. PAHs are hydrophobic, and partition to the organic phase of particulate matter in the environment. In the case of aquatic systems, PAHs are thus largely associated with sediments (Davenport and Spacie 1991; Boese et al. 2000; Ghosh et al. 2000; Marvin et al. 2000; Klamer et al. 2005).

Sediment transport is a process documented for movement of contaminants in aqueous environments (Baker and Eisenreich 1989), and during this process, sediments in the water column are likely to enter the photic zone. Photoactive wavelengths are known to penetrate into surface waters (Holst and Giesy 1989), and indeed particulate matter plays a large role in the attenuation of UV radiation in the water column (Smith et al. 2004). Thus, the formation of oxyPAHs via photomodification of PAHs on the sediment is possible. OxyPAHs are generally more toxic than their parent compounds, and unlike intact PAHs do not require UV radiation to manifest direct toxicity. This presents a concern, since the possibility arises that rather than photolysis/degradation of PAHs to non-toxic forms, a variety of toxic oxyPAHs could be formed. This would result in a change in the profile of contaminants associated with the sediments, and potentially, higher-than-expected toxicity.

Sediment samples were taken along a transect near Randle Reef in Hamilton Harbour, Hamilton, ON, Canada (Figure 2.1). Normal phase HPLC was used to separate extracts of sediments from three sites varying in distance from shore (Figure 2.3). A decrease in the contaminant load was observed, which correlated with increasing distance from shore. Six fractions were collected for further analysis, and toxicity testing. Subsequent analysis of the fractions with RP-HPLC revealed a wide range of intact PAHs, as well as the presence of oxyPAHs in sediments from all three sites (Table 2.1). Intact PAHs were found in all 6 NP fractions. Large amounts of 3 and 4 ring PAHs, including ANT, FLA, PHE, and PYR were detected in fraction 3. Fractions 4a through 5b contained a wide variety of larger 4 to 6 ring PAHs, all but one (TRI) of which are among the 16 PAHs the US EPA has designated as priority contaminants. Increasingly polar compounds were expected to have longer retention times. Indeed, fractions 4a to 5a contained modified PAHs, as well as putative oxyPAHs that were not identified. Fraction 6 is the most polar of the fractions, and appeared to contain PAH degradation products, including compounds such as phthalic acid, benzoic acid, benzaldehyde and various phenols. The phenols have end absorbance (<250 nm) with similar absorption spectra, and are thus difficult to specifically identify with diode array detection.

The primary photoproduct of ANT, ATQ (Mallakin et al. 2000) was identified in fractions 4a through 5a, based on comparison with the absorbance spectrum and retention time of a standard. A second ATQ, putatively 1,2-dhATQ was also observed in each of fractions 4a through 5a. The absorbance spectrum of this eluent was identical to the spectrum of a standard of 1,2-dhATQ, although the retention time differed from the standard. This could be due to chemical interactions/complexing since the fractions are complex mixtures. It is possible that a shift in retention time occurred, compared to a

standard, single compound run. A representative RP-HPLC chromatogram is presented in Figure 2.4, displaying both of these compounds. There are also numerous smaller peaks that are likely oxyPAHs, but at concentrations too low to allow for proper identification. This data is consistent with other studies regarding the presence of modified PAHs in the environment (Legzdins et al. 1995; Enya et al. 1997; Kosian et al. 1998).

One problem that was encountered was the presence of a high concentration of humic matter that eluted in fraction 5b (Figure 2.3). The NP-HPLC method was designed so that retention time would increase with polarity. Based on the presence of oxyPAHs in the preceding fractions, it is highly likely that there are other oxyPAHs present; however, they are probably masked by the high amount of humic material in this fraction. Indeed, other oxyPAHs have been identified in sediments, including benz[a]anthraquinone, and benzanthrone (Machala et al. 2001). This point raises an analytical issue regarding the detection of oxyPAHs in environmental samples. The use of HPLC with diode array detection (DAD), while adequate in this instance, cannot compare to a powerful analytical technique such as LC/MS/MS. Indeed, it has been shown that some oxyPAHs were only detectable with the use of such techniques (Mosi et al. 1997). Thus, it is likely that there were more oxyPAHs present, but not detectable with the 2D HPLC-DAD method used above. Characterization through alternative techniques such as GC/MS or LC/MS will facilitate greater insight into the components and toxicity of the polar fractions.

To assess changes in the profile of contaminants, as the distance from shore increased along the transect, it was necessary to find some representative compounds with which comparisons could be made. Since ATQ, a primary product of ANT

photomodification, was present, these two compounds were chosen. FLA was chosen as a third compound; it was present at all of the sites, is relatively stable, and has a much lower photomodification rate than ANT (0.017 vs. 0.347 h^{-1}) (Krylov et al. 1997). FLA is also known to manifest photoinduced toxicity through photosensitization, rather than photomodification (Ankley et al. 1995; Ahrens et al. 2002), and thus was considered an excellent choice for comparison. Relative amounts of these three compounds at each of the sites were compared in Figure 2.6. With increasing distance from shore, there is less of a relative decrease in ATQ than is present for ANT and FLA. A proposed mechanism for this is illustrated in Figure 2.5, where the parent and product are ANT and ATQ, respectively. Initially, as the distance from shore increases, there would be an increase in the amount of ATQ present. This reaches a peak which can be attributed to the continued photomodification of ANT, followed by a decrease in both of the compounds, presumably due to photomodification of both of the compounds, as ATQ may also undergo this process (Mallakin et al. 2000).

The ratios of ATQ:ANT, and ATQ:FLA were determined (Figure 2.7), and both rose initially, then declined at the latter two sites on the transect. The initial rise may be attributed to a large decrease in the amount of both ANT and FLA, between 100 and 200 m (Figure 2.6). An increase in both ratios was expected at 300 m, but was not observed. This may be attributed to a decrease in the amount of ANT present (Figure 2.6). Another reason for the decrease in ratio is due to further photomodification of ATQ, creating further oxygenated PAHs (Mallakin et al. 2000). Indeed, a putative hydroxylated-ATQ was detected in these samples. This also supports the mechanism proposed in Figure 2.5. McKinney et al. (1999) report the use of the ATQ:ANT ratio as an indicator of the source of contaminant inputs, maintaining that airborne particulate

46

matter has a different ratio than sediment, and that the ratio is source-dependent.

However, that study was conducted on a broad scale, with sample sites hundreds of

kilometers apart in some cases. Interestingly, they were able to increase this ratio in

laboratory studies exposing contaminated sediment to UV radiation (McKinney et al.

1999). The data presented in Figures 2.6 and 2.7 provide evidence that the contaminant

profile does change during sediment transport, and that the ratio of oxy- to intact PAHs

is altered with distance from a point source of contamination.

Whole sediment extract and fractions from sample site 1 from Hamilton Harbour were

tested for toxicity using a novel assay of inhibition of oxygen consumption by *V. fischeri*.

The highest inhibition of oxygen consumption in all fractions tested was produced by

fraction 4a, which contained oxyPAHs (Figure 2.8, Table 2.1). Indeed, all of the oxyPAH-

containing fractions exhibited toxicity on the order of the fractions containing intact PAHs

alone. Interestingly, the fractions were also close to the toxicity of the whole extract. One

explanation for this might be the amelioration of toxicity in the whole extract by the

presence of humic matter, which is known to decrease PAH toxicity (Gensemer 1998).

However, the proposed amelioration was not observed in fraction 5b, possibly due to

lower levels of humic matter than the whole extract, via loss through binding to the

HPLC column. Fractions containing confirmed and putative oxyPAHs were at least as

toxic as fractions expected to contain intact PAHs. Of note, this assay was performed in

the absence of UV radiation, indicating that photosensitization, a major mechanism of

PAH phototoxicity (Bowling et al. 1983; Oris and Giesy 1985; Newsted and Giesy 1987)

is not contributing to toxicity. Rather, the toxicants are acting directly. This supports

existing evidence that modified PAHs need neither biological activation, nor UV

radiation, to exhibit direct toxicity (Huang et al. 1993; Huang et al. 1995; Ren 1996; McConkey et al. 1997; Mallakin et al. 1999).

It is important that the compounds that make up the profile of modified PAHs in the environment are identified and quantified. The elucidation of the individual compounds present in environmental samples will enable further determination of possible synergistic effects that may be observed in these complex mixtures. Mixtures of photomodified anthracene have been found to inhibit photosynthesis (Huang et al. 1997b). There is evidence that 1,2-dhATQ has an inhibitory effect on the cytochrome b/c complex of the mitochondrial electron transport chain (Tripuranthakam et al. 1999). In addition, inhibition in the chloroplast at the cytochrome b_6/f complex has been observed, as has synergistic toxicity, when 1,2-dhATQ was mixed with copper (Babu et al. 2001). As many oxyPAHs affect toxicity via different mechanisms, knowledge of components of relevant mixtures would be integral to the evaluation of environmental risk.

2.5 Conclusions

Existing data, and that presented, indicates that the presence of modified PAHs in the environment should be studied more thoroughly. Further elucidation of the nature of the mixtures present is required to understand possible ramifications that may occur. Detailed evidence regarding the presence of a heretofore-unmonitored class of toxic, mutagenic and/or carcinogenic compounds in the environment would be of great value. The data are needed to reassess regulations, and to understand the consequences of future environmental disasters such as petroleum spills. The data will also help evaluate the risks associated with human and environmental exposure to these compounds.

Chapter 3

Photoinduced Toxicity of PAHs to *Daphnia magna*: UV-Mediated Effects and the Toxicity of PAH Photoproducts.

*This chapter is based on a manuscript that has been accepted for publication in Environmental Toxicology and Chemistry.

3.1 Introduction

Polycyclic aromatic hydrocarbons are ubiquitous contaminants present at high levels in the environment. They are continuously produced naturally and anthropogenically, with an estimated ~700 metric tonnes generated annually as waste in the United States alone (US EPA 2004). These compounds generally appear as complex mixtures, and are known to be toxic, mutagenic, and carcinogenic. An environmentally relevant aspect of PAH toxicity is that it increases in the presence of solar radiation (Allred and Giesy 1985; Newsted and Giesy 1987; Ankley et al. 1994; Arfsten et al. 1996; McConkey et al. 1997; Brack et al. 2003). Polycyclic aromatic hydrocarbons contain two or more conjugated benzene rings that facilitate the absorption of ultraviolet A radiation (UVA, 320 to 400 nm), ultraviolet B radiation (UVB, 290 to 320 nm) and, in some instances, visible light (400 to 700 nm). This can lead to photoactivation of mutagens, toxicity via the photosensitized production of singlet oxygen, and photomodification that results in toxic products (Newsted and Giesy 1987; Larson and Berenbaum 1988; Arfsten et al. 1996; Huang et al. 1997a; Huang et al. 1997b; Dong et al. 2000; Yu 2002).

Photoactivation of PAH promutagens to mutagens is a well-documented phenomenon, and may occur through a variety of mechanisms (Yan et al. 2004). Benzo[a]pyrene (BAP), anthracene (ANT), benz[a]anthracene (BAA), and several of

49

their methylated substituents have been shown to efficiently cleave DNA with co-exposure to UVA (Dong et al. 2000; Dong et al. 2002). Eleven of the sixteen EPA priority PAHs showed some degree of photomutagenicity using the Ames test (Yan et al. 2004), and several of these are known to form PAH-DNA adducts (Yu 2002).

The photosensitized production of highly reactive, and biologically damaging singlet oxygen is an important, and well-studied aspect of PAH phototoxicity (Larson and Berenbaum 1988; Arfsten et al. 1996). This phenomenon is known to affect a wide variety of aquatic organisms including those living within the water column, such as fish (Oris and Giesy 1985), zooplankton (Newsted and Giesy 1987; Nikkila et al. 1999; Diamond et al. 2000), and microbes (El-Alawi et al. 2001); sediment-associated organisms including benthic anthropods (Ankley et al. 1994) and bivalves (Weinstein and Polk 2001; Ahrens et al. 2002); and aquatic vegetation (Huang et al. 1997a; Huang et al. 1997b). Photosensitization has generally been considered the major mechanism of PAH phototoxicity, although the role of photomodification has become recognized as a key mechanism of toxicity (Huang et al. 1997a; Huang et al. 1997b; McConkey et al. 1997; Brack et al. 2003).

Photomodification of PAHs, primarily via oxygenation, is a widely acknowledged phenomenon. Photomodified PAHs are known to occur in the atmosphere (Fox and Olive 1979; Legzdins et al. 1995), and within aqueous environments, both in the water column (Papadoyannis et al. 2002; Kurihara et al. 2005) and in association with sediments (Marvin et al. 2000; Lampi et al. 2001). Many of the photoproducts generated through environmental photomodification exhibit greater toxicity than the parent PAHs. Mallakin et al. (1999) found that several hydroxylated anthraquinones inhibited growth in *Lemna gibba*. Similarly, El-Alawi et al. (2001) and Brack et al. (2003) observed toxicity of

anthracene photoproducts to *Vibrio fischeri*. Brack et al. (2003) also showed that anthracene genotoxicity was manifested only after irradiation with UV. A phenanthrene (PHE) photoproduct, 9,10-phenanthrenequinone (PHQ) has been shown to have greater toxicity that the parent compound in bacterial, plant and invertebrate assays (McConkey et al. 1997; Xie et al. 2005). Further, PHQ has been found to disrupt mitochondrial function *in vivo* (Xia et al. 2004), and is known to disrupt hormone production (Nykamp et al. 2001). 3,6-benzo[a]pyrenequinone (BPQ), as well as PAH quinone-containing organic extracts of diesel exhaust particulate matter cause elevated expression of heme oxygenase-1 (Li et al. 2000). This is one of many enzymes induced via antioxidant response elements, indicating a possible role of reactive oxygen species (ROS) in oxyPAH toxicity. Of concern, risk assessment of intact PAHs currently involves concentrations that are determined from laboratory toxicity data that do not include solar radiation effects, and environmental oxyPAHs are not currently regulated.

Another issue regarding the environmental presence of oxyPAHs is the potential for synergistic interactions with other contaminants. For instance, metals are common co-contaminants with PAHs in industrialized areas. It has been shown that mixtures of copper and an oxyPAH, 1,2-dihydroxyanthraquinone, exhibited synergistic toxicity to *L. gibba* (Babu et al. 2001). Recently, it has been observed that mixtures of copper and PHQ show synergistic toxicity to *D. magna* (Xie et al. 2005). It is highly likely that further interactions will become evident as more mixtures of these contaminants are investigated. However, to fully elucidate the characteristics of these mixtures, it is first necessary to understand the effects of the individual compounds.

In this chapter, sixteen intact PAHs were assayed for toxicity to the cladoceran *D. magna* under irradiation sources containing visible light + UVA ± UVB. This organism is

known to be sensitive to PAH photoinduced toxicity (Newsted and Giesy 1987; Nikkila et al. 1999), yet a complete set of EC50 data using these spectral manipulations is currently lacking. Toxicity is reported with UVA present as was an increase in toxicity with the addition of UVB to the irradiation source. Data is also presented on the toxicity of fourteen oxyPAHs to *D. magna*. These data included photoproducts of several common, intact PAHs, heretofore untested in *D. magna*. Several of the oxyPAHs showed high toxicity, with the most toxic compounds having EC50s in the low nanomolar range. This information serves to expand the body of knowledge of the toxicity of PAHs and oxyPAHs to *D. magna*, and provides information necessary for risk assessment, as well as future mechanistic and mixture studies.

3.2 Materials and Methods

3.2.1 Stock Cultures of *Daphnia magna*

Daphnia magna colonies that have been continuously maintained in our laboratory for several years, and cultured according to standard protocols were used (Environment Canada 1990). Mature daphnids were maintained in groups of 40, in 2 L glass culture vessels, from which neonates (<24 h old) were collected daily for use in acute lethality assays. Culture water consisted of Waterloo, Ontario, Canada well water diluted 1:1 with reverse osmosis-purified (RO) water, and was changed every 3 days. Stock cultures were fed daily with *Selenastrum capricornutum* and every 3 days with TetraMin® Flakes (Tetra GMBH, Melle, Germany). Animals were cultured under cool-white fluorescent (visible) light (10 μmol·m^{-2}·s^{-1}), with a 16 h:8 h, light:dark photoperiod. The temperature was maintained at 20 ± 2°C.

3.2.2 *Daphnia magna* Acute Bioassays

Acute bioassays were performed with *D. magna* neonates (<24 h old) to determine 48 h EC50 values for immobility, determined as lack of locomotion for 15s after gentle agitation of solution. Sixteen intact PAHs and fourteen oxyPAHs were assayed. Compounds used for all toxicity assays were purchased from a variety of companies in the highest purities available, and used as received. Structures of oxyPAHs are presented in Figure 3.1, and sources and purities for all chemicals are listed in Table 3.1. Stock solutions of the test compounds were prepared in molecular biology grade dimethylsulfoxide (DMSO) (Fisher Scientific, Nepean, ON, Canada), and diluted as necessary, with the final concentration in experimental vessels not exceeding 0.1% DMSO. This level of DMSO has no impact on the test organisms (Xie et al. 2005) and was used in the controls. Assays were conducted in the same medium used to maintain the *D. magna* cultures. Geometric dilution series of five concentrations for each chemical were used for toxicity assays. Each treatment was performed in triplicate, with 10 animals per replicate in 200 mL of test medium. The photoperiod was maintained at 16 h:8 h light:dark cycle under the irradiation regimes described below. Neonate immobility was assessed after 48 h. Assays were considered unacceptable if greater than 10% immobility was observed in control animals. All triplicate experiments were independently repeated at least 3 times.

3.2.3 Lighting Conditions

Irradiation sources for the *D. magna* bioassays with intact PAHs consisted of two different regimes: full spectrum simulated solar radiation (SSR) consisting of visible light + UVA + UVB, and visible light + UVA (Figure 3.2). To produce the SSR, standard cool

Intact PAHs		oxyPAHs	
Compound	Purity (%)	Compound	Purity (%)
ANT[a]	99	9,10-ATQ[a]	97
BAA[b]	99	1,4-ATQ[d]	99
BAP[a]	97	1,2-dhATQ[e]	98
BBA[a]	98	1,4-dhATQ[e]	96
BBF[a]	98	1,8-dhATQ[f]	95
BEP[b]	90	1,2,4-thATQ[a]	90
BGP[b]	98	1,2,5,8-thATQ[a]	93
CHR[b]	98	BAQ[g]	95
COR[b]	98	PHQ[a]	99
DAA[a]	97	1,6-BPQ[h]	99
DAP[c]	98	3,6-BPQ[h]	99
FLA[a]	99	1-hATQ[g]	95
FLU[a]	98	2-hATQ[g]	96
PHE[a]	96	BBQ[g]	98
PYR[a]	95		
TRI[a]	98		

[a]Sigma-Aldrich (Mississauga, ON, Canada)

[b]Acros Organics (Morris Plains, NJ, USA)

[c]AccuStandard (New Haven, CT, USA)

[d]LGC Promochem (Wesen, Germany)

[e]Lancaster Synthesis (Windham, NH, USA)

[f]Alfa Aesar (Ward Hill, MA, USA)

[g]Tokyo Chemical Industry (TCI) America (Portland, OR, USA)

[h]NCI Chemical Carcinogen Reference Standard Repository (Kansas City, MO, USA)

Table 3.1. Sources[a-h] and purities for all compounds used in *D. magna* bioassays.
Abbreviations for intact PAHs: anthracene (ANT), benz[a]anthracene (BAA), benzo[a]pyrene (BAP), benz[b]anthracene (BBA), benzo[b]fluorene (BBF), benzo[e]pyrene (BEP), benzo[g,h,i]perylene (BGP), chrysene (CHR), coronene (COR), dibenz[a,h]anthracene (DAA), dibenzo[a,i]pyrene (DAP), fluoranthene (FLA), fluorene (FLU), phenanthrene (PHE), pyrene (PYR), triphenylene (TRI). Abbreviations for oxyPAHs: 9,10-ATQ: 9,10-anthraquinone; 1,4-ATQ: 1,4-anthraquinone; 1,2dhATQ: 1,2-dihydroxyanthraquinone (alizarin); 1,4dhATQ: 1,4-dihydroxyanthraquinone (quinizarin); 1,8dhATQ: 1,8-dihydroxyanthraquinone (danthron, chrysazin); 1,2,4thATQ: 1,2,4-trihydroxyanthraquinone (purpurin); 1,2,5,8thATQ: 1,2,5,8-tetrahydroxyanthraquinone (quinalizarin); BAQ: benz[a]anthraquinone (1,2-benzanthraquinone, benz[a]anthracene-7,12-dione), PHQ: 9,10-phenanthrenequinone; 1,6-BPQ: 1,6-benzo[a]pyrenequinone; 3,6-BPQ: 3,6-benzo[a]pyrenequinone, 1-hATQ: 1-hydroxyanthraquinone, 2-hATQ: 2-hydroxyanthraquinone, BBQ: benzo[b]anthraquinone.
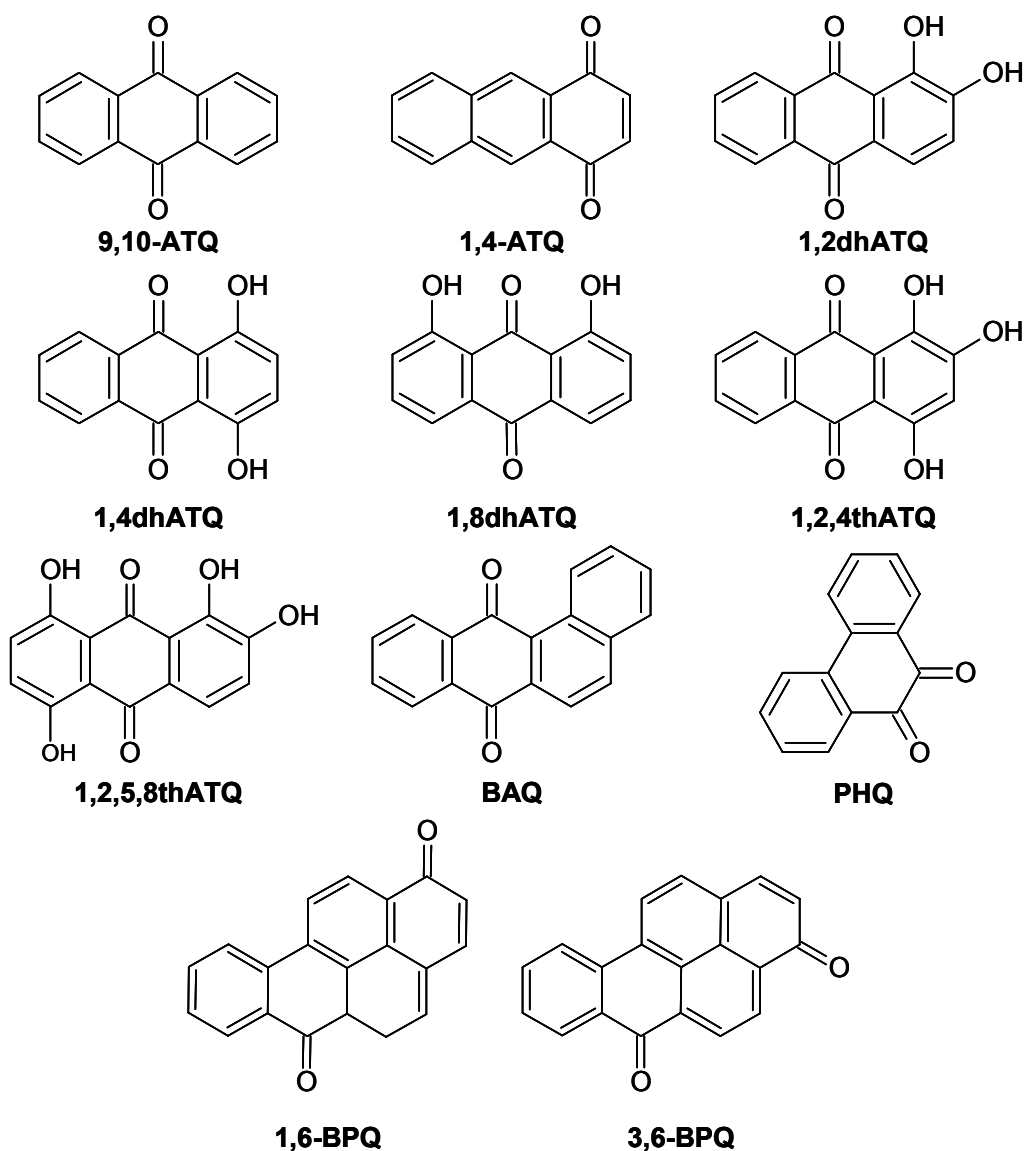
Figure 3.1 Structures of the oxyPAHs used for *D. magna* toxicity testing.
Abbreviations: 9,10-ATQ: 9,10-anthraquinone; 1,4-ATQ: 1,4-anthraquinone; 1,2dhATQ: 1,2-dihydroxyanthraquinone (alizarin); 1,4dhATQ: 1,4-dihydroxyanthraquinone (quinizarin); 1,8dhATQ: 1,8-dihydroxyanthraquinone (danthron, chrysazin); 1,2,4thATQ: 1,2,4-trihydroxyanthraquinone (purpurin); 1,2,5,8thATQ: 1,2,5,8-tetrahydroxyanthraquinone (quinalizarin); BAQ: benz[a]anthraquinone (1,2-benzanthraquinone, benz[a]anthracene-7,12-dione), PHQ: 9,10-phenanthrenequinone; 1,6-BPQ: 1,6-benzo[a]pyrenequinone; 3,6-BPQ: 3,6-benzo[a]pyrenequinone.
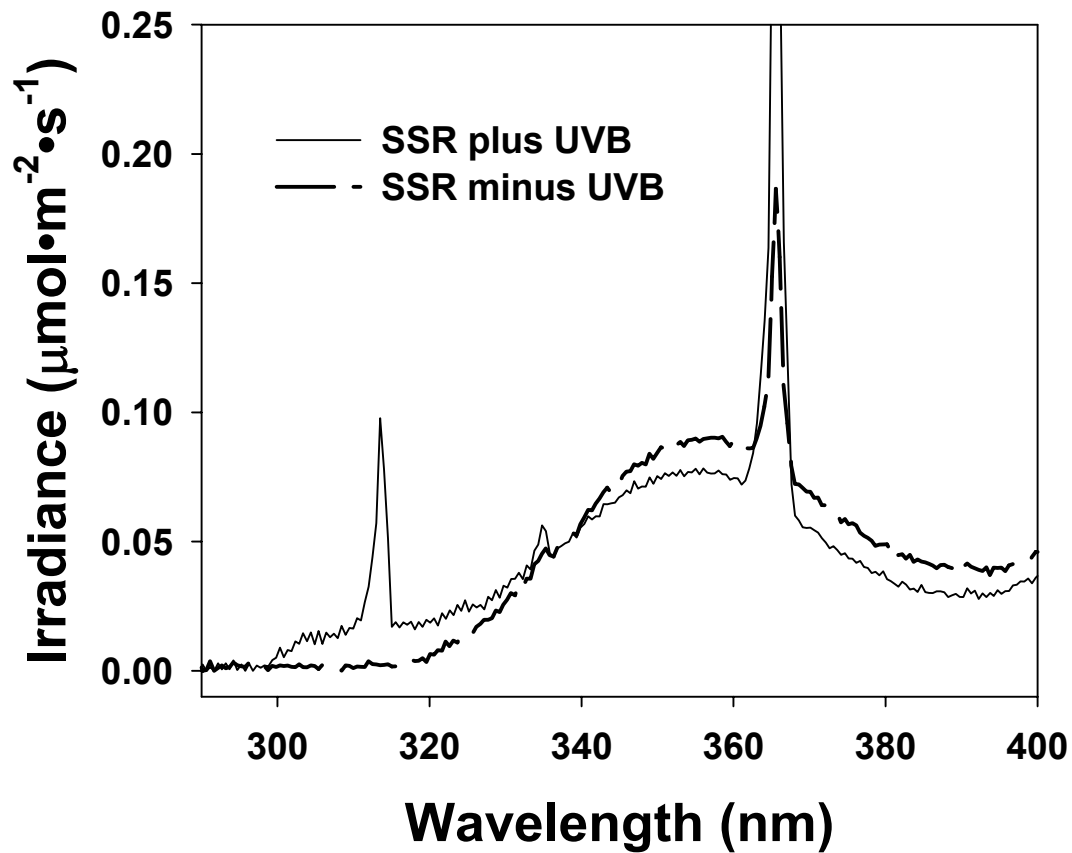
Figure 3.2 Ultraviolet spectral irradiance of light sources used for intact PAH toxicity experiments.
Irradiance levels were visible light:UVA:UVB[+], 61:4.4: 0.45 μmol•m^{-2}•s^{-1}, and visible light:UVA:UVB[-], 56:4.6:0 μmol•m^{-2}•s^{-1}. Irradiance spectra for visible light are as previously published (Mallakin et al. 1999).

white fluorescent (CWF) lamps plus RPR-3500 (UVA), and RPR-3000A (UVB) lamps (Southern New England Ultraviolet Co., Branford, USA) were combined to create spectral irradiance levels of 61:4.4:0.45 $\mu mol \cdot m^{-2} \cdot s^{-1}$ visible:UVA:UVB. Three layers of cellulose diacetate (0.08 mm) were used to remove UVC wavelengths (<290 nm). For the light source without UVB, CWF lamps and a F40T12/Type 2011 UVA lamp (Sylvania Inc., Mississauga, Canada) were used. A Mylar® screen (0.08 mm Mylar® D) was used to attenuate wavelengths below 320 nm (UVB), resulting in visible:UVA levels of 56:4.6 $\mu mol \cdot m^{-2} \cdot s^{-1}$ with no UVB present. For modified PAH bioassays, visible light was generated with CWF lamps, at an irradiance of 56 $\mu mol \bullet m^{-2} \bullet s^{-1}$. No UV was present. Spectral distribution and fluence rates for all light sources were periodically monitored using a calibrated spectroradiometer (Oriel, Inc. Stratford, CT).

3.2.4 Data Processing and Statistical Analysis

To determine the median effective concentration for 50% survival (EC50) for each replicate assay, survival data were first transformed using Equation 3.1, to enable the inclusion of zero values:

$$\text{Survival } = \frac{(m + 0.5)}{(n + 1)} \tag{3.1}$$

where m is the number of surviving neonates in a given replicate, and n is the total number of neonates. Survival data derived from Equation 3.1 were fit to the following logistic regression model adapted from Stephenson et al. (2000) (Equation 3.2):

$$\text{Survival } = \frac{1}{\left(1 + \left(\left(\frac{0.5}{0.5}\right) \times \left(\frac{x}{\mu}\right)^{b}\right)\right)} \tag{3.2}$$

57

where x is the log of the chemical concentration, μ is the log of the EC50, and b is a measure of the slope of the dose-response curve. Iterative regression with the *nonlin* function of Systat 10 (Systat Software Inc., Point Richmond, CA, USA) was used to solve for the EC50 and the slope. Average EC50 and standard deviation values were obtained from a minimum of three independent replicates. Figures were generated with SigmaPlot 6.10 (Systat Software Inc.), and ACD/Chemsketch 5.12 (Advanced Chemistry Development Inc., Toronto, ON, Canada).

3.3 Results and Discussion

3.3.1 Toxicity of Intact PAHs to *D. magna* Under Two Different UV Conditions

The toxicities of sixteen intact PAHs were assayed under two different irradiation sources: visible light + UVA and SSR. They were generally toxic to *D. magna* with and without UVB. Nonetheless, intact PAHs exhibited UV-dependent toxicity to *D. magna* with few exceptions (Table 3.2). Toxicity increased when UVB was present in the spectrum; an average decrease in EC50 of approximately 3-fold was observed in SSR versus visible + UVA exposures. Similar results were observed by Diamond et. al. (2000) in *Artemia salina*. A wide range of EC50s was observed under both irradiation regimes. In the absence of UVB, the EC50s ranged from 3.77 nM (BGP) to greater than maximum solubility for four PAHs (CHR, COR, FLU and TRI), and with UVB present, the EC50s

Compound	EC50:Visible + UVA (nM ± SD)	EC50: SSR (nM) ±SD	Fold-Decrease in EC50
ANT	110.02 ± 28.1	62.80 ± 15.7	1.8
BAA	6.49 ± 0.84	4.20 ± 0.84	1.5
BAP	6.44 ± 0.50	3.89 ± 0.81	1.7
BBA	15.09 ± 0.89	10.20 ± 2.97	1.5
BBF	483.62 ± 189	41.20 ± 4.25	11.7
BEP	5.66 ± 1.16	1.29 ± 0.60	4.4
BGP	3.77 ± 3.59	0.48 ± 0.34	7.9
CHR	NT	17.40 ± 7.36	N/A
COR	NT	NT	—
DAA	5.60 ± 4.16	1.98 ± 1.52	2.8
DAP	17.20 ± 16.2	2.27 ± 1.15	7.6
FLA	56.23 ± 10.6	19.70 ± 5.17	2.9
FLU	NT	17,100.00 ± 8410	N/A
PHE	3,923.13 ± 164	2,680.00 ± 286	1.4
PYR	21.40 ± 5.41	22.65 ± 15.0	0.9
TRI	NT	NT	—

Table 3.2. Toxicity of 16 PAHs to *D. magna* under visible light + UVA, or SSR.
Fold decrease in EC50: ratio of the visible + UVA to SSR EC50s. NT: non-toxic at levels below maximum solubility. N/A: Ratio not calculable due to zero numerator.
Abbreviations: anthracene (ANT), benz[a]anthracene (BAA), benzo[a]pyrene (BAP), benz[b]anthracene (BBA), benzo[b]fluorene (BBF), benzo[e]pyrene (BEP), benzo[g,h,i]perylene (BGP), chrysene (CHR), coronene (COR), dibenz[a,h]anthracene (DAA), dibenzo[a,i]pyrene (DAP), fluoranthene (FLA), fluorene (FLU), phenanthrene (PHE), pyrene (PYR), triphenylene (TRI).

ranged from 0.48 nM (BGP) to greater than maximum solubility for only two PAHs (COR and TRI). Among the non-toxic PAHs were two poor photosensitizers: FLU and TRI; and two highly insoluble PAHs: COR and CHR.

One compound, BBF, showed a greater than 10-fold decrease in the EC50 in the presence of UVB, and two other compounds, CHR and FLU, did not exhibit toxicity in the absence of UVB, while they became toxic with UVB (EC50s: 14.5 nM (CHR), 17,100 nM (FLU)). This can be explained by the poor absorption of UVA radiation by these compounds; they do not absorb wavelengths <350 nm, and absorb very weakly between 320 - 350 nm. Similarly, large decreases in the EC50s in the presence of UVB were also observed for BEP, BGP and DAP; these compounds also absorb weakly in the UVA spectral region, and strongly in the UVB spectral region.

It is known that photon absorbance by PAHs leads to photosensitized production of ROS, and that they photomodify to toxic products at environmentally relevant levels of UV radiation (McConkey et al. 1997; Mallakin et al. 2000; Lampi et al. 2001). Concentration-response curves representative of 3-, 4-, and 5-ring PAHs (Figure 3.3) indicate differences in mode of action. It is interesting to note that these compounds are known to photomodify, and given that photoinduced toxicity occurs via a bipartite mechanism that includes photosensitization and photomodification (Huang et al. 1997a), different modes of action are not unexpected. Indeed, a 4-fold range of slopes was observed in Figure 3.3. This may be due in part to the increase in the number of chemicals present in the solution that have formed during photomodification. The new compounds that have been generated likely have numerous mechanisms of toxicity, and each would contribute to the overall toxicity to the organism.
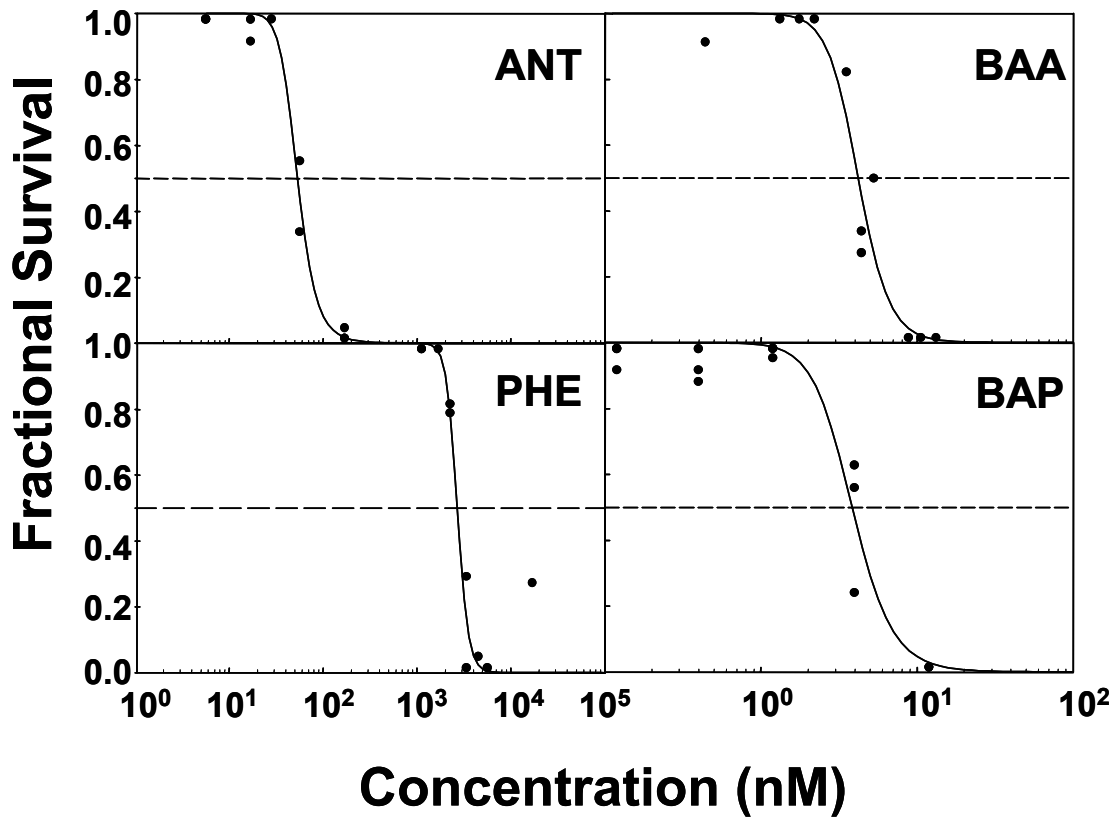
Figure 3.3. Concentration-response curves of selected intact PAHs to *D. magna*, under SSR.
Dashed line represents 50% effect. Abbreviations: ANT: anthracene, BAA: benz[a]anthracene, PHE: phenanthrene, BAP: benzo[a]pyrene.

An interesting observation was that the presence of UVB was not necessary for photoinduced toxicity of most PAHs to *D. magna*. Given that longer wavelength UVA may penetrate further into the water column than UVB, this mechanism of toxicity may be of environmental concern, particularly for those chemicals that absorb in the long wavelength UV/short wavelength visible regions. From the data, it is also evident that in some cases (e.g., a shallow streambed contaminated with PAHs), there may be sufficient penetration of UVB to result in the phototoxicity of a compound that does not necessarily absorb strongly in the UVA region. Thus, some compounds that show low toxicity without actinic radiation may in fact be highly toxic in photic environments.

3.3.2 Toxicity of PAH Photoproducts (oxyPAHs) to *D. magna*

It is a logical assumption that if a chemical is modified to other products, that some of these products could contribute to toxicity. This may also provide an explanation for the differences in the slopes of the intact PAH concentration-response curves, as the formation of new compounds during the course of a bioassay is likely to alter toxicity, and thus the shape of the curve. Based on previous knowledge of the toxicity of photomodified PAHs (Huang et al. 1997a; McConkey et al. 1997; Mallakin et al. 1999; Brack et al. 2003; Marwood et al. 2003), and the lack of a substantial set of *D. magna* toxicity data for these compounds, fourteen PAH quinones (Table 3.1) that are known PAH photooxidation products (oxyPAHs) were assayed for toxicity (Figure 3.1)

There was a wide range of EC50s for the oxyPAHs tested (Table 3.3). The most toxic photoproduct to *D. magna* was 1,6-BPQ, with an EC50 in the low nanomolar range (6.87 nM), which was nearly three orders of magnitude greater than the oxyPAH with the

Compound	EC50 (nM)	Vis + UVA Ratio	SSR Ratio
9,10-ATQ	1,108.66 ± 513	10.0	17.6
1,4-ATQ	134.53 ± 14.4	1.2	2.1
1-hATQ	NT	—	—
2-hATQ	NT	—	—
1,2-dhATQ	12,237.90 ± 4181	111.0	197.8
1,4-dhATQ	122.72 ± 16.9	1.1	2.0
1,8-dhATQ	801.25 ± 94.3	7.3	12.8
1,2,4-thATQ	196.69 ± 93.5	1.8	3.1
1,2,5,8-thATQ	685.19 ± 99.5	6.2	10.9
BAQ	14.75 ± 1.6	2.3	3.5
BBQ	NT	—	—
PHQ	1,720.53 ± 100	0.4	0.6
1,6-BPQ	6.87 ± 2.5	1.0	1.8
3,6-BPQ	10.33 ± 3.3	1.6	2.7

Table 3.3. Toxicity of oxyPAHs to *D. magna* under visible light.
Ratios are presented as $EC50_{oxyPAH}$: $EC50_{parent\ PAH}$, compared to the two irradiation conditions used for the parent PAHs. NT: non-toxic at levels below maximum aqueous solubility. Abbreviations: 9,10-ATQ: 9,10-anthraquinone; 1,4-ATQ: 1,4-anthraquinone; 1,2dhATQ: 1,2-dihydroxyanthraquinone (alizarin); 1,4dhATQ: 1,4-dihydroxyanthraquinone (quinizarin); 1,8dhATQ: 1,8-dihydroxyanthraquinone (danthron, chrysazin); 1,2,4thATQ: 1,2,4-trihydroxyanthraquinone (purpurin); 1,2,5,8thATQ: 1,2,5,8-tetrahydroxyanthraquinone (quinalizarin); BAQ: benz[a]anthraquinone (1,2-benzanthraquinone, benz[a]anthracene-7,12-dione), PHQ: 9,10-phenanthrenequinone; 1,6-BPQ: 1,6-benzo[a]pyrenequinone; 3,6-BPQ: 3,6-benzo[a]pyrenequinone.

highest measurable EC50, 1,2-dhATQ (EC50: 12.2 μM). Several anthracene photoproducts, including 1,4-ATQ, 1,4-dhATQ, 1,2,4-thATQ, 1,2,5,8-thATQ and 1,8-dhATQ showed high toxicity to *D. magna*, with the most toxic of these being 1,4-dhATQ (EC50: 122 nM). Three compounds (1-hATQ, 2-hATQ, and BBQ) did not display sufficient toxicity at concentrations soluble in the aqueous test solution to enable calculation of EC50s.

Representative concentration-response plots are given in Figure 3.4. There is no clear trend in the slope of the concentration-response curves, which range over 5-fold for the representative compounds. This would indicate that the individual PAHs and oxyPAHs have separate and distinct modes of action in *D. magna*. Indeed, several different mechanisms for PAH quinone toxicity have been reported in the literature (Jarabak et al. 1998; Penning et al. 1999; Li et al. 2000; Babu et al. 2001; Machala et al. 2001).

In general, the toxicity of oxyPAHs in visible light approaches that of intact PAHs in SSR. This is due in part to increased solubility of the oxyPAHs relative to intact PAHs. However, this data, which shows different toxicities and different slopes, indicates that increased solubility, which would imply narcosis, is not the sole explanation for the high toxicity. The manifestation of toxicity of oxyPAHs in visible light is in contrast to that of intact PAHs, which are not generally recognized as acutely toxic to aquatic organisms without UV radiation (Neff 1979). A further note of import is that oxyPAHs manifested toxicity in the absence of UV radiation, demonstrating that photoactivation is not required for these compounds. However, the implication is not that further
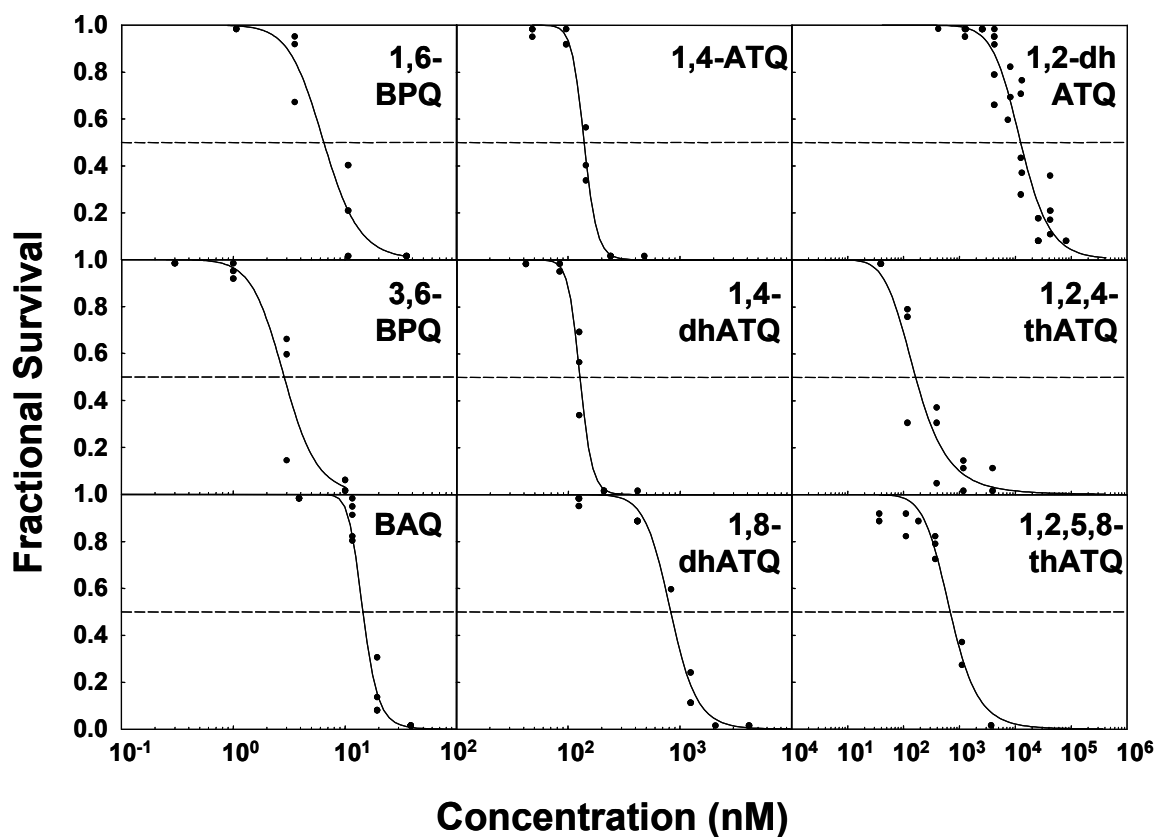
Figure 3.4. Concentration-response relationships for selected photomodified PAHs (oxyPAHs) to *D. magna* under visible light.
Dashed line represents 50% effect. Abbreviations: 1,6-BPQ: 1,6-benzo[a]pyrenequinone, 1,4-ATQ: 1,4-anthraquinone, 1,2-dhATQ: 1,2-dihydroxyanthraquinone, 3,6-BPQ: 3,6-benzo[a]pyrenequinone, 1,4-dhATQ: 1,4-dihydroxyanthraquinone, 1,22,4-thATQ: 1,2,4-trihydroxyanthraquinone, BAQ: benz[a]anthraquinone, 1,8-dhATQ: 1,8-dihydroxyanthraquinone, 1,2,5,8-thATQ: 1,2,5,8-tetrahydroxyanthraquinone.

photomodification, as observed by Mallakin et al. (2000), does not occur. Indeed, it is possible that photomodification of oxyPAHs could result in the formation of even more toxic oxyPAHs. A prime example of this is that ATQ, which itself is not highly toxic, can be further photomodified to a host of other highly toxic oxyPAHs (Mallakin et al. 2000). Thus, an important area for future study would be the toxicity of oxyPAHs to *D. magna* in the presence of UV radiation.

Photomodification of anthracene (ANT) has been shown to generate a wide range of products (Mallakin et al. 1999), many of which are anthraquinones (ATQs). Some of these have been found to exhibit greater toxicity than ANT in the absence of UV radiation (Huang et al. 1997b; Mallakin et al. 1999). The toxicity of nine different ATQs (Figure 3.1) to *D. magna* was assessed, with the resultant range of EC50s covering three orders of magnitude. The two most toxic of these compounds, 1,4-dhATQ and 1,4-ATQ, had nearly identical EC50s (122 and 134 nM) (Table 3.3). The ATQ with the highest calculable EC50 was 1,2-dhATQ (12237 nM), which is comparable to that determined in *L. gibba* (22900 nM) (Mallakin et al. 1999). 1,2-dhATQ has been studied extensively in our laboratory, and has been shown to block photosynthetic (Huang et al. 1997b), and mitochondrial (Tripuranthakam et al. 1999) electron transport. This is putatively the mode of action of toxicity of 1,2-dhATQ in *D. magna*. Greater-than-additive toxicity to *L. gibba* is also observed with 1,2-dhATQ when present in mixtures with copper (Babu et al. 2001). This occurs via Cu^{2+}-mediated, Fenton-like catalytic cycling of electrons from the pool of reduced plastoquinone caused by 1,2-dhATQ, resulting in a massive, toxic ROS burst.

It is interesting to note that the EC50s of the two unsubstituted anthraquinones, 9,10-ATQ and 1,4-ATQ, are an order of magnitude apart, and that two anthraquinones with 1-

and 4-oxygenated positions, 1,4-ATQ and 1,4-dhATQ have nearly identical EC50s (134

and 122 nM, respectively). This implies a mechanistic link between these positions and

toxicity. A third 1- and 4- substituted ATQ, with an additional hydroxy group at the 2-

position, is nearly as toxic, with an EC50 of 196 nM (Figure 3.1, Table 3.3). 1,2,5,8-

thATQ, although less toxic (EC50: 685 nM), also has hydroxy groups at positions that

are analogous to the 1- and 4- positions (Figure 3.1). This further supports the

importance of para-hydroxy groups or a para-quinone on the outside ring of the

anthracene core in determining toxicity to *D. magna*. This feature appears to be

favourable for the formation of a reactive site on this outside ring. Indeed, it has been

shown that 1,4-ATQ can form an adduct with cysteine at the 2-position on the quinone

ring (ortho to the 1-ketone) via a Michael addition (Briggs et al. 2003). This results in a

thioether linkage between the oxyPAH and the cysteine. In studies on 1,4-

naphthoquinone (structurally similar to 1,4-ATQ, with one less benzene ring) Michael

adducts ortho to the 1,4-naphthoquinone were detected with glutathione and bovine

serum albumin (Briggs et al. 2003). It is possible that similar adducts to biological

molecules would form with 1,4-ATQ. Further, 1,4-dhATQ has a resonance structure

whereby the para-hydroxy groups interact with the 9,10-quinone to form the tautomer

depicted in Figure 3.5 (Ferreiro and Rodriguez-Otero 2001; Fabriciova et al. 2004).

Similar resonance structures are likely for other anthraquinones with para-hydroxy

groups (Figure 3.5). One postulation is that this tautomerization of 1,4-dhATQ may

enable Michael adduct formation with biological molecules, and is likely the reason for

the similarities in EC50s of 1,4-dhATQ and 1,4-ATQ. Moreover, the lower toxicity of
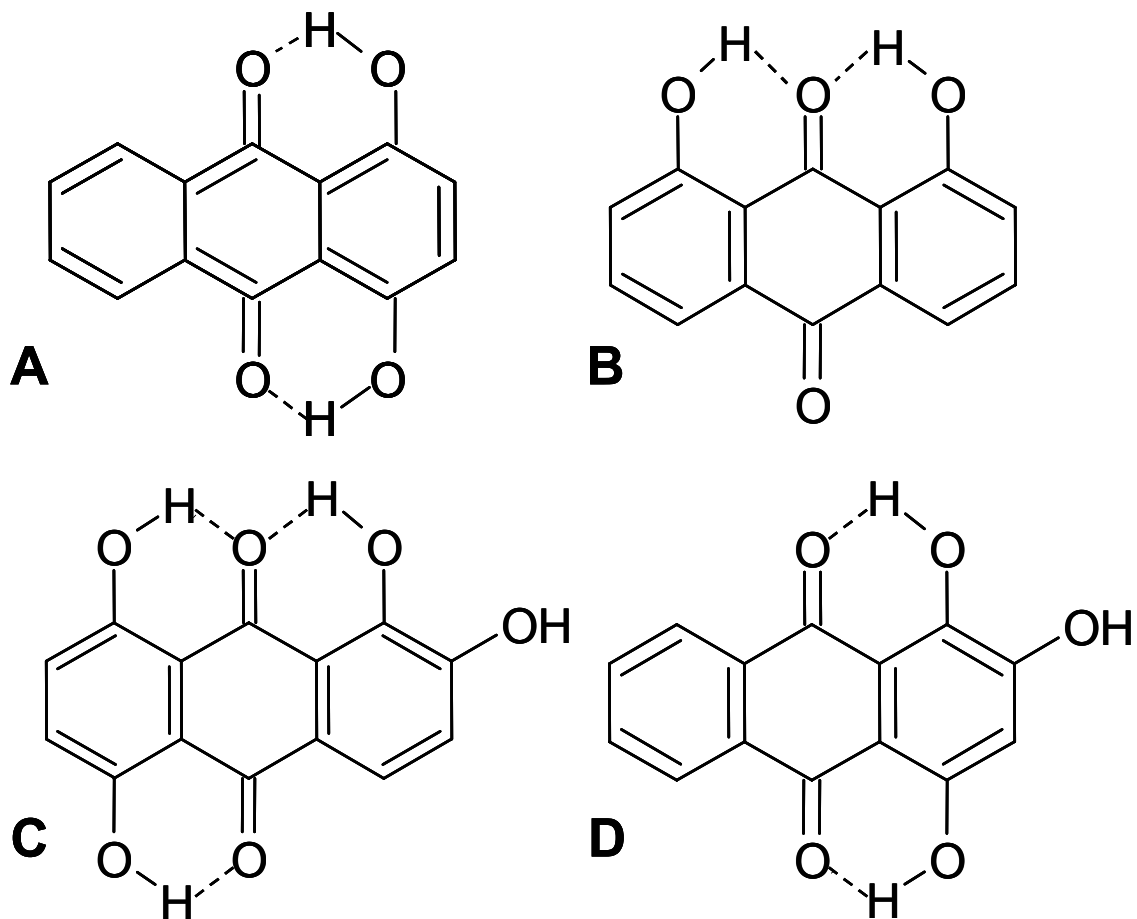
Figure 3.5. Tautomerization and hydrogen bonding of hydroxylated anthraquinones that may favour Michael addition.
A: 1,4-dihydroxyanthraquinone (1,4-dhATQ); **B:** 1,8-dihydroxyanthraquinone (1,8-dhATQ); **C:** 1,2,5,8-tetrahydroxyanthraquinone (1,2,5,8-thATQ); **D:** 1,2,4-trihydroxyanthraquinone (1,2,4-thATQ).

other para-hydroxy-containing compounds such as 1,2,4-thATQ and 1,2,5,8-thATQ

could be explained by the presence of extra hydroxy groups perturbing the resonance

structures and decreasing the efficiency of adduct formation.

Another anthraquinone showing high toxicity was 1,8-dhATQ, with an EC50 of 801

nM. This is an order of magnitude lower than that found in *L. gibba* (Mallakin et al.

1999). Despite the dearth of literature on the effects of this compound on aquatic

organisms, it has been widely studied in humans and other mammals. In addition to

being an inhibitor of topoisomerase II, an enzyme vital to DNA replication (Mueller and

Stopper 1999), 1,8-dhATQ can be metabolically activated from a weak mutagen into a

strong mutagen (Chesis et al. 1984). Bondy et al. (1994) noted the importance of

carbonyl-adjacent hydroxy groups on 1,8-dhATQ, and 1,4-dhATQ for toxicity to various

mammalian cell lines. They alluded to the importance of hydrogen bonding of these

adjacent hydroxy groups to the core ketones in retaining planar configuration of the

compounds. This planarity would facilitate intercalation of hydroxyATQs into DNA.

Furthermore, with new information regarding the formation of Michael adducts (Briggs et

al. 2003), it seems plausible that in addition to maintenance of planarity, the hydrogen

bonding of anthraquinones with carbonyl-adjacent hydroxy groups may act to increase

reactivity of the 2-position of the anthraquinone (Figure 3.5B). This could occur through

resonance tautomerization, resulting in a ketone group on the outer core ring, which

would have an electron-withdrawing effect, enabling the position ortho to the ketone

group (i.e. the 2-position on the quinone ring) to react with biomolecules.

The data of Bondy et al. (1994) are consistent with the tautomerization proposed

hypothesis; they found 1,4-dhATQ, 1,2,5,8-thATQ, 1,8-dhATQ and another

anthraquinone, leucoquinizarin (9,10-dihydroxy-1,4-anthraquinone) to be much more

toxic than anthraflavic acid (2,6-dhATQ) which does not have a carbonyl-adjacent

hydroxy group. It is interesting to note that leucoquinizarin is the resonance tautomer of

1,4-dhATQ (Figure 3.5A), and that this compound was found to be slightly more toxic

than 1,4-dhATQ (Bondy et al. 1994). Our data are also consistent with these

observations, as compounds that can hydrogen bond to the 9,10-quinone are all much

more toxic than 1,2-dhATQ. This latter compound, although able to hydrogen bond with

the 9-ketone, has the 2-position occupied by the second hydroxy group, in effect

blocking this position, which would render it incapable of undergoing Michael adduct

formation.

Phenanthrenequinone has been found to have a wide variety of detrimental biological

effects and is known to be toxic to *V. fischeri* and *L. gibba* (McConkey et al. 1997). The

EC50 for PHQ in this study with *D. magna* (1720 nM) is on the order of EC50s

previously reported for both *V. fischeri* (490 nM) and *L. gibba* (2550 nM). One reason for

elevated toxicity to *D. magna* could be higher solubility of PHQ, compared to the parent

PHE (Xie et al. 2005). This would result in greater bioavailability, and thus increased

toxicity of this oxyPAH to *D. magna*.

Several publications have implicated the importance of the *ortho*-quinone

configuration of PHQ as an important mechanism of toxicity (Flowers-Geary et al. 1996;

Jarabak et al. 1998; Penning et al. 1999). One reason this is important is that *ortho*-

quinones redox cycle. That is, a one- or two-electron reduction of the quinone, via *in

vivo* reductases, to a semiquinone or quinol would occur first. Subsequent production of

reactive oxygen species (ROS) such as superoxide (O_2^-) can occur when the

semiquinone or quinol is oxidized back to PHQ (Monks et al. 1992; Jarabak et al. 1998),

resulting in the catalytic production of ROS. However, previously an increase in ROS

production in *D. magna in vivo* was not observed (Xie et al. 2005), although redox cycling has been observed with PHQ (Jarabak et al. 1998). Further, O_2^- production by PHQ is quenched by superoxide dismutase (SOD) *in vitro* (Jarabak et al. 1998). Strikingly, this quenching effect almost completely disappears in the presence of Cu^{2+} (Jarabak et al. 1998). Mixtures of PHQ and Cu^{2+} have also been found to exhibit greater-than-additive toxicity to *D. magna* and likely via a ROS-mediated mechanism (Xie et al. 2005).

Another highly toxic compound was BAQ, a 9,10 para-quinone, with an EC50 of 14.8 nM. There is a large gap in the literature available on this compound despite its toxicity, although substantial effort has gone into the investigation of BAA *o*-quinones. BAQ is the major aqueous photodegradation product of BAA (Lehto et al. 2003), and has been detected in the environment in river sediments (Machala et al. 2001), and atmospheric aerosols (Legzdins et al. 1995; Oda et al. 1998). The few reports on this compound suggest that it may cleave DNA (Dong et al. 2002), and possess weak estrogenic activity (Machala et al. 2001). Clearly, further mechanistic investigations of this compound are warranted.

The most toxic oxyPAHs tested were both quinones of BAP: 1,6-BPQ (EC50: 6.87 nM) and 3,6-BPQ (EC50: 10.3 nM) (Figure 3.3, Table 3.3). These compounds are known BAP photoproducts (Li et al. 2000) and are present in environmental samples (Koeber et al. 1999). They may be formed within an organism through biological activation (Zhu et al. 1995) and photoactivation (Warshawsky et al. 1995). They are considered the most cytotoxic BAP metabolites, generally through formation of ROS (Grove et al. 2000). Zhu et al. (1995) observed a decrease in cellular ATP content in a stromal cell line, implicating mitochondria as a target for BPQs. Burdick et al. (2003)

affected signaling with BPQs in an epithelial cell line, likely via production of superoxide and hydrogen peroxide. It is clear that BPQs, whether generated by bioactivation or photomodification, will have negative impacts on a variety of organisms.

The fact that toxic photoproducts are generated from PAH photomodification provides substantial support for a bipartite mechanism of phototoxicity that includes both photosensitization and photomodification as suggested by Huang et al. (1997a). However, as with anthracene, which is an order of magnitude greater in toxicity than its primary photoproduct, 9,10-anthraquinone (Table 3.3), the role of photosensitization is clearly important: the sum of the individual toxicities of the anthracene photoproducts alone, would not explain the toxicity of this compound under UV. Therefore, there must be another factor contributing to toxicity. This was the case in *L. gibba*: only after the consideration of both photosensitization and photomodification could toxicity be explained (Huang et al. 1997a). This is particularly important for *D. magna* since the major site of PAH uptake would be the gill filaments which filter a high volume of water. As this organism is relatively transparent, it is highly likely that both photomodification and photosensitization would take place *in vivo*, and the tissue would be simultaneously impacted by both ROS, and metabolically active oxyPAHs.

It should be noted that the oxyPAHs tested were toxic in the absence of UV radiation. Although these compounds are formed in a photochemically favorable milieu, their detrimental biological effects are not necessarily limited to these locales as they may diffuse to other environmental compartments. This is in contrast to intact PAHs, which generally manifest toxicity via narcosis at high concentrations, with minimal toxicity at low concentrations in the absence of actinic radiation. With the exception of PHQ, all of
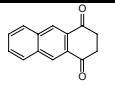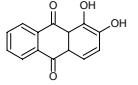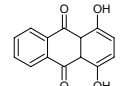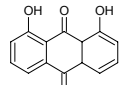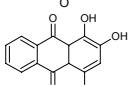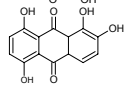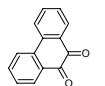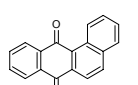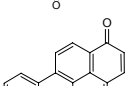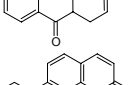
Compound	Structure	Mechanism	Reference
1,4-ATQ		Michael adducts with biological molecules.	(Briggs et al. 2003)
1,2-dhATQ		Inhibition of cytb$_6$/f (bc$_1$)	(Tripuranthakam et al. 1999; Babu et al. 2001)
1,4-dhATQ		Possible adduct formation.	Proposed
1,8-dATQ		Inhibits topoisomerase II, mutagen	(Chesis et al. 1984; Mueller and Stopper 1999)
1,2,4-thATQ		Possible adduct formation.	Proposed
1,2,5,8-thATQ		Possible adduct formation.	Proposed
PHQ		Redox production of ROS, mitochondrial disruption	(Jarabak et al. 1998; Xia et al. 2004)
BAQ		Weakly estrogenic, cleavage of DNA	(Machala et al. 2001; Dong et al. 2002)
1,6-BPQ		ROS production, decrease in ATP	(Zhu et al. 1995; Grove et al. 2000)
3,6-BPQ		ROS production, mitochondrial disruption	(Grove et al. 2000; Li et al. 2000)

Table 3.4. Possible mechanisms of toxicity of oxyPAHs.
Proposed: based on arguments presented in this study. Abbreviations: 1,4-ATQ: 1,4-anthraquinone, 1,2-dhATQ: 1,2-dihydroxyanthraquinone, 1,4-dhATQ; 1,4-dihydroxyanthraquinone, 1,8-dhATQ: 1,8-dihydroxyanthraquinone, 1,2,4-thATQ: 1,2,4-trihydroxyanthraquinone, 1,2,5,8-thATQ: 1,2,5,8-tetrahydroxyanthraquinone, PHQ: phenanthrenequinone, BAQ: benz[a]anthraquinone, 1,6-BPQ: 1,6-benzo[a]pyrenequinone, 3,6-BPQ: 3,6-benzo[a]pyrenequinone.

the PAH photoproducts displayed less toxicity than their parent compounds with UV radiation present (Tables 3.1 and 3.2). However, an examination of the ratios of toxicity of the intact PAHs to respective photoproducts (Table 3.3) shows clearly that environmental photomodification plays a role in photoinduced toxicity of PAHs, and evidence points to a wide variety of mechanisms of action (Table 3.4).

3.4 Conclusions

There is a lack of comprehensive dose-response relationship data for PAHs with UV, as well as oxyPAH toxicity to *D. magna*. Toxicity of PAHs to *D. magna* was observed in the presence and absence of UVB. UVB was not an absolute requirement for PAH phototoxicity, and as longer wavelength UVA can penetrate deeper into the water column, the longer wavelengths must be considered with risk assessment of PAHs. It was also observed that compounds that were non- or minimally toxic in the absence of UVB, exhibited considerable toxicity in the presence of actinic radiation. This confirms the known importance of spectral quality (Diamond et al. 2000), and emphasizes the need to analyze absorption spectra of new and known contaminants in the prediction of phototoxicity.

Several PAH photoproducts (oxyPAHs) demonstrated high toxicity to *D. magna*. These compounds showed remarkable toxicity for an unregulated group of chemicals, with EC50s from the low nanomolar to micromolar range. The variety of slopes for the concentration-response curves is indicative of different modes of action, which highlights the increased potential for interactions with environmental co-contaminants, some of which have already been documented. Because photomodified PAHs are known to

74

occur in the aquatic environment, they are likely to contribute to the toxic load of contaminants, individually or as components of mixtures.

The data presented here support the need to consider bipartite photoinduced toxicity as a mechanism in studies dealing with PAHs in the environment. These compounds manifest toxicity through photosensitized production of ROS, and via the production of unregulated photoproducts, many of which show great potential for interaction with existing co-contaminants. Clearly, environmental photomodification of PAHs has the potential to generate toxic compounds that could negatively impact various natural ecosystems and human health.

Chapter 4

A Predictive QSAR Model for the Photoinduced Toxicity of PAHs to *Daphnia magna* Using Factors for Photosensitization and Photomodification.

4.1 Introduction

As ubiquitous environmental contaminants of natural and anthropogenic origin, polycyclic aromatic hydrocarbons (PAHs) contribute substantially to environmental pollutant loads. They are generally found throughout urbanized regions as they are byproducts of many industrial processes (Neff 1985; Eisler 1987; Mastral and Callen 2000). There is risk of toxicity, mutagenicity and carcinogenicity to organisms in ecosystems contaminated with PAHs through a variety of well-documented modes of action (McCarty et al. 1992; Arfsten et al. 1996; Dong et al. 2000; White 2002).

Photoinduced toxicity is one such mode of action, and is an environmentally relevant phenomenon (Larson and Berenbaum 1988; Arfsten et al. 1996). PAH structure consists of two or more fused benzene rings. Their extended conjugated π-bonding orbitals allow for absorption of radiation in the UV/far blue region of the solar spectrum (Nikolaou 1984; Larson and Berenbaum 1988). Photoinduced toxicity occurs via photosensitization (Foote 1968; Huang et al. 1997a; Krylov et al. 1997), and photomodification (Huang et al. 1995; McConkey et al. 1997; Marwood et al. 1999; Lampi et al. 2005). The former involves the production of highly reactive singlet oxygen ($^1O_2$) (Foote 1968) after photodynamic generation of PAHs in their triplet states. The long triplet state lifetimes of PAHs allows $^1O_2$ production to occur with high efficiency (Morgan et al. 1977).

76

Photomodification generally occurs through photooxidation of a parent PAH to one or several photoproducts, usually oxygenated PAHs (oxyPAHs), which are detectable in the environment (Fox and Olive 1979; Andino et al. 1996; Jang and McDow 1997; Lampi et al. 2001; Machala et al. 2001; Reed et al. 2003). Many oxyPAHs exhibit greater biological activity than their parent compounds through a variety of mechanisms (McConkey et al. 1997; Babu et al. 2001; Blaha et al. 2001; Machala et al. 2001; Brack et al. 2003; Choi and Oris 2003; Seike et al. 2003; Lampi et al. 2005).

Quantitative structure-activity relationships (QSARs) in environmental toxicology are designed to accurately predict ecotoxicological impacts of a chemical or class of chemicals. They must correctly account for environmental modifying factors, and ultimately, attain this for a variety of species. There have been several models presented that account for the enhanced toxicity of PAHs in UV radiation. Newsted and Giesy (1987) showed a hyperbolic relationship between lowest triplet state energy and LT50s for *D. magna*. Mekenyan et al. (1994b), using data from Newsted and Giesy, showed that toxicity was related to the HOMO-LUMO gap energy. However, there are factors that these models overlooked. First, these pioneering models did not explicitly account for photomodification of PAHs. Second, the solar simulating light sources employed by Newsted and Giesy did not encompass the full range of solar UV wavelengths that contribute to toxicity at environmentally relevant levels (Newsted and Giesy 1987; Holst and Giesy 1989).

Previously, it was shown that an empirical QSAR model for photoinduced toxicity of PAHs was explanatory for *Lemna gibba* (Huang et al. 1997a; Krylov et al. 1997). In this model, the sum of a photosensitization factor (PSF_{LG}) and a photomodification factor (PMF_{LG}) (Equation 4.1):

$$\text{Toxicity} = \text{PSF}_{LG} + \text{PMF}_{LG}$$

$$\text{PSF}_{LG} = f\{[C]_L, \varphi, J\}, \text{PMF}_{LG} = f\{k_m, T_{PM}\} \tag{4.1}$$

correlated well with toxicity. These factors were composed of photophysical properties obtained in the literature, as well as variables that were organism-specific, and experimentally derived. Subsequently, this model was also found to be predictive by correlating with photoinduced toxicity in a long-term *Vibrio fischeri* assay (El-Alawi et al. 2002). This provided initial evidence that the *L. gibba* model could cross a species barrier for photoinduced toxicity. To further investigate the inter-species applicability of the *L. gibba* model, the next step was to determine whether it would carry over to an animal system. *Daphnia magna*, an ecologically relevant, and well-studied organism was chosen, with concentration causing 50% immobilization (EC50) and time to 50% immobilization (ET50) as the endpoints.

This chapter shows that after simple alteration of the terms that were *Lemna*-specific in the previous model, an excellent correlation to *D. magna* EC50s is observed. These findings demonstrate that a QSAR that is highly predictive has been derived, which requires little empirical data, as was required for the *Lemna* QSAR. This also provides further evidence of the development of a model that is able to accurately predict inter-species photoinduced toxicity of PAHs. Thus, it was possible to gain insight into the mechanism of photoinduced toxicity. In contrast to photoinduced toxicity in *L. gibba*, photosensitization processes contributed to a greater degree in the toxicity model than photomodification processes in *D. magna*. It is also likely that this model can be applied to other photoactive chemicals that are present in the environment, including heterocyclic and substituted PAHs.

4.2 Materials and Methods

4.2.1 Stock Cultures of *Daphnia magna*

A *D. magna* colony that has been continuously maintained in our laboratory for several years, and cultured according to standard protocols was used for these experiments (Environment Canada 1990). Mature daphnids were maintained in groups of 40, in 2 L glass culture vessels from which neonates (<24 h old) were collected daily for use in acute lethality assays. Culture water consisted of Waterloo, Ontario, Canada well water diluted 1:1 with reverse osmosis-purified (RO) water, and was changed every 3 days. Stock cultures were fed daily with *Selenastrum capricornutum* and every 3 days with TetraMin® Flakes (Tetra GMBH, Melle, Germany). Animals were cultured under cool-white fluorescent (visible) light, with a 16 h:8 h, light:dark photoperiod. The temperature was maintained at $20\pm2^{o}C$.

4.2.2 Test Compounds

Compounds used for all toxicity assays were purchased from a variety of companies in the highest purities available, and used as received. The following chemicals were used, with abbreviations and purities in parentheses. Structures are shown in Figure 4.1. Benz[a]anthracene (BAA, 99%), benzo[e]pyrene (BEP, 90%), benzo[g,h,i]perylene (BGP, 98%), chrysene (CHR, 98%), and coronene (COR, 95%) were purchased from Acros Organics (Morris Plains, NJ, USA). Anthracene (ANT, 99%), benzo[a]pyrene (BAP, 97%), benzo[b]anthracene (BBA, 98%), benzo[b]fluorene (BBF, 98%), dibenz[a,h]anthracene (DAA, 97%), fluorene (FLU, 98%), fluoranthene (FLA, 99%),
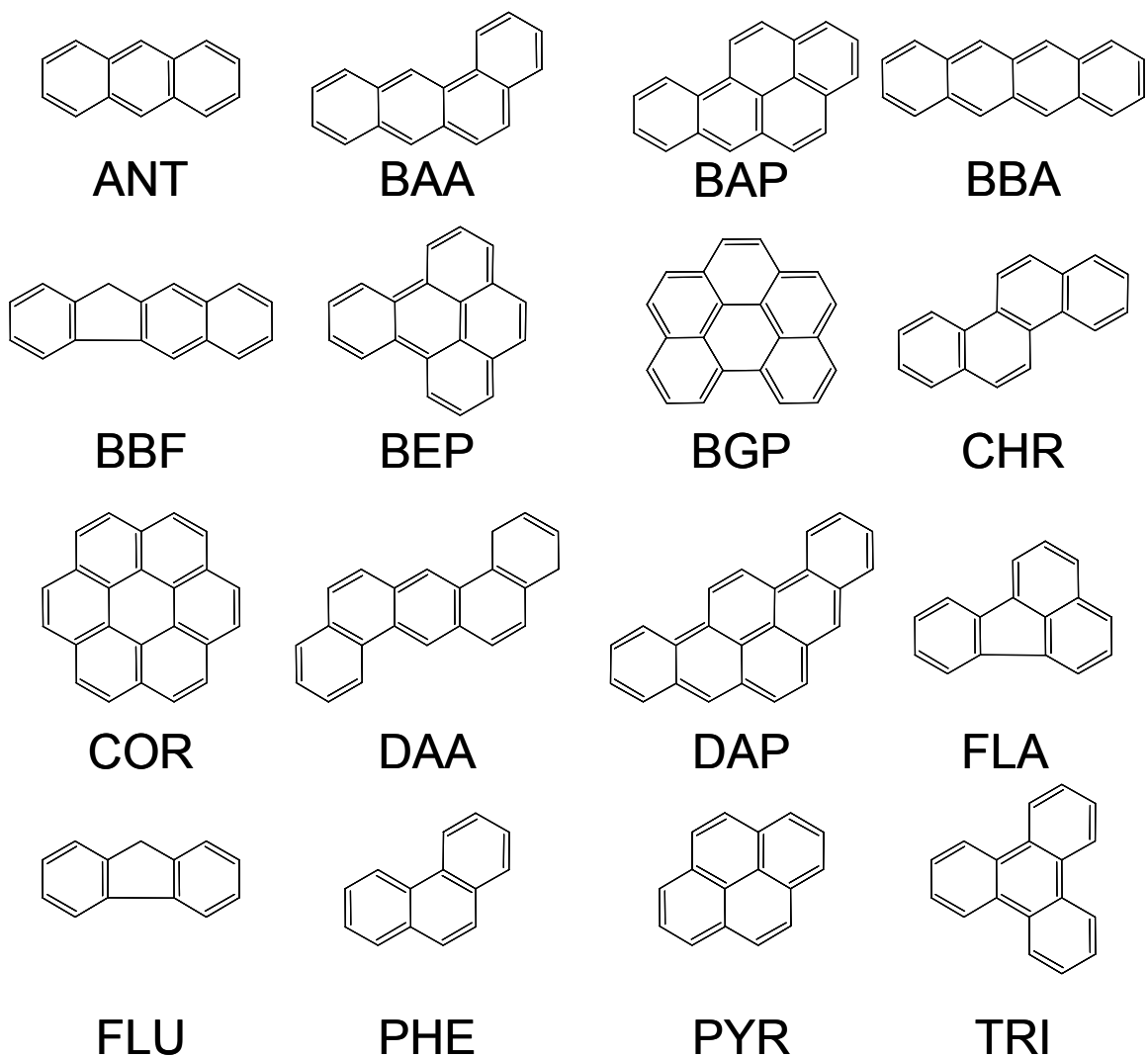
Figure 4.1. Structures of the PAHs used in this study.
Abbreviations: anthracene (ANT), benz[a]anthracene (BAA), benzo[a]pyrene (BAP), benz[b]anthracene (BBA), benzo[b]fluorene (BBF), benzo[e]pyrene (BEP), benzo[g,h,i]perylene (BGP), chrysene (CHR), coronene (COR), dibenz[a,h]anthracene (DAA), dibenzo[a,i]pyrene (DAP), fluoranthene (FLA), fluorene (FLU), phenanthrene (PHE), pyrene (PYR), triphenylene (TRI).
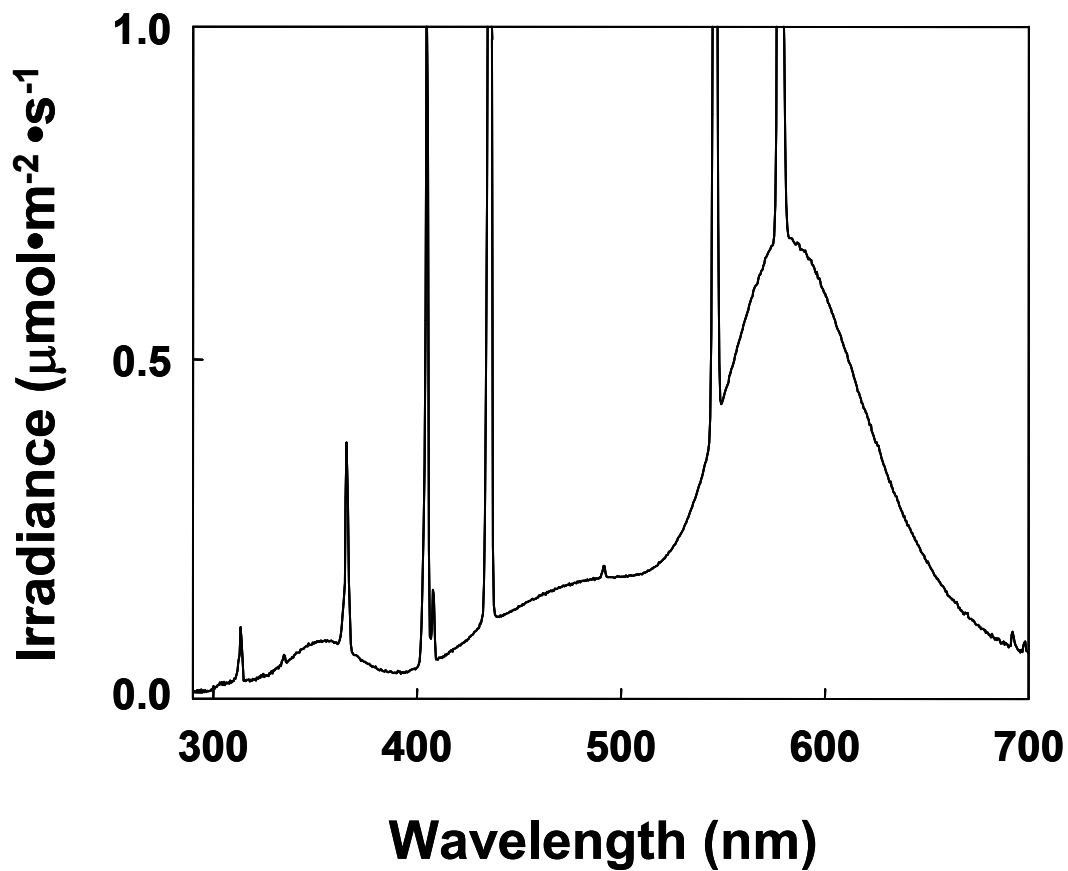
Figure 4.2. Ultraviolet spectral irradiance of the light source used for PAH toxicity experiments.
Irradiance levels were visible light:UVA:UVB, 61:4.4: 0.45 μmol•m^{-2}•s^{-1}.

phenanthrene (PHE, 96%), pyrene (PYR, 95%), and triphenylene (TRI, 98%), were purchased from Sigma-Aldrich (Mississauga, ON, Canada). Dibenzo[a,i]pyrene (DAP, 98%) was purchased from AccuStandard (New Haven, CT, USA).

4.2.3 *D. magna* Toxicity Data

Acute bioassays with *D. magna* to ascertain ET50 values of the PAHs were conducted in the same medium used to maintain the *D. magna* cultures. All assays were conducted at the same concentration for each chemical (300 nM). This is the 48 h EC90 for ANT, a known phototoxic PAH. This level was chosen with the intent of having assays run for a maximum of 96 h, while also providing a sufficient dose of chemical to manifest toxicity within the assay time limit. Light (see below) was maintained throughout the entire duration of the assay. Each treatment was performed in triplicate, with 10 animals per replicate in glass vessels. Each vessel contained 200 mL of test medium. The number of immobilized neonates was counted at appropriate time intervals. If assays ran longer than 24 h, animals were fed as per culture procedure for 1 h preceding a change of toxicant-containing assay medium via static renewal. This was repeated at 24 h intervals, up to a maximum of 96 h, after which time it was concluded that chemicals were non-toxic at this dose, and/or the organisms had lost sensitivity due to increases in biomass through normal growth. EC50 toxicity data was obtained from Lampi et al. (2005, Chapter 3).

4.2.4 Lighting Conditions

The light source for the *D. magna* toxicity assays was simulated solar radiation (SSR, Figure 4.2) (Lampi et al. 2005, Chapter 3). To produce the SSR, cool white fluorescent

(CWF) lamps, RPR-3500 (UVA) and RPR-3000A (UVB) lamps (Southern New England Ultraviolet Co., Branford, USA) were combined to create spectral irradiance levels of 61:4.4:0.45 μmol•m^{-2}•s^{-1} visible:UVA:UVB. The light was filtered through three layers of cellulose diacetate (0.08 mm) to remove UVC (<290 nm). All toxicity tests were run under continuous SSR. This is to prevent a burst in toxicity following a dark period where bioaccumulation would occur without photoinduced effects (Allred and Giesy 1985). Spectral distribution and fluence rates for the SSR source were periodically monitored using a calibrated spectroradiometer (Oriel, Inc. Stratford, CT).

4.2.5 Data Processing and Statistical Analysis

To determine the median effective time for 50% survival (ET50) for each replicate assay, toxicity data was first transformed using Equation 4.2, to enable the inclusion of zero values:

$$\text{Survival} = \frac{(m + 0.5)}{(n + 1)} \qquad (4.2)$$

where m is the number of surviving neonates in a given replicate, and n is the total number of neonates. Time and survival data derived from Equation 4.2 were fit to the following logistic regression model adapted from Stephenson et al. (2000) (Equation 4.3):

$$\text{Survival} = \frac{1}{1 + \left[\left(\frac{0.5}{0.5}\right) \times \left(\frac{t}{\mu}\right)^b\right]} \qquad (4.3)$$

where t is the time at which survival was assessed, μ is the ET50 value, and b is a measure of the slope of the curve. Iterative regression with the *nonlin* function of Systat

10 (Systat Software Inc., Point Richmond, USA) was used to solve for the ET50. Average ET50 and 95% confidence interval values were obtained from a minimum of three independent replicates. Figures were generated with SigmaPlot 6.10 (Systat Software Inc.), and ACD/Chemsketch 5.12 (Advanced Chemistry Development Inc., Toronto, ON, Canada). Regression analyses were performed using JMP 5.1 (SAS Institute Inc., Cary, USA), and Systat 10 (Systat Software Inc.).

4.3 Results and Discussion

4.3.1 *Daphnia magna* EC50 and ET50 Toxicity Data

To evaluate the fit of the previous QSAR model developed for *L. gibba*, a complete set of *D. magna* toxicity data for 16 PAHs was required. One goal was to use data at one concentration (e.g. ET50 data), which mathematically fits the *L. gibba* QSAR model better than EC50 data (Krylov et al. 1997). Thus, *D. magna* ET50 toxicity data for 16 PAHs, each at 300 nM, were generated. A set of EC50 data from Lampi et al. (2005, Chapter 3) was also used. Both sets of data are presented in Table 4.1.

ET50s ranged from 94.8 min (FLA) to non-toxic (COR, FLU, PHE, and TRI). The most toxic compound was FLA, with an ET50 of 94.8 min, followed by BEP, PYR and BAP with ET50s of 116, 121, and 147 min, respectively. Two other highly toxic compounds were ANT (174 min) and BAA (184 min). Mid-level toxicity range was observed for some of the larger compounds, including BBA, DAP, DAA, BGP, BBF and CHR (Table 4.1). Of the non-toxic compounds, three of the four (FLU, PHE, and TRI)

84

Compound	ET50 (min) ± SD	EC50 (nM) ± SD
ANT	173.6 ± 45.1	62.80 ± 15.7
BAA	183.9 ± 68.5	4.20 ± 0.84
BAP	147.4 ± 23.0	3.89 ± 0.81
BBA	369.5 ± 9.46	10.20 ± 2.97
BBF	727.5 ± 66.8	41.20 ± 4.25
BEP	116.2 ± 42.5	1.29 ± 0.60
BGP	454.5 ± 222.0	0.48 ± 0.34
CHR	764.3 ± 45.5	17.40 ± 7.36
COR	NT	NT
DAA	425.6 ± 111.8	1.98 ± 1.52
DAP	397.1 ± 149.5	2.27 ± 1.15
FLA	94.8 ± 38.7	19.70 ± 5.17
FLU	NT	17,100.00 ± 8410
PHE	NT	2,680.00 ± 286
PYR	121.3 ± 16.05	22.65 ± 15.0
TRI	NT	NT

Table 4.1. Toxicity of 16 intact PAHs to *D. magna* under SSR presented as ET50 and EC50 for immobilization.
NT: non-toxic. Abbreviations are as follows: anthracene (ANT), benz[a]anthracene (BAA), benzo[a]pyrene (BAP), benz[b]anthracene (BBA), benzo[b]fluorene (BBF), benzo[e]pyrene (BEP), benzo[g,h,i]perylene (BGP), chrysene (CHR), coronene (COR), dibenz[a,h]anthracene (DAA), dibenzo[a,i]pyrene (DAP), fluoranthene (FLA), fluorene (FLU), phenanthrene (PHE), pyrene (PYR), triphenylene (TRI).

were also found to be non-toxic by Newsted and Giesy (1987). The fourth, COR, was not assayed by Newsted and Giesy (1987), although it was predicted to be non-toxic by Mekenyan et al. (1994a).

In contrast to the results presented by Newsted and Giesy (1987) BAA, BEP, and FLA were found to be quite toxic, and DAA to be only moderately toxic. It is likely that the contrasting results for BAA, BEP and FLA are due to differences in light source emission spectra. Each of these compounds absorbs strongly in the UVB region. Newsted and Giesy (1987) did not use wavelengths below 312 nm. However, the SSR source used contains the full range of UVB wavelengths (290-320 nm). The difference in DAA toxicity may be explained by the 24 h pre-exposure to the experimental solution in their protocol. It is likely in our case, that had this compound been allowed to equilibrate within the organism, similar results would have been observed. The proposed hypothesis is that since this compound is a relatively poor photosensitizer, at a low body concentration it will have less of an impact than a compound such as PYR, which is a good photosensitizer (Krylov et al. 1997).

The EC50 data is spread over a wide range of concentrations (Table 4.1). BGP was the most toxic compound, with an EC50 of 0.48 nM, while COR and TRI were non-toxic. ANT was only moderately toxic to *D. magna*, which is in contrast to data for *L. gibba* (Huang et al. 1997a) and *V. fischeri* (El-Alawi et al. 2002). ANT was the most toxic compound for both of those organisms. Excellent correlation was observed between *L. gibba* and *V. fischeri* toxicity (El-Alawi et al. 2002), although in this study *D. magna* ET50 toxicity correlated poorly with *L. gibba* toxicity and *V. fischeri* toxicity (Table 4.2). This might be attributed to the nature of the uptake of the compounds, and effects of the

Variables	r^2	p
D. magna ET50 vs. *L. gibba* Toxicity	.235	0.110
D. magna ET50 vs. *V. fischeri* Toxicity	.265	0.087
D. magna ET50 vs. PSF_{LG}	.140	0.232
D. magna ET50 vs. PMF_{LG}	.0004	0.953
D. magna EC50 vs. PSF_{LG}	.240	0.072
D. magna EC50 vs. PMF_{LG}	.004	.835

Table 4.2. Regression data for analyses not graphically represented.
All regressions were performed on $\log_{10}$-transformed relative toxicity data. For *D. magna* EC50, and ET50 data, values were inverted to keep a positive relationship to toxicity.

irradiation source on the organisms. *L. gibba* is a static organism, floating on top of the test solution. Uptake occurs via equilibration of the compound into the organism (Krylov et al. 1997). *D. magna* are non-static organisms that move within the water column, and several mechanisms could contribute to the observed differences in toxicity. In contrast to *L. gibba*, the movement of *D. magna* neonates within the test solution could facilitate chemical uptake through exposure to a greater volume of the solution. This could occur dermally, and as the test solution passes through the gill filaments as well as through the gut during feeding. When combined with the huge differences in K_{OW} between a smaller PAH such as ANT, and larger PAHs such as BGP, the described exposure effect would likely result in greater bioaccumulation of the large PAHs by *D. magna*. The fact that many of these larger compounds are the most toxic to *D. magna* supports this hypothesis. Secondly, *D. magna* actively acquire oxygen through a gill filament system. An increase in both surface area exposure, as well as overall volume of test solution, would likely result in greater chemical uptake than would be the case for *L. gibba*. Finally, *D. magna* are relatively transparent compared to *L. gibba*, which would likely result in a higher rate of *in vivo* photochemical reactions of the PAHs. This could result in higher toxicity due to a higher availability of target biomolecules for ROS produced through photosensitization. As well, increased localized concentrations of oxyPAHs formed within *D. magna* through photomodification could also result in higher toxicity.

A poor overall correlation was observed between the *D. magna* EC50 and ET50 data (Figure 4.3). Chemicals that are strong photosensitizers (ANT, PYR, and FLA) were more toxic in the ET50 assay, while larger chemicals (BGP, DAA, and DAP) were more toxic in EC50 assays (Figure 4.3). Interestingly, without these two groups of chemicals
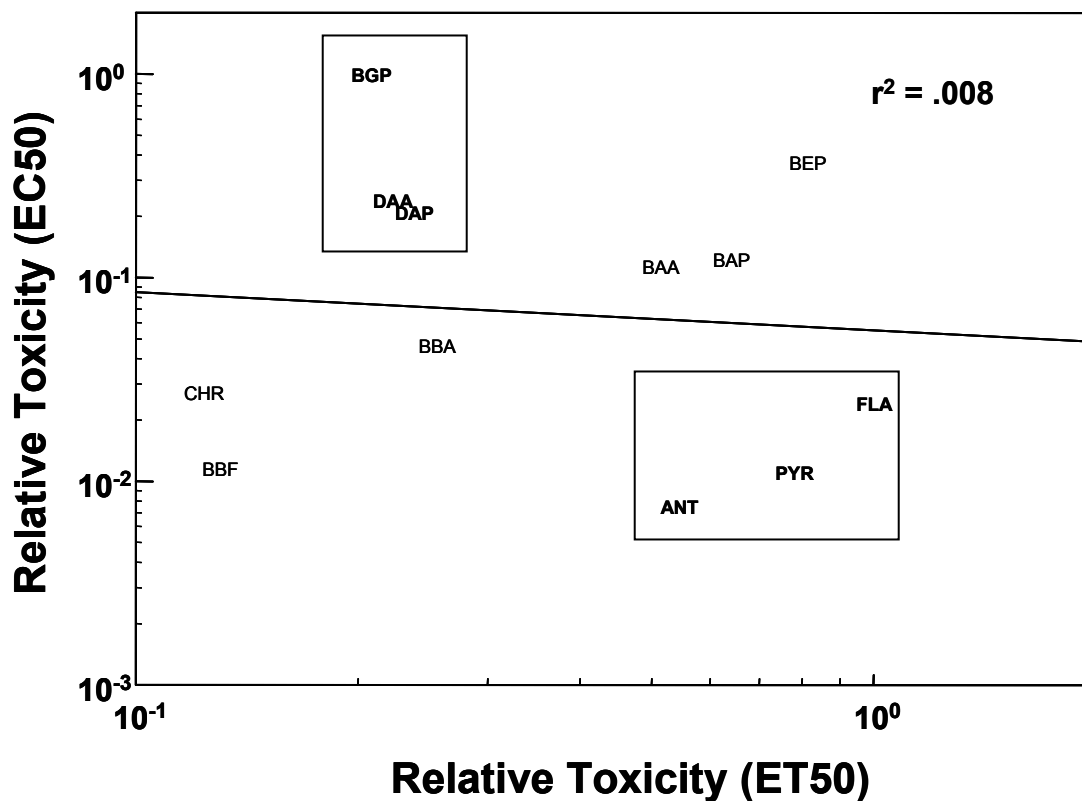
Figure 4.3. Comparison of normalized *D. magna* ET50 data to normalized EC50 data.
Compounds in bold indicate either strong photosensitizers (ANT, FLA, PYR) or large, insoluble compounds (BGP, DAA, DAP) that fall away from an apparent correlation. Abbreviations are as follows: anthracene (ANT), benz[a]anthracene (BAA), benzo[a]pyrene (BAP), benz[b]anthracene (BBA), benzo[b]fluorene (BBF), benzo[e]pyrene (BEP), benzo[g,h,i]perylene (BGP), chrysene (CHR), coronene (COR), dibenz[a,h]anthracene (DAA), dibenzo[a,i]pyrene (DAP), fluoranthene (FLA), fluorene (FLU), phenanthrene (PHE), pyrene (PYR), triphenylene (TRI).

a correlation is evident with several of the compounds. Clearly, a single model will not be adequate in describing toxicity for both sets of data. The *D. magna* ET50 data is similar in metric to the *L. gibba* data, in that both are continuous measurements (growth inhibition, and time) with a single chemical concentration applied. Thus, it is plausible that the *L. gibba* QSAR model will correlate better to the *D. magna* ET50 toxicity data, than EC50 data. Nonetheless, weak correlations are anticipated overall, as the *L. gibba* and *D. magna* toxicity data do not themselves correlate (Table 4.2).

4.3.2 QSAR Model for Photoinduced Toxicity

Previously in our laboratory, a QSAR model based on a bipartite mechanism of photoinduced toxicity was developed for *L. gibba*. The model attributed photoinduced toxicity to two different processes: photosensitization and photomodification. Previous models only used photosensitization as a factor (Newsted and Giesy 1987; Mekenyan et al. 1994b; Mekenyan et al. 1994a). The two factors were found to contribute to toxicity as a sum: a *L. gibba* factor for photosensitization (PSF_{LG}), and a *L. gibba* factor for photomodification (PMF_{LG}) (Equation 4.1). Photosensitization was expressed as a function of assimilation of PAH by *L. gibba* $[C]_L$, the quantum yield for triplet state formation of the PAH (φ), and the integral of the overlap between the light source irradiance spectrum and the test compound absorbance spectrum (*J*). Photomodification was expressed as a function of photomodification rate of the PAH (k_m), and the toxicity of the photoproducts of each PAH (T_{pm}). The values for all terms used in modeling are presented in Table 4.3. The factors were generated by multiplying the terms, after normalization. For those studies (Huang et al. 1997a; Krylov et al. 1997), it was necessary to experimentally generate several of the constants, including $[C_L]$, k_m, and

90

PAH	PSF_{LG}	PMF_{LG}	SUM_{LG}	J^n	φ^n	k_m^n	K_{OW}	K_{OW}^n	Sol (mM)	$(Sol^{-1})^n$	PSF_{DM}	PMF_{DM}	SUM_{DM}
ANT	1.87×10^{-2}	1.00	1.02	1.19×10^{-1}	6.30×10^{-1}	1.00	[a]4.79×10^{4}	3.02×10^{-3}	[a]5.22×10^{-4}	8.93×10^{-4}	7.50×10^{-2}	2.70×10^{-6}	7.50×10^{-2}
BAA	6.06×10^{-3}	4.01×10^{-1}	4.07×10^{-1}	1.90×10^{-1}	8.40×10^{-1}	4.01×10^{-1}	[a]8.13×10^{5}	5.13×10^{-2}	[a]5.69×10^{-5}	8.19×10^{-3}	1.60×10^{-1}	1.68×10^{-4}	1.60×10^{-1}
BAP	3.91×10^{-3}	3.67×10^{-2}	7.58×10^{-2}	6.47×10^{-1}	4.20×10^{-1}	3.75×10^{-2}	[a]1.35×10^{6}	8.51×10^{-2}	[b]7.21×10^{-6}	6.46×10^{-2}	2.72×10^{-1}	2.06×10^{-4}	2.72×10^{-1}
BBA	8.89×10^{-3}	7.27×10^{-2}	8.16×10^{-2}	1.20×10^{-1}	6.80×10^{-1}	7.49×10^{-2}	[b]7.94×10^{5}	5.01×10^{-2}	[b]2.50×10^{-6}	1.87×10^{-1}	8.16×10^{-2}	7.01×10^{-4}	8.23×10^{-2}
BBF	2.31×10^{-2}	1.90×10^{-2}	4.22×10^{-2}	1.50×10^{-1}	5.30×10^{-1}	2.88×10^{-2}	[b]5.62×10^{5}	3.55×10^{-2}	[b]9.25×10^{-6}	5.04×10^{-2}	7.95×10^{-2}	5.15×10^{-5}	7.96×10^{-2}
BEP	3.00×10^{-2}	2.02×10^{-2}	5.02×10^{-2}	2.55×10^{-1}	7.40×10^{-1}	2.59×10^{-2}	[b]2.75×10^{6}	1.74×10^{-1}	[b]1.59×10^{-5}	2.94×10^{-2}	1.89×10^{-1}	1.33×10^{-4}	1.89×10^{-1}
BGP	4.34×10^{-2}	5.24×10^{-3}	4.87×10^{-2}	4.08×10^{-1}	6.30×10^{-1}	2.02×10^{-2}	[a]1.66×10^{6}	1.05×10^{-1}	[a]4.96×10^{-7}	9.40×10^{-1}	2.57×10^{-1}	1.99×10^{-3}	2.59×10^{-1}
CHR	9.56×10^{-3}	2.56×10^{-2}	3.52×10^{-2}	1.12×10^{-1}	7.00×10^{-1}	3.46×10^{-2}	[a]6.46×10^{5}	4.07×10^{-2}	[a]6.57×10^{-6}	7.09×10^{-2}	7.84×10^{-2}	9.99×10^{-5}	7.85×10^{-2}
COR	3.22×10^{-2}	1.11×10^{-2}	4.33×10^{-2}	3.30×10^{-1}	8.40×10^{-1}	2.02×10^{-2}	[c]1.58×10^{7}	1.00	[b]4.66×10^{-7}	1.00	2.77×10^{-1}	2.02×10^{-2}	2.97×10^{-1}
DAA	4.47×10^{-2}	1.54×10^{-2}	6.01×10^{-2}	4.66×10^{-1}	5.30×10^{-1}	1.24×10^{-1}	[b]5.62×10^{6}	3.55×10^{-1}	[b]2.16×10^{-6}	2.16×10^{-1}	2.47×10^{-1}	9.51×10^{-3}	2.56×10^{-1}
DAP	7.47×10^{-2}	2.40×10^{-3}	7.71×10^{-2}	1.00	5.30×10^{-1}	4.90×10^{-2}	[c]2.95×10^{6}	1.86×10^{-1}	[d]1.98×10^{-6}	2.35×10^{-1}	5.30×10^{-1}	2.14×10^{-3}	5.32×10^{-1}
FLA	1.55×10^{-1}	2.40×10^{-3}	1.58×10^{-1}	2.74×10^{-1}	6.30×10^{-1}	4.90×10^{-2}	[b]1.58×10^{5}	1.00×10^{-2}	[b]1.29×10^{-3}	3.63×10^{-4}	1.73×10^{-1}	1.78×10^{-7}	1.73×10^{-1}
FLU	2.44×10^{-2}	1.14×10^{-2}	1.38×10^{-2}	1.00×10^{-2}	3.30×10^{-1}	1.07×10^{-1}	[a]1.51×10^{4}	9.55E-04	[a]1.25×10^{-3}	3.74×10^{-4}	3.30×10^{-3}	3.81×10^{-8}	3.30×10^{-3}
PHE	2.44×10^{-2}	2.07×10^{-2}	4.51×10^{-2}	2.90×10^{-2}	8.40×10^{-1}	1.44×10^{-1}	[a]2.14×10^{3}	1.35E-04	[a]4.62×10^{-3}	1.01×10^{-4}	2.44×10^{-2}	1.96×10^{-9}	2.44×10^{-2}
PYR	5.16×10^{-2}	1.86×10^{-3}	5.34×10^{-3}	2.35×10^{-1}	2.80×10^{-1}	4.32×10^{-2}	[b]1.51×10^{5}	9.55×10^{-3}	[b]6.68×10^{-4}	6.98×10^{-4}	6.58×10^{-2}	2.88×10^{-7}	6.58×10^{-2}
TRI	8.53×10^{-3}	1.01×10^{-3}	9.54×10^{-3}	2.90×10^{-2}	1.00	3.17×10^{-2}	[b]2.82×10^{5}	1.78×10^{-2}	[b]1.88×10^{-4}	2.47×10^{-3}	2.90×10^{-2}	1.40×10^{-6}	2.90×10^{-2}

Table 4.3. Phototoxicity factors and physical constants used for QSAR modeling.
Phototoxicity factors for photosensitization (PSF_{LG}) and photomodification (PMF_{LG}) and the sum, were obtained from Huang et al. (1997a). Individual terms used for the calculation of the modified PSF (PSF_{DM}), modified PMF (PMF_{DM}) and their sum (SUM_{DM}) are as follows: J^n represents the normalized absorption of simulated solar radiation (SSR) by the PAH ; φ^n is the normalized quantum yield for triplet state formation ; k_m^n is the normalized photomodification rate (Huang et al. 1997a). K_{OW} is the octanol/water partition coefficient, and Sol is the solubility in water. Please see individual compounds for references for K_{OW} and Sol. K_{OW}^n is K_{OW} normalized to the highest value, and $(Sol^{-1})^n$ is the inverse of solubility, normalized to the highest value. PSF_{DM} is the product of k_m^n, K_{OW}^n, and $(Sol^{-1})^n$. SUM_{DM} is the sum of PSF_{DM} and PMF_{DM}. a – from de Maagd et al. (1998); b – from Mackay et al. (1992); c – from Güsten et al. (1991); d – from OSPAR (2002).

T_{pm}, while φ was available from the photochemistry literature, and J was calculated from the spectral data. These constants were used in this study.

The full bipartite model seen in Equation 4.3 was explanatory, rather than predictive of inhibition of growth in *L. gibba*; several of the variables had to be generated experimentally. In a later study, the model was found to be highly predictive of long-term toxicity to *V. fischeri* without any alteration (El-Alawi et al. 2002). Thus, one goal was to use this model to test for additional inter-species predictive capabilities using *D. magna* as the test organism.

The initial step in this study was to determine whether a correlation existed between the *L. gibba* model and the toxicity data generated for *D. magna*. However, because the *L. gibba* toxicity data and the *D. magna* were not correlated (Table 4.2), it was not anticipated that the *L. gibba* model would be highly predictive of PAH photoinduced toxicity to *D. magna*. Indeed, upon analysis, the PSF_{LG} and PMF_{LG} neither independently (Table 4.2) nor additively correlated to the *D. magna* EC50 toxicity data. The sum of the two factors resulted in the best correlation (Figure 4.4A), as was the case in the previous studies (Huang et al. 1997a; El-Alawi et al. 2002). Clearly, there is little correlation between the Huang et al. (1997a) constants and *D. magna* toxicity as EC50 (Table 4.2, Figure 4.4A).
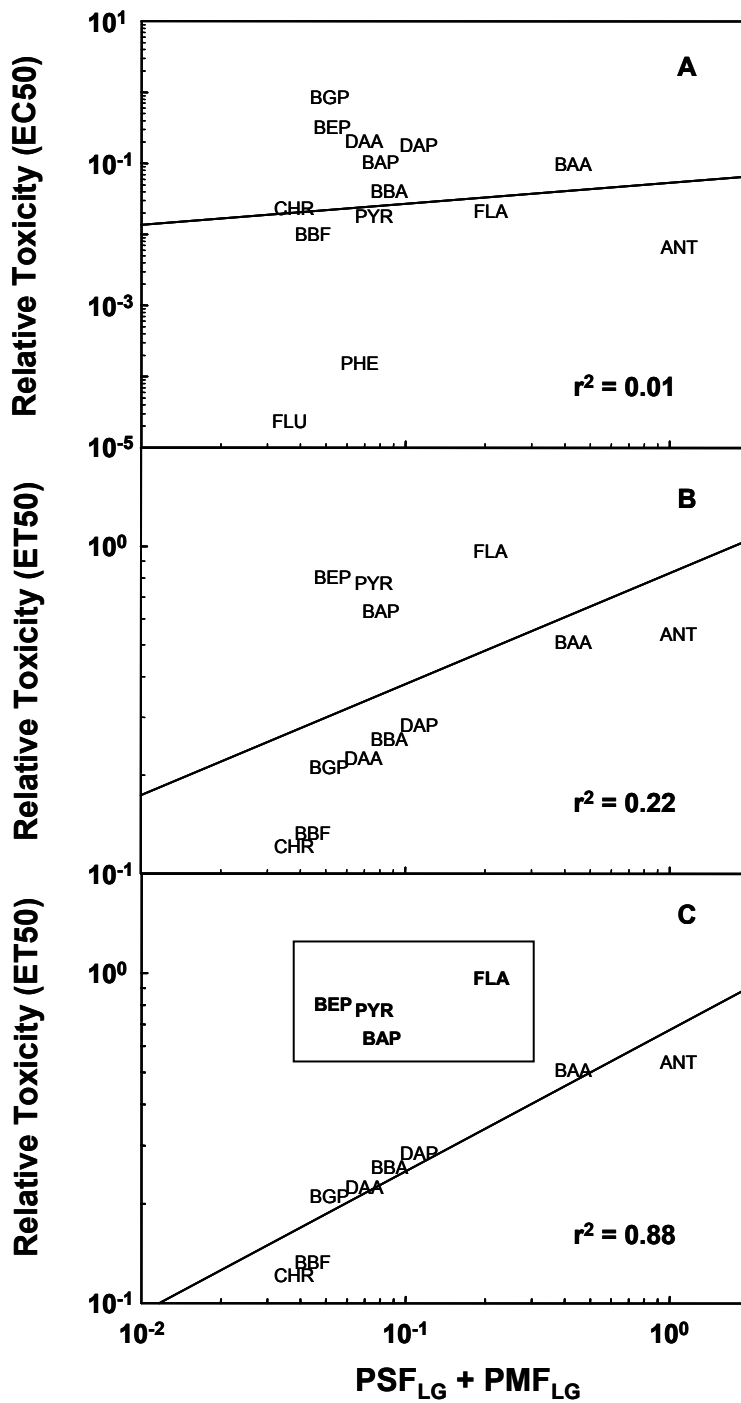
Figure 4.4. Toxicity of intact PAHs to *D. magna* compared to the sum of the PSF$_{LG}$ and PMF$_{LG}$.
Toxicity data as EC50 or ET50 were normalized from 0 to 1, and plotted against the PSF. A. Toxicity as EC50. B. Toxicity as ET50. C. Toxicity as ET50, with four outlying compounds (in bold) removed.

Further analysis of the *D. magna* ET50 toxicity data did not reveal a clear correlation using the PSF$_{LG}$ and PMF$_{LG}$ independently (Table 4.2). There also does not appear to be a correlation to the sum of the factors (Figure 4.4B). However, if four compounds that appear to be outliers are removed (BAP, BEP, FLA and PYR), an excellent correlation was found (Figure 4.4C). These four outliers are the four most toxic compounds as assessed via the ET50 assay (Table 4.1). Thus, while a correlation is clear, and the *L. gibba* QSAR model does appear to be appropriate for the ET50 data, it falls short of true prediction, since the toxicities of the most toxic PAHs are underestimated.

4.3.2.1 Adaptation of the L. gibba *QSAR Model to* D. magna

This QSAR model developed for *L. gibba* was not predictive of toxicity in *D. magna* as measured by EC50, and was only moderately successful for the ET50. Some correlation was expected with the ET50 data, since toxicity data at a single concentration was predicted successfully with the *L. gibba* model (Huang et al. 1997a; El-Alawi et al. 2002). However, the underestimation of the most toxic compounds to *D. magna* (as measured by ET50) was a serious shortcoming of the *L. gibba* QSAR. It was postulated that some of the constants in the Huang model (Huang et al. 1997a) developed for *L. gibba*, were not appropriate for *D. magna*. First, it was suspected that differences in PAH uptake between these two organisms resulted in differences in relative toxicity. This means the *L. gibba* PSF (PSF$_{LG}$) will not be useful for *D. magna*. Second, oxyPAHs have markedly different levels of toxicity to *D. magna* and *L. gibba* (Mallakin et al. 1999; Lampi et al. 2005). This led us to believe that the *L. gibba* PMF (PMF$_{LG}$) was not appropriate for *D. magna*. This implied that alterations were necessary in the *L. gibba* QSAR model. The

approach taken was to alter the model to account for differences in the ways that *L. gibba* and *D. magna* interact and respond to PAHs.

4.3.2.2 Generation of a D. magna *Photosensitization Factor (PSF_DM)*

The *L. gibba* PSF (PSF$_{LG}$) incorporates a term for assimilation of PAHs into the plants ([C]$_L$). It was desirable to replace this term with a property that was not species-specific. Alternatives included *D. magna* bioconcentration factors, although standard, non-specific terms (e.g., K$_{OW}$) would be preferable; they would make the new model less organism-specific. Huang et al. (1997a) stated that the octanol-water partition coefficient (K$_{OW}$) could be used as an alternative variable. Generally, K$_{OW}$ is presented as a logarithm (log K$_{OW}$), however the untransformed value, normalized to the highest value was used. Use of the logarithmic value would have masked the wide range of the toxicity data, which covered several orders of magnitude (Table 4.1). Subsequent replacement of *L. gibba* uptake ([C]$_L$) with K$_{OW}$ in the PSF resulted in excellent correlation to the *D. magna* EC50 toxicity data (r^2 = 0.83, p< 0.0001; data not shown). However, elimination of uptake (Equation 4.4) resulted in an even better PSF (designated PSF$_{DM}$) with an improved fit to the EC50 data (r^2 = 0.86, p < 0.0001; Equation 4.5).

$$\text{Toxicity} = \text{PSF}_{DM} = f\{J, \varphi\} \tag{4.4}$$

$$\log \text{Toxicity}(\text{EC50}^{-1}) = 0.56 + 2.13 \log(\text{PSF}) \tag{4.5}$$

The correlation is evident in Figure 4.5A, and it is interesting to note that chemicals farther from the line, such as PHE and DAP are poor photosensitizers.

Figure 4.5. Toxicity of PAHS to *D. magna* as EC50 plotted versus PSF$_{DM}$ (A), PMF$_{DM}$ (B), and their sum (C). Normalized toxicity data (as in Fig. 4.3) were plotted against each factor and their sum.

The high degree of correlation after removal of uptake as a contributor to the PSF indicates that photosensitization does not appear to be an uptake-dependent process in *D. magna*.

The gill filament of *D. magna* is the expected site of uptake, and gill cells are highly susceptible to PAH photosensitization (Schirmer et al. 1998). Whereas passive uptake was an important factor in *L. gibba* and *V. fischeri* (Huang et al. 1997a; El-Alawi et al. 2002), locomotion of neonates in the test solution likely facilitates rapid accumulation of toxic levels of PAHs in the gill filament of *D. magna*. Consequently, toxicity is almost completely described by the photon absorption (J) and quantum yield (φ) factors.

A correlation was not observed with the ET50 data and PSF_{DM} (Figure 4.6A). This is not unexpected, due to the lack of correlation between the ET50 data and the EC50 data (Figure 4.3). This is perhaps due to the exclusion of uptake. Indeed, when both solubility, and K_{OW} were included in the PSF_{DM}, a modest fit was present (data not shown). Similar observations were made by Newsted and Giesy (1987), and Mekenyan et al. (1994b). They found that lowest triplet energy, and HOMO-LUMO gap, respectively, both correlated well with photoinduced toxicity of PAHs to *D. magna*, only after adjustments were made to account for uptake.

4.3.2.3 Generation of a D. magna *Photomodification Factor (PMF_{DM})*

Huang et al. (1997a) generated a factor for activity of photomodified PAHs (T_{PM}) by using toxicity values of PAHs following their photooxidation to form oxyPAHs. This term was combined with the photomodification rate (k_m) to give a PMF_{LG}. The PMF_{LG} correlated modestly with *L. gibba* PAH photoinduced toxicity. However, the
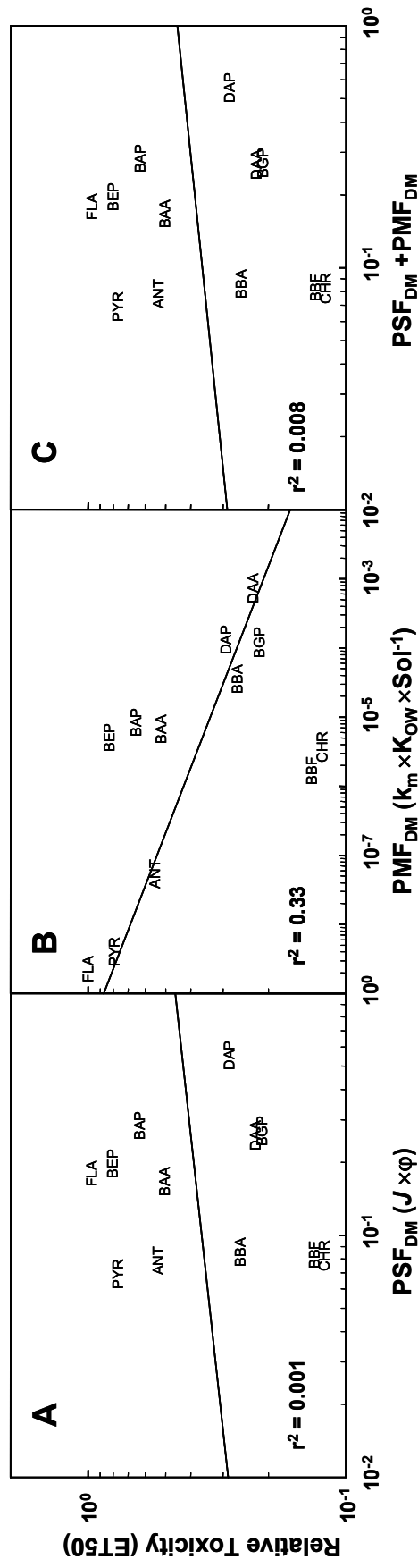
Figure 4.6. Toxicity of PAHS to *D. magna* as ET50 plotted against a PSF$_{DM}$ (A), a PMF$_{DM}$ (B), and their sum (C). Normalized toxicity data (as in Fig. 4.3) were plotted against each factor and their sum.

98

use of the PMF$_{LG}$ was not predictive of either the ET50s or EC50s for *D. magna* (Table 4.2). Huang et al. (1997a) used a high PAH concentration (2 mgL^{-1}) in the experimental solution to generate the T$_{PM}$ factor for photoproduct toxicity. This corresponds to a range of PAH concentrations from 6.6 to 12 μM, which is between 10 and 1000 times greater than 12 of the 14 *D. magna* EC50s, and more than 10 times greater than the concentration used to generate the ET50s (300 nM). It was postulated that the concentration of the PAHs used in generating both sets of *D. magna* toxicity data used here, was not high enough to generate toxic levels of PAH photoproducts (oxyPAHs) in the test solution. However, accumulation of intact PAHs by the organism, and subsequent photomodification within the organism could result in high, localized concentrations of oxyPAHs. Further, accumulation would likely occur at the gill filament, which is rich in mitochondria, the function of which, is known to be disrupted by several oxyPAHs (Babu et al. 2001; Xia et al. 2004). This could result in toxicity to *D. magna*. For this reason an uptake factor for the intact PAHs was incorporated into the PMF (PMF$_{DM}$).

An alternative strategy for improving the PMF$_{LG}$ would have been to generate a *Daphnia*-specific photoproduct toxicity variable. However, as this term is organism-specific, its use was avoided to maintain a non-species-specific model. It has also been demonstrated that oxyPAHs are toxic to *D. magna* (Lampi et al. 2005), and *L. gibba* (Mallakin et al. 1999); however, photoproducts that were highly toxic to *L. gibba*, such as 1,2-dihydroxyanthraquinone (1,2-dhATQ) and 2-hydroxyanthraquinone (2-hATQ) demonstrated remarkably little effect in *D. magna* (Mallakin et al. 1999; Lampi et al. 2005). This indicates differences in modes of

action of PAH photoproducts between species, and is a strong argument for the omission of T_{PM} term that was specific for *L. gibba*, as well as avoiding the use of a new species-specific term.

As with the PSF, the base K_{OW} was used, rather than the logarithmic value, to avoid masking the range of toxicity. In addition to adding a term for uptake, water solubility was also incorporated, since both chemical availability and uptake would affect overall toxicity to an organism, particularly in an environmentally relevant scenario. To keep the correlation positive, the inverse of the solubility was used, also normalized. Subsequently, it was found that the inclusion of normalized K_{OW} and solubility in the PMF_{DM} (Equation 4.6, Figure 4.5B), and exclusion of the T_{PM} resulted in a good correlation to the *D. magna* EC50 data ($r^2=0.70$, $p< 0.001$; Equation 4.7).

$$\text{Toxicity} = PMF_{DM} = f\{K_{OW}, Sol, k_m\} \tag{4.6}$$

$$\log \text{Toxicity}(EC50^{-1}) = 0.85 + 0.52 \log(PMF) \tag{4.7}$$

A negative correlation to the *D. magna* ET50 was observed with the PMF_{DM} (Figure 4.6B), to which no conclusion is made.

Daphnia magna are relatively transparent organisms, and it is likely that photomodification can occur *in vivo*. One reason is that the inclusion of K_{OW} and solubility to the PMF_{DM} would account for uptake and photomodification within the organism. This would explain the greater fit when uptake (K_{OW}) and solubility are included in the PMF_{DM}. Indeed, PAHs that have high uptake potential and low solubility, such as DAA and BAP, or high photomodification rates, such as ANT and BAA, lie close to the regression line (Figure 4.5B). Conversely, FLA and PYR, which

are good photosensitizers fall away from the line, and diminish the fit. One explanation for the increased toxicity of some of the larger compounds may be attenuation of UVB by the test solution. Larger PAHs can absorb into the visible region of the solar spectrum. This region is attenuated less by water and the organism itself, and would increase the potential for photoinduced toxicity to occur, since more light at photoactive wavelengths is available. With the subsequent scenario, in which an easily photomodified compound bioaccumulates into a transparent organism, the possibilities for the manifestation of toxicity are evident.

4.3.2.4 Correlation of D. magna *Toxicity Data to the sum of the PSF$_{DM}$ and PMF$_{DM}$*

To determine whether the modified factors (Equations 4.4 and 4.6) would jointly predict toxicity, they were summed as in Equation 4.1. In Figure 4.5C, the terms are treated as equal contributors to toxicity, and together they do not appear to improve correlation compared to the PSF$_{DM}$ alone (Figure 4.5B). Again, the ET50 data correlated poorly with the *D. magna* QSAR (Figure 4.6C). Multiple regression analysis to determine the independent contributions of the PSF$_{DM}$ and PMF$_{DM}$ to toxicity as EC50 revealed an extremely strong correlation (r^2 = 0.92, p < .0001) described by Equation 4.8:

$$\log \text{Toxicity}(\text{EC50}^{-1}) = 0.98 + 1.55 \log(\text{PSF}_{DM}) + 0.22 \log(\text{PMF}_{DM}) \quad (4.8)$$

Both of the terms are significant in this regression (PSF$_{DM}$: p= 0.0002, PMF$_{DM}$: p= .019), and upon observation of the predicted toxicity vs. actual toxicity (Figure 4.7),
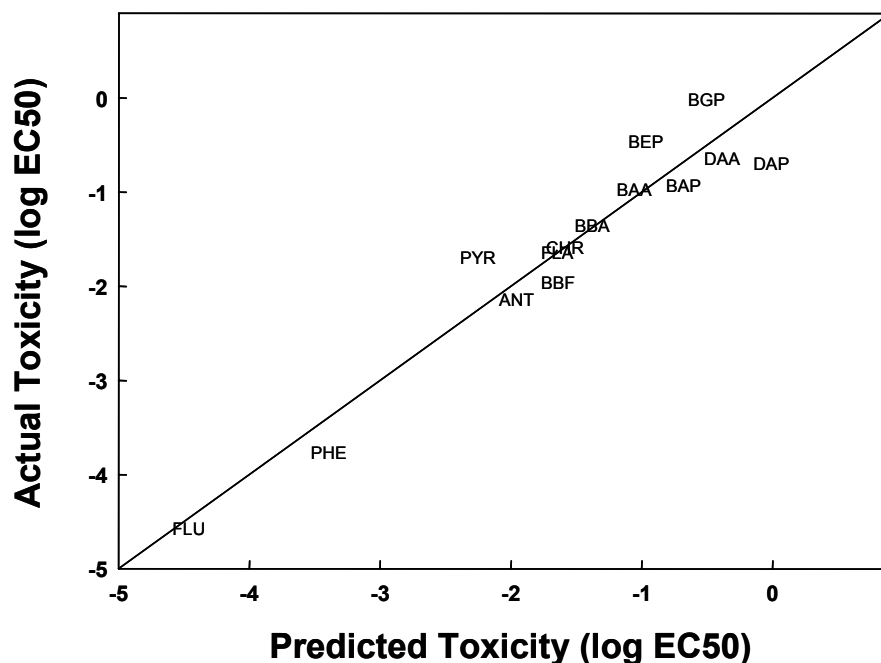
Figure 4.7. Predicted toxicity (log EC50) of PAHs to *D. magna* versus actual toxicity (log EC50).
Predicted toxicity was calculated using Equation 8: log Toxicity(EC50) = 0.98 + 1.55 log(PSF) + 0.22 log(PMF), and plotted against normalized experimental data (Table 4.1). Abbreviations are as follows: anthracene (ANT), benz[a]anthracene (BAA), benzo[a]pyrene (BAP), benz[b]anthracene (BBA), benzo[b]fluorene (BBF), benzo[e]pyrene (BEP), benzo[g,h,i]perylene (BGP), chrysene (CHR), coronene (COR), dibenz[a,h]anthracene (DAA), dibenzo[a,i]pyrene (DAP), fluoranthene (FLA), fluorene (FLU), phenanthrene (PHE), pyrene (PYR), triphenylene (TRI).

the increase in correlation resulting from the sum of the PSF_{DM} and PMF_{DM} is obvious. However, the regression shows that PSF_{DM} is weighted greater than the PMF_{DM}. This is contrary to what was observed in both *L. gibba* and *V. fischeri* (Huang et al. 1997a; El-Alawi et al. 2002), where the PMF had a greater contribution to toxicity. It is possible that several oxyPAHs share similar mechanisms of toxicity in *L. gibba* and *V. fischeri*. In this case, the presence of the T_{PM} term would increase the correlation to the PMF_{LG}, as well as the contribution of the PMF_{LG} to the sum of the two factors. The high weighting of the PSF_{DM} indicates that photosensitization appears to be the greatest contributing factor to *D. magna* toxicity in these assays. It is likely that the high correlation of the PSF_{DM} alone overshadowed the PMF_{DM}, resulting in the lower contribution to the regression. However, the importance of photomodification is evident in Figure 4.5, which illustrates that the addition of the PMF_{DM} did improve correlation. With the high correlation from the PSF alone, which accounted for 86% of the variance in the data ($r^2 = 0.86$), any improvement would be minor. When external factors such as experimental error, generally 5% to 10%, are taken into account, it is evident that an improvement on the correlation due to the PMF_{DM} is meaningful, as this factor removes some of the remaining unexplained variance.

Strikingly, despite the apparent lack of fit of the ET50 data to the sum of the PSF_{DM} and PMF_{DM}, multiple regression analysis reveals a moderate, though significant fit ($r^2 = .581$, $p = .02$; Equation 4.9):

$$\log \text{Toxicity}(ET50^{-1}) = -2.65 + 0.64 \log(PSF_{DM}) - 0.19 \log(PMF_{DM}) \quad (4.9)$$

Interestingly, both of the terms are significant in this equation (PSF_{DM}, p = .048; PMF_{DM}, p = .007), although the greater importance of photosensitization in PAH toxicity to *D. magna* is clear. The fact that the contribution of the PMF_{DM} is negative is somewhat perplexing. It is likely that the PAH concentration, which was held constant during the course of the ET50 assays, was not sufficiently high to result in toxic levels of oxyPAHs. Therefore, removal of intact PAH via photomodification, would only act to decrease the effect of photosensitization, and could explain the negative contribution of the PMF_{DM} to the regression. Indeed, these two factors cannot operate concurrently, as PAHs can only photosensitize until they have undergone photomodification (Huang et al. 1997a; El-Alawi et al. 2002). However, the fact that there is in fact a fit, although modest, is encouraging regarding the success of the modified, universal model for photoinduced toxicity of PAHs.

4.4 Conclusions

The photosensitization and photomodification factors (PSF_{LG} and PMF_{LG}) developed for *L. gibba* neither independently nor additively correlated to EC50 data in *D. magna*. A poor correlation of the PSF_{LG} plus the PMF_{LG} to ET50 data was observed, and after removal of four outlying compounds, excellent correlation was seen with the sum of the two factors.

The removal of uptake as a contributor to the PSF_{LG}, and substitution with K_{OW} resulted in improved correlation. Subsequently, the removal of uptake altogether from the equation further improved the correlation, indicating that in *D. magna*,

photosensitization does not appear to be an uptake-dependent process. This is likely due to accelerated chemical uptake via the movement of *D. magna* neonates within the test solution: all chemicals are rapidly bioconcentrated, making the importance of uptake that was observed with *L. gibba* and *V. fischeri* superfluous. This resulted in the complete dependence of the PSF_{DM} on absorbance (J) and quantum efficiency (φ). However, contrary to what was observed in *L. gibba*, where uptake did not play a role in the PMF_{LG}, incorporating K_{OW} and solubility of the intact PAHs resulted in improved correlation to EC50 toxicity data. This is possibly due to a localization effect; with uptake being an important factor, as PAH photomodification *in vivo* could result in toxic oxyPAHs at their sites of action.

The model resulting from the sum of the PSF_{DM} plus the PMF_{DM} successfully predicted the EC50s for *D. magna*. Strikingly, it was also successful, albeit modestly, at predicting toxicity as ET50s, although this was only evident after multiple regression analysis. Indeed, Huang et al. (1997a) hypothesized that modifications might be necessary for application to animal systems. Further, contrary to the original model presented by Huang et al. (1997a), this adapted model was based solely on photophysical descriptors (J, φ, and k_m) and physical properties (K_{OW} and solubility).

This study shows that both the PSF_{DM} and the PMF_{DM} individually predicted PAH toxicity to *D. magna*, although the correlation was higher with the PSF_{DM}, possibly due to the high sensitivity of *D. magna* to reactive oxygen species (ROS) such as singlet oxygen. When the two factors were summed, multiple regression analysis

105

revealed an extremely strong correlation to toxicity. This research further supports

the role of photomodification to the photoinduced toxicity of PAHs, as a

mathematical model was highly predictive of toxicity when a factor for

photomodification was included. Further, it has been shown that a model for

photoinduced toxicity that includes factors for both photosensitization, and

photomodification is able to successfully predict toxicity for multiple species.

Chapter 5

An Application of Structural Equation Modeling to Ecotoxicology: PAH Photoinduced Toxicity as a Test Case

5.1 Introduction

Recent advances in the technological fields related to computing have led to a large increase in the use of sophisticated modeling techniques. The field of ecotoxicology is no different and indeed, there has been a wide applicability of such technology. The use of techniques to predict various properties of chemicals has made use of advances in computing. Many semiempirical and *ab initio* techniqes are used to calculate physical and quantum properties of various chemicals for subsequent use in modeling (Mekenyan et al. 1994a; Chen et al. 2000; Warne et al. 2003; Netzeva et al. 2005). Application of these methods has blossomed, particularly with respect to different types of relationship modeling, such as structure-activity relationships (SAR), quantitative structure-activity relationships (QSAR), and quantitative structure-property relationships (QSPR) (Tuppurainen and Ruuskanen 2000; Ferreira 2001; Altenburger et al. 2003; de Lima Ribeiro and Ferreira 2003; Huuskonen 2003).

There is great interest in techniques that can predict the fate, distribution, and toxic effects of contaminants in the environment. Currently, there are a vast number of chemicals that have not undergone full assessment for environmental risk (Nendza 1998; Cronin et al. 2003). The economic impact of such testing would be

enormous, and researchers are constantly developing and improving methods to predict negative effects of pollutants. The intent being to use predictive modeling to screen potential candidates of concern, and to more comprehensively assess these alone, thereby reducing the overall cost.

A more recent introduction to the field has been the use of complicated modeling techniques, particularly artificial neural network models (ANN) (Kaiser et al. 2002; Kaiser 2003; Niculescu et al. 2004). However, data presentation can be obscure, and interpretation is often difficult for the inexperienced user, and even more so for the inexperienced reader. A complementary technique that has not been widely employed in the biological sciences is structural equation modeling (SEM). This method encompasses many statistical techniques including regression, factor and path analysis. The initial concept of this type of modeling was introduced by Wright (Wright 1934), who derived a manner of mathematically describing correlations and hypotheses regarding causal relationships between traits in guinea pigs. These relationships were represented as path diagrams, leading to the term path analysis. The reintroduction of SEM was described in the early 1970s (Jöreskog 1973), as a combination of path analysis, and factor analysis, which enabled testing of causal claims by comparing the covariance of original data, with that of a hypothesized model (Iriondo et al. 2003). The fundamental null hypothesis is that the covariance of the original data is equal to the covariance of the model, and in contrast to standard statistical technique, the goal is to accept the null hypothesis (Reckhow et al. 2005). Thus, if the model was solved, and the parameters therein estimated with no error,

108

the model covariance would be equal to that of the original data, and the model would not be rejected.

Initially, SEM programming involved complex matrix algebra and variable syntax (Bollen 1989). This syntax has been translated by many statistical packages into the simple construction of diagrams that are pictorially represented as detailed flow charts, or path diagrams (Figure 5.1). The subsequent development of SEM-specific software packages has resulted in the wide use of this technique in psychology, sociology, and economics (Hoyle 1995; Malaeb et al. 2000), and currently, most of these packages are user-friendly (Loehlin 2004).

Structural equation modeling allows for the testing of hypotheses regarding relations between observed and latent (unobserved) variables. It is the use of latent variables wherein lies the strength of this technique. Latent variables are theoretical concepts that unite phenomena under a single term, and can be expressed in terms of directly measured variables (Bollen 1989). With this technique, it is possible to construct theoretical concepts, test their reliability, as well as hypothesize and test theories about their relationships (Malaeb et al. 2000). For example, for photoinduced toxicity of PAHs (Chapter 4), photosensitization, a phenomenon that is not directly observed, but is known to contribute to photoinduced toxicity, could be described in terms of a variety of photodynamic descriptors, and shown to predict toxicity. This is somewhat different than ANN models, which employ hidden layers, or nodes to complete the analysis: SEM modeling allows the user to define the unobserved variables.
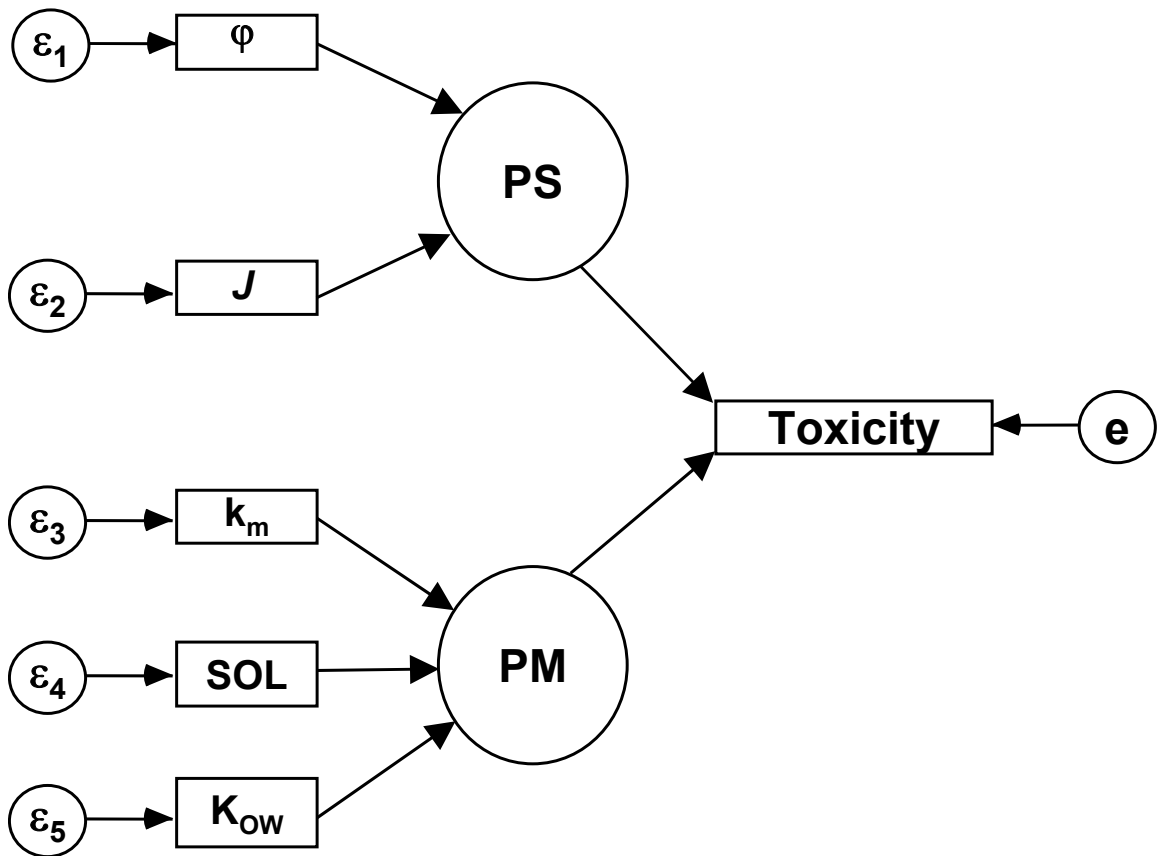
Figure 5.1. Path diagram used in structural equation modeling of photoinduced toxicity of PAHs.
Squares represent observed variables. Circles represent unobserved, latent variables for photosensitization (PS) or photomodification (PM), or error terms (e, and ε_{1-5}). J^n represents the normalized absorption of simulated solar radiation (SSR) by the PAH; φ^n is the normalized quantum yield for triplet state formation; k_m^n is the normalized photomodification rate. K_{OW}^n is K_{OW} normalized to the highest value, and $(Sol)^n$ is the solubility, normalized to the highest value.

Structural equation modeling is becoming increasingly recognized as a useful technique in the biological sciences. Recently, there have been publications employing SEM modeling in the literature in a variety of biological fields (Taylor and Irwin 2004; Wall et al. 2005). In the environmental sciences, Reckhow et al. (2005) employed SEM modeling to identify water quality criteria that predicted the successful function of different bodies of water for pre-determined uses such as availability of habitat, and fisheries production. Taylor and Irwin (2004) were able to evaluate two models for the prediction of the presence of exotic plant species, and employ the better-suited model successfully to different data. These are two prime examples of environmental applications of SEM modeling, an area likely to expand rapidly in the near future.

This chapter expands on the prediction of photoinduced toxicity of PAHs as described in Chapter 4. A novel application of structural equation modeling was used to validate the assumption of a bipartite mechanism of photoinduced toxicity of PAHs. Based on the *D. magna* QSAR in Chapter 4, two latent variables were created to represent the processes of photosensitization and photomodification, respectively. The preceding chapter, and several published works support this view (Huang et al. 1997a; Krylov et al. 1997; El-Alawi et al. 2002; Estrada and Patelwicz 2004). As with that research, physicochemical and photophysical properties of PAHs were hypothesized to contribute to photosensitization and photomodification. In Chapter 4, the former was described by two terms: triplet state quantum efficiency (φ), and the photon absorbance, or the integral of the overlap of the absorbance

111

spectra of the chemicals with the emission spectrum of the irradiation source (J).

Three variables contributed to photomodification: the PAH photomodification rate

(k_m), the aqueous solubility, and the K_{OW} value. Previous models simply utilized the

product of these variables to create factors for each process, and subsequently

determined the relative contribution of each factor to toxicity. The use of SEM will

enable the determination of the relative contribution, or weighting of these properties

to each process individually.

5.2 Materials and Methods

The toxicity data were collected as part of the studies in Chapters 3 and 4 (Table

5.1). *Daphnia magna* 48 h EC50s, as well as ET50s under full spectrum simulated

solar radiation (SSR) were used. Additionally, toxicity data were obtained for *L.*

gibba (Huang et al. 1997a), *Vibrio fischeri* (El-Alawi et al. 2002) as well as other

published data for *D. magna* (Newsted and Giesy 1987). Several of the

physicochemical properties described in Chapter 4 were also employed (Table 5.2).

A model was developed, based on the *D. magna* QSAR presented in Chapter 4.

Two latent (unobserved) variables were set to contribute causally to each of the

toxicity data sets. These latent variables were based on the factors for

photosensitization and photomodification described in Chapter 4. The base model is

described in Figure 5.1. The variables used were as follows: *J*, the integral of the

overlap of the absorption spectrum of the PAH and the spectrum of the irradiance

PAH	$\log(Dm\ \text{EC50}^{-1})_n$	$\log(Dm\ \text{ET50}^{-1})_n$	*Lemna*	*Vf* EC50	*Vf* Inhib	log(NG)
ANT	-2.12	-.256	1.00	1.00	1.00	-.208
BAA	-.946	-.281	.745	.724	.933	-.608
BAP	-.913	-.185	.255	.227	.338	-.159
BBA	-1.33	-.576	.259	.231	.358	-.726
BBF	-1.94	-.864	.354	.166	.402	-.861
BEP	-.435	-.081	.165	.123	.234	-.695
BGP	0.00	-.660	.139	.011	.132	-.651
CHR	-1.56	-.902	.016	.002	.020	-.891
COR	NT	NT	.118	.002	.039	NA
DAA	-.620	-.635	.085	.150	.137	0.00
DAP	-.679	-.532	.458	.143	.410	NA
FLA	-1.62	0.00	.580	.210	.543	-.545
FLU	-4.56	NT	.160	.117	.185	NA
PHE	-3.75	NT	.104	.067	.136	NA
PYR	-1.68	-.100	.170	.101	.211	-.052
TRI	NT	NT	.071	.002	.047	NA

Table 5.1. Toxicity data for 16 intact PAHs to various organisms for use with structural equation modeling.
D. magna as $\log(\text{ET50}^{-1}_n)$ and $\log(\text{EC50}^{-1}_n)$ for immobilization (from Chapter 4), *L. gibba* (*Lemna*), presented as inhibition of growth (Huang et al. 1997a), and *V. fischeri* presented as inhibition of luminescence, and EC50 for inhibition of bioluminescence (El-Alawi et al. 2002). A second set of *D. magna* ET50s was obtained from Newsted and Giesy (1987), and presented identically to the other ET50 data [log(NG)]. Abbreviations are as follows: anthracene (ANT), benz[a]anthracene (BAA), benzo[a]pyrene (BAP), benz[b]anthracene (BBA), benzo[b]fluorene (BBF), benzo[e]pyrene (BEP), benzo[g,h,i]perylene (BGP), chrysene (CHR), coronene (COR), dibenz[a,h]anthracene (DAA), dibenzo[a,i]pyrene (DAP), fluoranthene (FLA), fluorene (FLU), phenanthrene (PHE), pyrene (PYR), triphenylene (TRI). NG: Newsted and Giesy, NT: non-toxic, NA: not assayed.

PAH	J^n	φ^n	$k_m{}^n$	$K_{OW}{}^n$	$(Sol)^n$
ANT	1.19×10^{-1}	6.30×10^{-1}	1.00	3.02×10^{-3}	8.93×10^{-4}
BAA	1.90×10^{-1}	8.40×10^{-1}	4.01×10^{-1}	5.13×10^{-2}	8.19×10^{-3}
BAP	6.47×10^{-1}	4.20×10^{-1}	3.75×10^{-2}	8.51×10^{-2}	6.46×10^{-2}
BBA	1.20×10^{-1}	6.80×10^{-1}	7.49×10^{-2}	5.01×10^{-2}	1.87×10^{-1}
BBF	1.50×10^{-1}	5.30×10^{-1}	2.88×10^{-2}	3.55×10^{-2}	5.04×10^{-2}
BEP	2.55×10^{-1}	7.40×10^{-1}	2.59×10^{-2}	1.74×10^{-1}	2.94×10^{-2}
BGP	4.08×10^{-1}	6.30×10^{-1}	2.02×10^{-2}	1.05×10^{-1}	9.40×10^{-1}
CHR	1.12×10^{-1}	7.00×10^{-1}	3.46×10^{-2}	4.07×10^{-2}	7.09×10^{-2}
COR	3.30×10^{-1}	8.40×10^{-1}	2.02×10^{-2}	1.00	1.00
DAA	4.66×10^{-1}	5.30×10^{-1}	1.24×10^{-1}	3.55×10^{-1}	2.16×10^{-1}
DAP	1.00	5.30×10^{-1}	4.90×10^{-2}	1.86×10^{-1}	2.35×10^{-1}
FLA	2.74×10^{-1}	6.30×10^{-1}	4.90×10^{-2}	1.00×10^{-2}	3.63×10^{-4}
FLU	1.00×10^{-2}	3.30×10^{-1}	1.07×10^{-1}	9.55E-04	3.74×10^{-4}
PHE	2.90×10^{-2}	8.40×10^{-1}	1.44×10^{-1}	1.35E-04	1.01×10^{-4}
PYR	2.35×10^{-1}	2.80×10^{-1}	4.32×10^{-2}	9.55×10^{-3}	6.98×10^{-4}
TRI	2.90×10^{-2}	1.00	3.17×10^{-2}	1.78×10^{-2}	2.47×10^{-3}

Table 5.2. Phototoxicity factors and physical constants used for structural equation modeling.
All factors were taken from Chapter 4. J^n represents the normalized absorption of simulated solar radiation (SSR) by the PAH; φ^n is the normalized quantum yield for triplet state formation; $k_m{}^n$ is the normalized photomodification rate. $K_{OW}{}^n$ is K_{OW} normalized to the highest value, and $(Sol)^n$ is the solubility, normalized to the highest value.

source; φ, the triplet state quantum yield, K_{OW}, the octanol-water partition coefficient; Sol, aqueous solubility; k_m, photomodification rate. It should be noted that the inverse of solubility was not used in the SEM presented in this chapter. While it was appropriate for prediction of toxicity in the QSAR, this term did not allow model convergence for several of the data sets using SEM.

Structural equation modeling was used to explore the contributions of the observed variables to each of the latent variables, which subsequently account for a portion of the variance of toxicity. The base path diagram used for analysis is illustrated in Figure 5.1. This diagram was input into Amos 4.0 (Amos Development Corp., Spring House, PA, USA) SEM software, using the graphical user interface. Data was entered, and linked to the path diagram with SPSS 11.0 (SPSS Inc., Chicago, IL, USA). Analysis was performed for all data sets via maximum likelihood (ML) estimation in Amos 4.0, and model parameters were subsequently estimated. The ML method has been shown to be accurate with smaller data sets (n<100), as is the case for all of the toxicity data sets (Loehlin 2004). Goodness of fit indices were calculated concurrently to the parameter estimation, with Amos 4.0.

5.3 Results and Discussion

There are several steps involved in the basic SEM procedure; included in these are specification of the model, parameter estimation and assessment of model fit. Specification of the model involves the development of the path diagram that will form the main model. Parameter estimation is the application of the software to

compute the model, and subsequent generation of a series of estimates for the paths and variables. Goodness of fit must then be analyzed using a variety of different indices, assuming the model has indeed converged, and a solution computed.

5.3.1 Model Specification

In this study, a model was adapted from the QSAR described in Chapter 4. This path diagram of the SEM is represented in Figure 5.1. The assumption of the bipartite mechanism of toxicity led to the utilization of two latent, unobserved constructs. These are represented as circles, with one construct representing photosensitization (PS), and the second, photomodification (PM). Both of these processes are known to contribute to photoinduced toxicity of PAHs (Newsted and Giesy 1987; Mekenyan et al. 1994b; Huang et al. 1997a; Krylov et al. 1997; Estrada and Patelwicz 2004). As with the QSAR model from Chapter 4, each of the observed variables account for a part of the designated latent construct. These constructs were designed so that the variables loading on to each mimicked the factors from the *D. magna* QSAR. Thus, φ and *J* were set to contribute to PS, and k_m, solubility, and K_{OW} were set to contribute to PM. Each latent variable was then set to contribute to photoinduced toxicity of PAHs, as given in each of the data sets.

5.3.2 Estimation of Model Parameters

Parameters were estimated for each of the six sets of toxicity data (Figures 5.2 and 5.3). The numbers on the paths from the observed variables to the latent

116

variables represent the percentage of the contribution of the respective observed variable, to the variance of the latent variable. The numbers on the paths from the latent variables to the toxicity, represent the absolute contribution of the respective latent variable to the r^2 value, as indicated. Thus, the sum of the values from the two latent variables is equal to the r^2 value.

In Figure 5.2, the estimated parameters for the toxicity data for *D. magna* from Chapter 4, along with another set of *D. magna* ET50 data obtained from Newsted and Giesy (1987) are presented. A large portion of the variance (i.e. high r^2) was accounted for with all three sets of data. That of Newsted and Giesy exhibited the highest r^2 value (0.96, Figure 5.2), with the ET50 data and the EC50 data following, with r^2 values of 0.87 and 0.80 respectively.

The *D. magna* EC50 had a slightly weaker correlation than either set of ET50 data (Figure 5.2). However, in this case, and unlike the *D. magna* ET50 toxicity data, the PS and PM variables contributed similarly to explaining the variance in toxicity. This reflects the QSAR model presented in Chapter 4, which suggested that photosensitization is an important mechanism of PAH phototoxicity to *D. magna* in EC50 assays. Both *J* and φ contribute strongly to PS, indicating that photon absorbance, and triplet state quantum efficiency are important descriptors in this case. Solubility and K_{OW} accounted for the majority of PM, which agrees with the *D. magna* QSAR model in Chapter 4, which required both of these variables to enable prediction of toxicity.
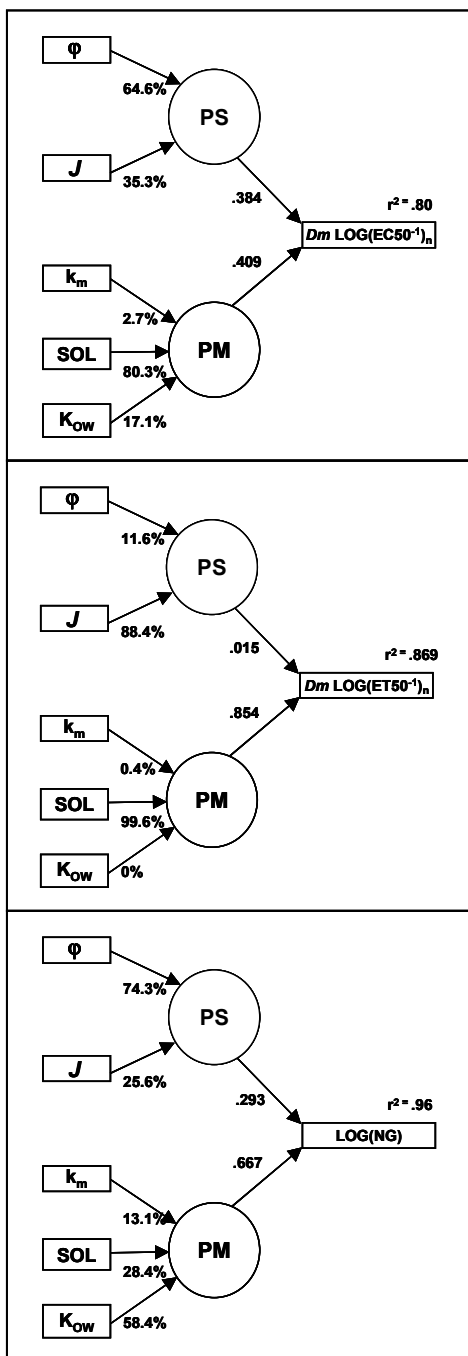
Figure 5.2. Parameter estimations for the SEM of photoinduced toxicity of PAHs to _D. magna_.
Percentages represent contribution of the corresponding factor to the variance explained by the latent variables for photosensitization (PS) or photomodification (PM). Values on the path from latent variable to toxicity represent absolute contribution to the r^2 value for toxicity. For abbreviations, see Table 5.2.

Figure 5.3. Parameter estimations for the SEM of photoinduced toxicity of PAHs to *L. gibba* and *V. fischeri*.
Percentages represent contribution of the corresponding factor to the variance explained by the latent variables for photosensitization (PS) or photomodification (PM). Values on the path from latent variable to toxicity represent absolute contribution to the r^2 value for toxicity. For abbreviations, see Table 5.2.
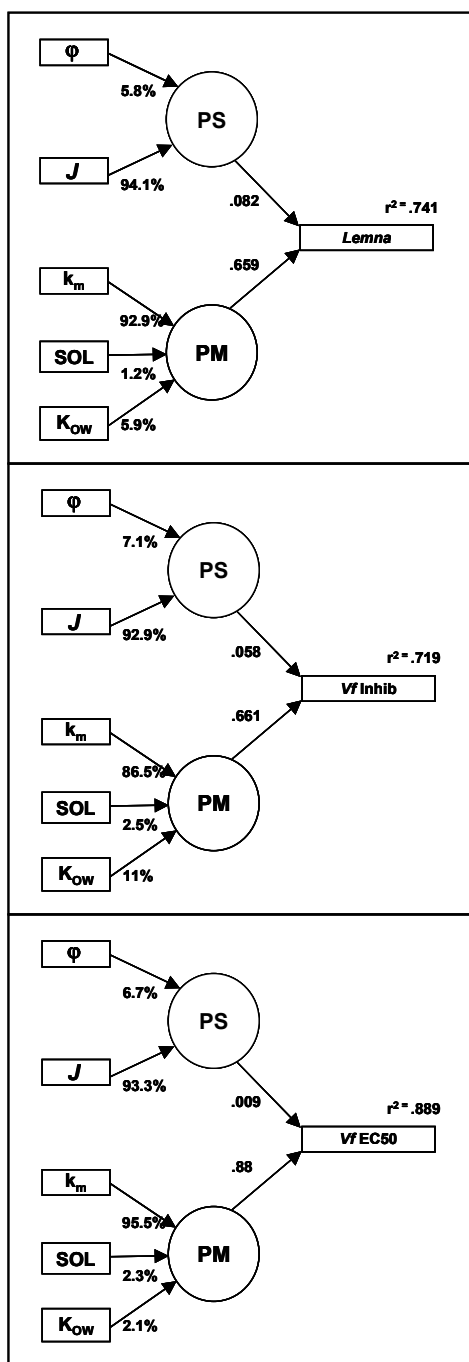
In each set of ET50 data (Figure 5.2), the PM variable is the greater contributor to the overall correlation of the model. K_{OW} and solubility account for over 90% of the contribution to PM with the data from Newsted and Giesy (1987), while solubility is almost the sole contributor to PM with the ET50 data from Chapter 4. Both of these results suggest that uptake factors are extremely important in the manifestation of toxicity to *D. magna* via photomodification within the animal in this type of continuous assay. These results also illustrate the flexibility of this type of modeling. The *D. magna* QSAR model from Chapter 4 was only moderately predictive of the ET50. Further, the PMF_{DM}, which was the product of the contributing variables, had a negative contribution to the correlation. With the SEM able to freely determine the contribution of the descriptors to PM, a greater amount of the variance was explained (*D. magna* QSAR: $r^2 = 0.581$; SEM: $r^2 = 0.869$).

The two descriptors of PS, *J* and φ, vary in contribution between the data sets. With ET50 data from Newsted and Giesy (1987), φ contributes highly to PS. This may be due to differences in irradiation source emission spectra between data sets; Newsted and Giesy (1987) filtered wavelengths below 312 nm, while the variable *J* was generated with an irradiance source including UV wavelengths down to 290 nm. Thus, it is not surprising that φ is the greater contributing variable to the Newsted and Giesy (1987) data.

In their work, Newsted and Giesy (1987) were not able to facilely discern a correlation to toxicity with their chosen photodynamic descriptors, and the use of a hyperbolic model was required. This is perhaps because they did not account for

photomodification. Estrada and Patelwicz (2004) argued that a sole contributor to toxicity such as photosensitization was unlikely. Indeed the model presented in Figure 5.2 illustrates that PM contributed more to toxicity than PS. It is noteworthy that although using a different method, Newsted and Giesy (1987) were able to improve their model after incorporating PAH uptake. Two variables that would be important in chemical uptake, K_{OW} and solubility are present in the PM term. Interestingly, the photomodification rate (k_m) did not contribute greatly to the PM term for any *D. magna* toxicity data set. This further indicates that general uptake is an important descriptor for photomodification as a mechanism of PAH photoinduced toxicity to *D. magna*.

The toxicity data used for the parameter estimation in Figure 5.3 was obtained from studies on the photoinduced toxicity of PAHs to *L. gibba* (Huang et al. 1997a), and *V. fischeri* (El-Alawi et al. 2002). In these studies, an explanatory QSAR model was developed for the *L. gibba* data, which was subsequently found to be predictive of toxicity as inhibition of bioluminescence in *V. fischeri*. The SEM (Figure 5.3) accounted for less variance in the toxicity for both the *L. gibba* data ($r^2 = 0.741$), and the *V. fischeri* inhibition data ($r^2 = 0.719$) relative to the *D. magna* data. However, it is encouraging that the SEM was indeed capable of accounting for a large portion of the variance in these data sets. The lower r^2 values for the *L. gibba* data and the *V. fischeri* inhibition data compared to the *D. magna* data could be attributed to the omission of a factor for uptake in PS, as well as the factor for toxicity of photoproducts from PM. Both of these variables were required in the *L. gibba* QSAR.

121

An excellent r^2 value of 0.889 was determined for the *V. fischeri* EC50 data, again with a high contribution of k_m and the PM term.

With each set of estimates in Figure 5.3, PS had a minor contribution to toxicity compared to PM. This is perhaps due to the mechanism of uptake, which is passive in the case of *L. gibba*, and could be due to the exclusion of an uptake-related variable from PS. It is clear that for both organisms, the photomodification rate was the highest contributing descriptor to PM, and thus toxicity. This is in contrast to *D. magna* in which uptake-related factors were the greater contributors to toxicity.

An argument can be made that SEM, as a sophisticated iterative modeling technique, could compute a solution to any data set given enough observed variables. However, it should be noted that not all of the variables used in the *D. magna* QSAR model in Chapter 4 were applicable to SEM. The QSAR model employed the inverse of solubility (sol^{-1}) as part of the PMF_{DM}, in order to keep a positive correlation to toxicity. The intent was originally to use sol^{-1} in the SEM. However, after model estimation with this term included, several of the data sets did not converge. This is important in that it provided evidence that not all variables are appropriate, as might be interpreted after observing the success of the estimations illustrated in Figures 5.2 and 5.3. One might postulate that unlike the QSAR model, in which the PMF_{DM} was a product of the variables, the extreme difference in values between K_{OW} and sol^{-1} precluded SEM convergence. However, the success that was evident with the use of solubility indicates the importance of the inclusion of this

Data Set	χ^2 Value	df	p-value	NNFI	IFI
$\log(Dm\ EC50^{-1}_n)$	8.13	10	0.616	1.048	1.02
$\log(Dm\ ET50^{-1}_n)$	8.15	10	0.614	1.059	1.024
Lemna	8.13	10	0.616	1.050	1.021
Vf Inhib	8.13	10	0.616	1.050	1.021
Vf EC	8.13	10	0.616	1.045	1.019
$\log(NG)$	8.13	10	0.616	1.047	1.02

Table 5.3. Goodness of fit indices for the structural equation model of photoinduced toxicity of PAHs to various organisms.
df: degrees of freedom; NNFI: nonnormed fit index; IFI: incremental fit index. Index values >0.9 are considered acceptable, while p values >0.05 are desirable (Bollen 1989).

variable in the SEM. These results are highly encouraging for the applicability of this

type of modeling. With each data set, a good deal of the variance was accounted for,

with an r^2 value of 0.719 (71.9%) at the low end of the range. This was

accomplished not only across a range of organisms, but with data of different

metrics: ET50, EC50, inhibition of growth, and inhibition of luminescence.

5.3.3 Determination of Model Fit

To determine whether a model fits a given data set, a goodness of fit test is

performed. Generally, the test statistic is presented as a χ^2 value, and in contrast to

that generally expected, a significant test indicates that the model is a poor fit to the

data. A non-significant value indicates that the covariance pattern predicted by the

model is not distinct from the observed pattern, and thus that the model fits.

However, it is generally accepted that the χ^2 value for goodness of fit should be

interpreted with caution, and supplemented with other indices when sample sizes

are small (Bollen 1989). Two indices of fit that have been extensively analyzed for

SEM application, and have been recommended for use are the nonnormed-fit index

(NNFI), and incremental fit index (IFI) (Marsh et al. 1996). These indices were

employed in this study, and presented in Table 5.3. Values for NNFI, and IFI that are

>0.9 are indicative of an acceptable fit of the model to the data (Bollen 1989). In the

case of all data sets, p-values for the χ^2 statistic are greater than 0.05, indicating

non-significance. The null hypothesis (H_0) is that the observed and predicted

variables are similar, acceptance of H_0 is an indication that the model does fit, and

that the observed and predicted values are in fact similar. To further support this, NNFI and IFI values were all greater than 0.9, which strengthens the argument for the fit of the model to each data set.

5.4 Conclusions

In this chapter, a structural equation model was developed based on a QSAR model for photoinduced toxicity of PAHs to *D. magna*. This model accounted for a high amount of variance in six different sets of PAH phototoxicity data from different organisms, while providing insight regarding the contribution of different physicochemical and photodynamic descriptors. SEM appears to be a complementary technique to QSAR modeling in general, and specifically the model in Chapter 4. Indeed, the SEM confirms the relevance of the variables used in the *D. magna* QSAR, and could be used to explore the use of other common descriptors of photoinduced toxicity, such as HOMO-LUMO gap energy. Additionally, this technique could be used to compare various proposed models that exist, providing the means to select a general best-fit model. The flexibility of SEM is evident, in that the relative contributions of each factor are determined. This study illustrates the promise for this type of modeling in ecotoxicology, potential future uses which include assessment of possible synergism of pollutant mixtures, chemical fate and dispersal modeling, as well further application to QSAR models of other contaminants.

Chapter 6
General Conclusions

Polycyclic aromatic hydrocarbons are ubiquitous environmental contaminants, produced naturally and anthropogenically. These compounds present broad environmental health implications, one of which, photoinduced toxicity, has been examined in the preceding chapters of this thesis.

Environmental photomodification of PAHs results in the formation of compounds different in structure than the parent PAH, with generally increased toxicity. An assessment of the occurrence and toxicity of photomodified PAHs in PAH-contaminated sediments was made. The presence and toxicity of modified PAHs (oxyPAHs) was confirmed, as was an evident change in contaminant profile along a transect of sediment samples increasing in distance from shore.

Subsequent to the confirmation of the presence of oxyPAHs in environmental samples, the photoinduced toxicity of 16 PAHs to *D. magna* was assayed under two different irradiation schemes, one with, and one without UVB. Toxicity was observed in both schemes, with generally higher toxicity observed with UVB present, indicating the importance of spectral quality to PAH phototoxicity. Several oxyPAHs were also assayed for toxicity to *D. magna* under visible light. Many of these were highly toxic, although less so than the parent PAH compounds with UV radiation present in the irradiation schemes.

To enable the prediction of toxicity, there are several modeling techniques available for use. In this thesis, the use of quantitative structure-activity relationship (QSAR) techniques was employed. A bipartite model for photoinduced toxicity of PAHs to *D. magna* was developed based on a previously existing model developed for *L. gibba*. Some modifications were necessary to account for differences in assay method, and species. This model was based on factors for photosensitization, and unlike several previous models, photomodification. Ultimately the new model proved to be highly predictive ($r^2 = 0.92$) of photoinduced toxicity.

As an expansion of the modeling theme, a statistical technique that is relatively novel to ecotoxicology was used to further validate the QSAR model. Structural equation modeling (SEM), is a technique that is widely used in the psychological sciences, and employs the use of latent, or unobserved variables. This technique was used to generate models for six sets of toxicity data, which provided insight into the contribution of different descriptors to toxicity. This technique appears to be complimentary to QSAR modeling, and it is hoped that it will be more widely used in the future.

Chapter 7

References

Ahrens MJ, Nieuwenhuis R, Hickey CW. 2002. Sensitivity of Juvenile *Macomona liliana* (bivalvia) to UV-Photoactivated Fluoranthene Toxicity. *Environ Toxicol* 17:567-577.

Allen JO, Dookeran NM, Taghizadeh K, Lafleur AL, Smith KA, Sarofim AF. 1997. Measurement of Oxygenated Polycyclic Aromatic Hydrocarbons Associated with a Size-Segregated Urban Aerosol. *Environ Sci Technol* 31:2064-2070.

Allred PM, Giesy JP. 1985. Solar Radiation-Induced Toxicity of Anthracene to *Daphnia pulex*. *Environ Toxicol Chem* 4:219-226.

Altenburger R, Nendza M, Schüürmann G. 2003. Mixture Toxicity and Its Modeling by Quantitative Structure-Activity Relationships. *Environ Toxicol Chem* 22:1900-1915.

Andino JM, Smith JN, Flagan TC, Goddard I, W.A., Seinfeld JH. 1996. Mechanism of Atmospheric Photooxidation of Aromatics: A Theoretical Study. *J Phys Chem* 100:10967-10980.

Ankley GT, Burkhard LP, Cook PM, Diamond SA, Erickson RJ, Mount DR. 2003. Assessing Risks from Photoactivated Toxicity of PAHs to Aquatic Organisms. In: Douben PET, editor. PAHs: An Ecotoxicological Perspective. Etobicoke, ON, Canada: John Wiley & Sons Inc.

Ankley GT, Collyard SA, Monson PD, Kosian PA. 1994. Influence of Ultraviolet Light on the Toxicity of Sediments Contaminated with Polycyclic Aromatic Hydrocarbons. *Environ Toxicol Chem* 13:1791-1796.

Ankley GT, Erickson RJ, Phipps GL, Mattson VR, Kosian PA, Sheedy BR, Cox JS. 1995. Effects of Light Intensity on the Phototoxicity of Fluoranthene to a Benthic Macroinvertbrate. *Environ Sci Technol* 29:2828-2833.

Arey J, Atkinson R. 2003. Photochemical Reactions of PAHs in the Atmosphere. In: Douben PET, editor. PAHs: An Ecotoxicological Perspective. Etobicoke, ON: John Wiley & Sons Canada Ltd.

128

Arfsten DP, Schaeffer DJ, Mulveny DC. 1996. The Effects of Near Ultraviolet Radiation on the Toxic Effects of Polycyclic Aromatic Hydrocarbons in Animals and Plants: A Review. *Ecotoxicol Environ Saf* 33:1-24.

Babu TS, Marder JB, Tripuranthakam S, Dixon DG, Greenberg BM. 2001. Synergistic Effects of a Photooxidized Polycyclic Aromatic Hydrocarbon and Copper on Photosynthesis and Plant Growth: Evidence that *In Vivo* Formation of Reactive Oxygen Species is a Mechanism of Copper Toxicity. *Environ Toxicol Chem* 20:1351-1358.

Baker JE, Eisenreich SJ. 1989. PCBs and PAHs as Tracers of Particulate Dynamics in Large Lakes. *J Great Lakes Res* 15:84-103.

Baker JE, Eisenreich SJ. 1990. Concentrations and Fluxes of Polycyclic Aromatic Hydrocarbons and Polychlorinated Biphenyls across the Air-Water Interface of Lake Superior. *Environ Sci Technol* 24:342-352.

Betowski LD, Enlow M, Riddick L. 2002. The Phototoxicity of Polycyclic Aromatic Hydrocarbons: A Theoretical Study of Excited States and Correlation to Experiment. *Comput Chem* 26:371-377.

Blaha L, Machala M, Vondracek J, Breinekova K. 2001. Multiple Oxidative Stress Parameters are Modulated *In vitro* by Oxygenated Polycyclic Aromatic Hydrocarbons Identified in River Sediments. *Adv Exp Med Biol* 500:225-228.

Boese BL, Ozretich, RJ, Lamberson, JO, Swartz, RC, Cole, FA, Pelletier, J, Jones, J. 1999. Toxicity and Phototoxicity of Highly Lipophilic PAH Compounds in Marine Sediment: Can the ΣPAH Model Be Extrapolated? *Arch Environ Contam Toxicol* 36:270-280.

Boese BL, Ozretich RJ, Lamberson JO, Cole FA, Swartz RC, Ferraro SP. 2000. Phototoxic Evaluation of Marine Sediments Collected from a PAH-Contaminated Site. *Arch Environ Contam Toxicol* 38:274-282.

Bollen KA. 1989. Structural Equations with Latent Variables. Toronto, ON, Canada: John Wiley and Sons, Inc.

Bondy GS, Armstrong CL, Dawson BA, Heroux-Metcalf C, Neville GA, Rogers CG. 1994. Toxicity of Structurally Related Anthraquinones and Anthrones to Mammalian Cells *in vitro. Toxicol in Vitro* 8:329-335.

Bowling JW, Leversee GJ, Landrum PF, Giesy LP. 1983. Acute Mortality of Anthracene-Contaminated Fish Exposed to Sunlight. *Aquat Toxicol* 3:79-90.

Brack W, Altenburger R, Kuster E, Meissner B, Wenzel K-D, Schüürmann G. 2003. Identification of Toxic Products of Anthracene Photomodification in Simulated Sunlight. *Environ Toxicol Chem* 22:2228-2237.

Briggs MK, Desavis E, Mazzer PA, Sunoj RB, Hatcher SA, Hadad CM, Hatcher PG. 2003. A New Approach to Evaluating the Extent of Michael Adduct Formation to PAH Quinones: Tetramethylammonium Hydroxide (TMAH) Thermochemolysis with GC/MS. *Chem Res Toxicol* 16:1484-1492.

Burdick AD, Davis II JW, Liu KJ, Hudson LG, Shi H, Monske ML, Burchiel SW. 2003. Benzo(*a*)pyrene Quinones Increase Cell Proliferation, Generate Reactive Oxygen Species and Transactivate the Epidermal Growth Factor Receptor in Breast Epithelial Cells. *Cancer Res* 63:7825-7833.

Burgess RM, Ahrens MJ, Hickey CW. 2003. Geochemistry of PAHs in Aquatic Environments: Source, Persistence and Distribution. In: Douben PT, editor. PAHs: An Ecotoxicological Perspective. Etobicoke, ON: John Wiley & Sons Canada Ltd.

Butt CM, Diamond JT, Truong J, Ikonomou MG, Helm PA, Stern GA. 2004. Semivolatile Organic Compounds in Window Films from Lower Manhattan After the September 11th World Trade Center Attacks. *Environ Sci Technol* 38:3514-3524.

Chen B, Xuan X, Zhu L, Wang J, Gao Y, Yang K, Shen X, Lou B. 2004. Distributions of Polycyclic Aromatic Hydrocarbons in Surface Waters, Sediments and Soils of Hangzhou City, China. *Water Res* 38:3558-3569.

Chen J, Peijnenburg WJGM, Quan X, Chen S, Zhao Y, Yang F. 2000. The Use of PLS Algorithms and Quantum Chemical Parameters Derived from PM3 Hamiltonian in QSPR Studies on Direct Photolysis Quantum Yields of Substituted Aromatic Halides. *Chemosphere* 40:1319-1326.

Chesis PL, Levin DE, Smith MT, Ernster L, Ames BN. 1984. Mutagenicity of Quinones: Pathways of Metabolic Activation and Detoxification. *Proc Natl Acad Sci U S A* 81:1696-1700.

Choi J, Oris JT. 2000. Evidence of Oxidative Stress in Bluegill Sunfish (*Lepomis Macroshirus*) Liver Microsomes Simultaneously Exposed to Solar Ultraviolet Radiation and Anthracene. *Environ Toxicol Chem* 19:1795-1799.

Choi J, Oris JT. 2003. Assessment of the Toxicity of Anthracene Photo-Modification Products Using the Topminnow (*Poeciliopsis lucida*) Hepatoma Cell Line (PLHC-1). *Aquat Toxicol* 65:243-251.

Cody TE, Radike MJ, Warshawsky D. 1984. The phototoxicity of benzo[a]pyrene in the green alga *Selenastrum capricornutum*. *Environ Res* 35:122-132.

Cronin MT, Jaworska JS, Walker JD, Comber MH, Watts CD, Worth AP. 2003. Use of QSARs in International Decision-Making Frameworks to Predict Health Effects of Chemical Substances. *Environ Health Persp* 111:1391-401.

Davenport R, Spacie A. 1991. Acute Phototoxicity of Harbor and Tributary Sediments from Lower Lake Michigan. *J Great Lakes Res* 17:51-56.

de Lima Ribeiro FA, Ferreira MMC. 2003. QSPR Models of Boiling Point, Octanol-Water Partition Coefficient and Retention Time Index of Polycyclic Aromatic Hydrocarbons. *J Mol Struct (Theochem)* 663:109-126.

de Maagd PG-J, Ten Hulscher DTEM, Van Den Heuvel H, Opperhuizen A, Sijm DTHM. 1998. Physicochemical Properties of Polycyclic Aromatic Hydrocarbons: Aqueous Solubilities, *n*-Octanol/Water Partition Coefficients, and Henry's Law Constants. *Environ Toxicol Chem* 17:251-257.

Diamond SA, Milroy NJ, Mattson VR, Heinis LJ, Mount DR. 2003. Photoactivated Toxicity in Amphipods Collected from Polycyclic Aromatic Hydrocarbon-Contaminated Sites. *Environ Toxicol Chem* 22:2752-2760.

Diamond SA, Mount DR, Burkhard LP, Ankley GT, Makynen EA, Leonard EN. 2000. Effect of Irradiance Spectra on the Photoinduced Toxicity of Three Polycyclic Aromatic Hydrocarbons. *Environ Toxicol Chem* 19:1389-1396.

Dong S, Fu PP, Shisat RN, Hwang H-M, Leszczynski J, Yu H. 2002. UVA Light-Induced DNA Cleavage by Isomeric Methylbenz[*a*]anthracenes. *Chem Res Toxicol* 15:400-407.

Dong S, Hwang H-M, Harrison C, Holloway L, Shi X, Yu H. 2000. UVA Light-Induced DNA Cleavage by Selected Polycyclic Aromatic Hydrocarbons. *Bull Environ Contam Toxicol* 64:467-474.

Durant JL, Busby WF, Lafleur AL, Penman BW, Crespi CL. 1996. Human Cell Mutagenicity of Oxygenated, Nitrated and Unsubstituted Polycyclic Aromatic Hydrocarbons Associated with Urban Aerosols. *Mutat Res-Gen Tox En* 371:123-157.

Durant JL, Lafleur AL, Plummer EF, Taghizadeh K, Busby WF, Thilly WG. 1998. Human Lymphoblast Mutagens in Urban Airborne Particles. *Environ Sci Technol* 32:1894-1906.

Duxbury CL, Dixon, D.G., Greenberg, B.M. 1997. Effects of Simulated Solar Radiation on the Bioaccumulation of Polycyclic Aromatic Hydrocarbons by the Duckweed *Lemna gibba*. *Environ Toxicol Chem* 16:1739-1748.

Ehrhardt MG, Burns KA. 1993. Hydrocarbons and related photo-oxidation products in Saudi Arabian Gulf coastal waters and hydrocarbons in underlying sediments and bioindicator bivalves. *Mar Poll Bull* 27:187-197.

Eisler R. 1987. Polycyclic Aromatic Hydrocarbon Hazards to Fish, Wildlife, and Invertebrates: A Synoptic Review. : U.S. Fish and Wildlife Service. Report nr 85(1.11).

El-Alawi YS, Dixon DG, Greenberg BM. 2001. Effects of a Pre-incubation Period on the Photoinduced Toxicity of Polycyclic Aromatic Hydrocarbons to the Luminescent Bacterium *Vibrio fischeri*. *Environ Toxicol* 16:277-286.

El-Alawi YS, Huang X-D, Dixon DG, Greenberg BM. 2002. Quantitative Structure-Activity Relationship for the Photoinduced Toxicity of Polycyclic Aromatic Hydrocarbons to the Luminescent Bacteria *Vibrio fischeri. Environ Toxicol Chem* 21:2225-2232.

Environment Canada. 1990. Biological Test Method: Acute Lethality Test Using *Daphnia* spp. (Report EPS 1/RM/11). Ottawa, ON Canada. Report nr EPS 1/RM/11.

Environment Canada. 2005. National Pollutant Release Inventory: http://www.ec.gc.ca/pdb/querysite/query_e.cfm. : Environment Canada.

Enya T, Suzuki H, Watanabe T, Hirayama T, Hisamatsu Y. 1997. 3-Nitrobenzanthrone, a Powerful Bacterial Mutagen and Suspected Human Carcinogen Found in Diesel Exhaust and Airborne Particulates. *Environ Sci Technol* 31:2772-2776.

Epstein SS, Falk HL, Mantel N, Small M. 1964. On Association Between Photodynamic and Carcinogenic Activities in Polycyclic Compounds. *Cancer Res* 24:855-862.

Estrada E, Patelwicz G. 2004. On the Usefulness of Graph-Theoretic Descriptors in Predicting Theoretical Parameters. Phototoxicity of Polycyclic Aromatic Hydrocarbons (PAHs). *Croat Chem Act* 77:203-211.

Fabriciova G, Garcia-Ramos JV, Miskovsky P, Sanchez-Cortes S. 2004. Adsorption and Acidic Behavior of Anthraquinone Drugs Quinizarin and Danthron on Ag Nanoparticles Studied by Raman Spectroscopy. *Vib Spectrosc* 34:273-281.

Fasnacht MP, Blough NV. 2003. Mechanisms of the Aqueous Photodegradation of Polycyclic Aromatic Hydrocarbons. *Environ Sci Technol* 37:5767-5772.

Feilberg A, Nielsen, T. 2000. Effect of Aerosol Chemical Composition on the Photodegradation of Nitro-Polycyclic Aromatic Hydrocarbons. *Environ Sci Technol* 34:789-797.

Feilberg A, Ohura T, Nielsen T, Poulsen MWB, Amagai T. 2002. Occurrence and Photostability of 3-Nitrobenzanthrone Associated with Atmospheric Particles. *Atmos Environ* 36:3591-3600.

Fernandez M, L'Haridon J. 1992. Influence of Lighting Conditions on Toxicity and Genotoxicity of Various PAH in the Newt *in vivo. Mut Res* 298:31-41.

Ferreira MMC. 2001. Polycyclic Aromatic Hydrocarbons: A QSPR Study. *Chemosphere* 44:125-146.

Ferreiro ML, Rodriguez-Otero J. 2001. Ab initio Study of the Intramolecular Proton Transfer in Dihydroxyanthraquinones. *J Mol Struct (Theochem)* 542:63-77.

Fioressi S, Arce R. 2005. Photochemical Transformations of Benzo[e]pyrene in Solution and Adsorbed on Silica Gel and Alumina Surfaces. *Environ Sci Technol* 39:3646-3655.

Flowers-Geary L, Bleczinski W, Harbey RG, Penning TM. 1996. Cytotoxicity and Mutagenicity of Polycyclic Aromatic Hydrocarbon *o*-Quinones Produced by Dihydrodiol Dehydrogenase. *Chem Biol Interact* 99:55-72.

Foote CS. 1968. Mechanisms of Photosensitized Oxidation. *Science* 162:963-970.

Foote CS. 1976. Photosensitized Oxidation and Singlet Oxygen: Consequences in Biological Systems. In: Pryor WA, editor. Free Radicals in Biology. New York, NY, USA: Academic Press. p 85-133.

Foote CS. 1991. Definition of Type I and Type II Photosensitized Oxidation. *Photochem Photobiol* 54:659.

Fox MA, Olive S. 1979. Photooxidation of Anthracene on Atmospheric Particulate Matter. *Science* 205:582-583.

Gala WR, Giesy JP. 1992. Photo-induced toxicity of anthracene to the green alga, *Selenastrum capricornutum. Arch Environ Contam Toxicol* 23:316-323.

Gensemer RW, Dixon, D.G., Greenberg, B.M. 1998. Amelioration of the Photo-Induced Toxicity of Polycyclic Aromatic Hydrocarbons by a Commercial Humic Acid. *Ecotoxicology and Environmental Safety.* 9:57-64.

Gewurtz SB, Lazar R, Haffner GD. 2000. Comparison of Polycyclic Aromatic Hydrocarbon and Polychlorinated Biphenyl Dynamics in Benthic Invertebrates of Lake Erie, USA. *Environ Toxicol Chem* 19:2943-2950.

Gewurtz SB, Lazar R, Haffner GD. 2003. Biomonitoring of Bioavailable PAH and PCB Water Concentrations in the Detroit River Using the Freshwater Mussel, *Elliptio complanata. J Great Lakes Res* 29:242-255.

Ghosh U, Gillette JS, Luthy RG, Zare RN. 2000. Microscale Location, Characterization, and Association of Polycyclic Aromatic Hydrocarbons on Harbor Sediment Particles. *Environ Sci Technol* 34:1729-2736.

Gibson RL, Smart, V.B, Smith, L.L. 1978. Non-Enzymic Activation of Polycyclic Aromatic Hydrocarbons as Mutagens. *Mut Res* 49:153-151.

Gingrich SE, Diamond ML, Stern GA, McCarry BE. 2001. Atmospherically Derived Organic Surface Films Along an Urban-Rural Gradient. *Environ Sci Technol* 35:4031-4037.

Girotti A, W. 1983. Mechanisms of Photosensitization. *Photochem Photobiol* 38:745-751.

Greenstock CL, Wiebe RH. 1978. Photosensitized Carcinogen Degradation and Possible Role of Singlet Oxygen in Carcinogen Activation. *Photochem Photobiol* 28:863-867.

Grove AD, Llewellyn GC, Kessler FK, White Jr. KL, Crespi CL, Ritter JK. 2000. Differential Protection by Rat UDP-Glucuronosyltransferase 1A7 against Benzo[a]pyrene-3,6-quinone versus Benzo[a]pyrene-Induced Cytotoxic Effects in Human Lymphoblastoid Cells. *Toxicol Appl Pharmacol* 162:34-43.

Güsten H, Horvatic D, Sablijic A. 1991. Modeling n-Octanol/Water Partition Coefficients by Molecular Topology: Polycyclic Aromatic Hydrocarbons and Their Alkyl Derivatives. *Chemosphere* 23:199-213.

Hader DP, Worrest RC, Kumar HD, Smith RC. 1995. Effects of Increased Solar Ultraviolet-Radiation On Aquatic Ecosystems. *Ambio* 24:174-180.

Halliwell B, Gutteridge JMC. 1999. Free Radicals in Biology and Medicine. New York, NY, USA: Oxford University Press, Inc.

Hannigan MP, Cass, G.R., Penman, B.W., Crespi, C.L., Lafleur, A.L., Busby Jr., W.F., Thilly, W.G., Simoneit, B.R.T. 1998. Bioassay-Directed Chemical Analysis of Los Angeles Airborne Particulate Matter Using a Human Cell Mutagenicity Assay. *Environ Sci Technol* 32:3502-3514.

Hannigan MP, Cass.G.R., Penman BW, Crespi CL, Lafleur AL, Busby WF, Thilly WG. 1997. Human Cell Mutagens in Los Angeles Air. *Environ Sci Technol* 31:438-447.

He L, Jurs PC. 2005. Probabilistic Neural Network Multiple Classifier System for Predicting the Genotoxicity of Quinolone and Quinoline Derivatives. *Chem Res Toxicol* 18:428-440.

Holst L, Giesy JP. 1989. Chronic Effects of the Photoenhanced Toxicity of Anthracene on *Daphnia magna* Reproduction. *Environ Toxicol Chem* 8:933-942.

Hornung MW, Cook PM, Flynn KM, Lothenbach DB, Johnson RD, Nichols JW. 2004. Use of Multi-Photon Laser-Scanning Microscopy to Describe the Distribution of Xenobiotic Chemicals in Fish Early Life Stages. *Aquat Toxicol* 67:1-11.

Hoyle RH. 1995. The Structural Equation Modeling Approach: Basic Concepts and Fundamental Issues. In: Hoyle RH, editor. Structural Equation Modeling: Concepts, Issues, and Applications. Thousand Oaks, CA, USA: Sage Publications, Inc.

Huang X-D, Dixon DG, Greenberg BM. 1993. Impacts of UV Radiation and Photomodification on the Toxicity of PAHs to the Higher Plant *Lemna gibba* (Duckweed). *Environ Toxicol Chem* 12:1067-1077.

Huang X-D, Dixon DG, Greenberg BM. 1995. Increased Polycyclic Aromatic Hydrocarbon Toxicity Following Their Photomodification in Natural Sunlight: Impacts on the Duckweed *Lemna gibba* L. G-3. *Ecotoxicol Environ Saf* 32:194-200.

Huang X-D, Krylov SN, Ren L, McConkey BJ, Dixon DG, Greenberg BM. 1997a. Mechanistic Quantitative Structure-Activity Relationship Model for the Photoinduced Toxicity of Polycyclic Aromatic Hydrocarbons: II. An Empirical Model for the Toxicity of 16 Polycyclic Aromatic Hydrocarbons to the Duckweed *Lemna gibba* L. G-3. *Environ Toxicol Chem* 16:2296-2303.

Huang X-D, McConkey BJ, Babu TS, Greenberg BM. 1997b. Mechanisms of Photoinduced Toxicity of Photomodified Anthracene to Plants: Inhibition of Photosynthesis in the Aquatic Higher Plant *Lemna gibba* (Duckweed). *Environ Toxicol Chem* 16:1707-1715.

Huberman E, Sachs L, Yang SK, Gelboin HV. 1976. Identification of Mutagenic Metabolites of Benzo[a]pyrene in Mammalian Cells. *Proc Natl Acad Sci U S A* 73:607-612.

Huuskonen J. 2003. QSAR Modeling with the Electrotopological State Indices: Predicting the Toxicity of Organic Chemicals. *Cemosphere* 50:949-953.

Iriondo JM, Albert MJ, Escudero A. 2003. Structural Equation Modeling: An Alternative for Assessing Causal Relationships in Threatened Plant Populations. *Biol Conserv* 113:367-377.

Jang M, McDow SR. 1995. Benz[*a*]anthracene Photodegradation in the Presence of Known Organic Constituents of Atmospheric Aerosols. *Environ Sci Technol* 29:2654-2660.

Jang M, McDow SR. 1997. Products of Benz[*a*]anthracene Photodegradation in the Presence of Known Organic Constituents of Atmospheric Aerosols. *Environ Sci Technol* 31:1046-1053.

Jarabak R, Harvey RG, Jarabak J. 1998. Redox Cycling of Polycyclic Aromatic Hydrocarbon *o*-Quinones: Metal Ion-Catalyzed Oxidation of Catechols Bypasses Inhibition by Superoxide Dismutase. *Chem Biol Interact* 115:201-213.

Jöreskog KG. 1973. A General Method for Estimating a Linear Structural Equation System. In: Goldberger AS, Duncan OD, editors. Structural Equation Models in the Social Sciences. New York, NY, USA: Seminar Press. p 85-112.

Kagan J, Kagan, E.D., Kagan, I.A., Kagan, P.A. and S. Quigley. 1985. The Phototoxicity of Non-Carcinogenic Polycyclic Aromatic Hydrocarbons in Aquatic Organisms. *Chemosphere* 14:1829-1834.

Kaiser KLE. 2003. The Use of Neural Networks in QSARs for Acute Aquatic Toxicological Endpoints. *J Mol Struct (Theochem)* 622:85-95.

Kaiser KLE, Niculescu SP, Schultz TW. 2002. Probabilistic Neural Network Modeling of the Toxicity of Chemicals to *Tetrahymena pyriformis* with Molecular Fragment Descriptors. *SAR QSAR Environ Res* 13:57-67.

Katz M, Chan C, Tosine H, Sakuma T. 1979. Relative Rates of Photochemical and Biological Oxidation *In vitro* of Polynuclear Aromatic Hydrocarbons. In: Jones PW, Leber P, editors. Polynuclear Aromatic Hydrocarbons. Ann Arbor, MI: Ann Arbor Science. p 171-189.

Kepley CL, Lauer FT, Oliver JM, Burchiel SW. 2003. Environmental Polycyclic Aromatic Hydrocarbons, Benzo(a)pyrene (BaP) and BaP-Quinones Enhance IgE-Mediated Histamine Release and IL-4 Production in Human Basophils. *Clin Immunol* 107:10-19.

Kilemade M, Hartl MGJ, Sheehan D, Mothersil C, van Pelt FNAM, O'Brien NM, O'Halloran J. 2004. An Assessment of the Pollutant Status of Surficial Sediment in Cork Harbour in the South East of Ireland with Particular Reference to Polycyclic Aromatic Hydrocarbons. *Mar Poll Bull* 49:1081-1096.

Kishikawa N, Wada M, Ohba Y, Nakashiima K, Kuroda N. 2004. Highly Sensitive and Selective Determination of 9,10-Phenanthrenequinone in Airborne Particulates Using High-Performance Liquid Chromatography with Pre-Column Derivatization and Fluorescence Detection. *J Chromatogr A* 1057:83-88.

Klaassen CD, Amdur MO, Doull J, editors. 1996. Casarett and Doull's Toxicology: The Basic Science of Poisons. Fifth Edition. Toronto, ON, Canada: McGraw-Hill Inc.

Klamer HJC, Leonards PEG, Lamoree MHl, Villerius LA, Akerman JE, Bakker JF. 2005. A Chemical and Toxicological Profile of Dutch North Sea Surface Sediments. *Chemosphere* 58:1579-1587.

Koeber R, Bayona JM, Niessner R. 1999. Determination of Benzo[a]pyrene Diones in Air Particulate Matter with Liquid Chromatography Mass Spectrometry. *Environ Sci Technol* 33:1552-1558.

Kohen E, Santus R, Hirschberg JG. 1995. Photobiology. Toronto, ON, Canada: Academic Press, Inc.

Konig J, Balfanz E, Funcke W, Romanowski T. 1983. Determination of Oxygenated Polycyclic Aromatic-Hydrocarbons in Airborne Particulate Matter By Capillary Gas-Chromatography and Gas-Chromatography Mass-Spectrometry. *Anal Chem* 55:599-603.

Kosian PA, Makynen EA, Monson PD, Mount DR, Spacie A, Mekenyan OG, Ankley GT. 1998. Application of Toxicity-Based Fractionation Techniques and Structure-Activity Relationship Models for the Identification of Phototoxic Polycyclic Aromatic Hydrocarbons in Sediment Pore Water. *Environ Toxicol Chem* 17:1021-1033.

Krylov SN, Huang X-D, Zeiler LF, Dixon DG, Greenberg BM. 1997. Mechanistic Quantitative Structure-Activity Relationship Model for the Photoinduced Toxicity of Polycyclic Aromatic Hydrocarbons: I. Physical Model Based on Chemical Kinetics in a Two-Compartment System. *Environ Toxicol Chem* 16:2283-2295.

Kumagai Y, Koide S, Taguchi K, Endo A, Nakai Y, Yohikawa T, Shimojo N. 2002. Oxidation of Proximal Protein Sulfhydryls by Phenanthraquinone, a Component of Diesel Exhaust Particles. *Chem Res Toxicol* 15:483-489.

Kummerová M, Kmentová E. 2004. Photoinduced Toxicity of Fluoranthene on Germination and Early Development of Plant Seedling. *Chemosphere* 56:387-393.

Kurihara R, Shiraishi F, Tanaka N, Hashimoto S. 2005. Presence and Estrogenicity of Anthracene Derivatives in Coastal Japanese Waters. *Environ Toxicol Chem* Accepted, xx:xxxx-xxxx.

Lampi MA, Gurska Y, McDonald KIC, Xie F, Huang X-D, Dixon DG. 2005. Photoinduced Toxicity of PAHs to *Daphnia magna:* UV-Mediated Effects and the Toxicity of PAH Photoproducts. *Accepted to Environmental Toxicology and Chemistry, May 25, 2005*.

Lampi MA, Huang X-D, El-Alawi YS, McConkey BJ, Dixon DG, Greenberg BM. 2001. Occurrence and Toxicity of Photomodified Polycyclic Aromatic Hydrocarbon Mixtures Present in Contaminated Sediments. In: Greenberg BM, Hull RN, Roberts MH, Gensemer RW, editors. Environmental Toxicology and Risk Assessment: Science, Policy, and Standardization - Implications for Environmental Decisions: Tenth Volume STP 1403. West Conshohocken, PA, USA: American Society for Testing and Materials.

Lamy E, Kassie F, Gminski R, Schmeiser HH, Mersch-Sundermann V. 2004. 3-Nitrobenzanthrone (3-NBA) Induced Micronucleus Formation and DNA Damage in Human Hepatoma (HepG2) Cells. *Toxicol Lett* 146:103-109.

Larson RA, Berenbaum MR. 1988. Environmental Phototoxicity. *Environ Sci Technol* 22:354-360.

Legzdins AE, McCarry BE, Marvin CH, Bryant DW. 1995. Methodology for Bioassay-Directed Fractionation Studies of Air Particulate Material and Other Complex Environmental Matrices. *Int J Environ Anal Chem* 60:79-94.

Lehto K-M, Puhakka JA, Lemmetyinen H. 2003. Photodegradation Products of Polycyclic Aromatic Hydrocarbons in Water and their Amenability to Biodegradation. *Polcycl Aromat Comp* 23:401-416.

Li N, Venkatesan MI, Miguel A, Kaplan R, Gujuluva C, Alam J, Nel A. 2000. Induction of Heme Oxygenase-1 Expression in Macrophages by Diesel Exhaust Particle Chemicals and Quinones via the Antioxidant-Responsive Element. *J Immunol* 165:3393-3401.

Loehlin JC. 2004. Latent Variable Models: An Introduction to Factor, Path, and Structural Equation Analysis. Fourth Edition. Mahwah, NJ, USA: Lawrence Erlbaume Associates.

Lors C, Mossmann J-R. 2005. Characteristics of PAHs Intrinsic Degradation in Two Coke Factory Soils. *Polcycl Aromat Comp* 25:67-85.

Machala M, Giganek M, Blaha L, Minksova K, Vondrack J. 2001. Aryl Hydrocarbon Receptor-Mediated and Estrogenic Activities of Oxygenated Polycyclic Aromatic Hydrocarbons and Azaarenes Originally Identified in Extracts of River Sediments. *Environ Toxicol Chem* 20:2736-2743.

Mackay D, Shiu WY, Ma KC. 1992. Illustrated Handbook of Physical-Chemical Properties and Environmental Fate for Organic Chemicals. Volume II. Ann Arbor: Lewis Publishers.

Malaeb ZA, Summers JK, Pugesek BH. 2000. Using Structural Equation Modeling to Investigate Relationships Among Ecological Variables. *Environ Ecol Stat* 7:93-111.

Malkin J. 1992. Photophysical and Photochemical Properties of Aromatic Compounds. Ann Arbor, MI, USA: CRC Press Inc.

Mallakin A, Dixon DG, Greenberg BM. 2000. Pathway of Anthracene Modificaton Under Simulated Solar Radiation. *Chemosphere* 40:1435-1441.

Mallakin A, McConkey BJ, Miao G, McKibben B, Snieckus V, Dixon DG, Greenberg BM. 1999. Impacts of Structural Photomodification on the Toxicity of Environmental Contaminants: Anthracene Photooxidation Products. *Ecotoxicol Environ Saf* 43:204-212.

Marsh HW, Balla JR, Hau K-T. 1996. An Evaluation of Incremental Fit Indices: A Clarification of Mathematical and Empirical Properties. In: Marcoulides GA, Schumacker RE, editors. Advanced Structural Equation Modeling: Issues and Techniques. Mahway, NJ, USA: Lawrence Erlbaum Associates. p 315-353.

Marvin CH, Tessaro, M., McCarry, B.E., Bryant, D.W. 1994. A Bioassay-Directed Investigation of Sydney Harbour Sediment. *Sci Total Environ* 156:119-131.

Marvin CH, McCarry BE, Villella J, Allan LM, Bryant DW. 2000. Chemical and Biological Profiles of Sediments as Indicators of Sources of Genotoxic Contamination in Hamilton Harbour. Part I: Analysis of Polycyclic Aromatic Hydrocarbons and Thia-Arene Compounds. *Chemosphere* 41:979-988.

Marwood CA, Smith REH, Charlton MN, Solomon KR, Greenberg BM. 2003. Photoinduced Toxicity to Lake Erie Phytoplankton Assemblages from Intact and Photomodified Polycyclic Aromatic Hydrocarbons. *J Great Lakes Res* 29:558-565.

Marwood CA, Smith REH, Solomon KR, Charlton MN, Greenberg BM. 1999. Intact and Photomodified Polycyclic Aromatic Hydrocarbons Inhibit Photosynthesis in Natural Assemblages of Lake Erie Phytoplankton Exposed to Solar Radiation. *Ecotoxicol Environ Saf* 44:322-327.

Mastral AM, Callen MS. 2000. A Review on Polycyclic Aromatic Hydrocarbon (PAH) Emissions from Energy Generation. *Environ Sci Technol* 34:3051-3057.

McCarthy LH, Thomas RL, Mayfield CI. 2004. Assessing the Toxicity of Chemically Fractionated Hamilton Harbour (Lake Ontario) Sediment Using Selected Aquatic Organisms. *Lakes Reserv Res Manage* 9:89-102.

McCarty LS, Mackay D, Smith AD, Ozburn GW, Dixon DG. 1992. Residue-Based Interpretation of Toxicity and Bioconcentration QSARs from Aquatic Bioassays - Neutral Narcotic Organics. *Environ Toxicol Chem* 11:917-930.

McConkey BJ, Duxbury CL, Dixon DG, Greenberg BM. 1997. Toxicity of a PAH Photooxidation Product to the Bacteria *Photobacterium phosphoreum* and the Duckweed *Lemna gibba*: Effects of Phenanthrene and its Primary Photoproduct, Phenanthrenequinone. *Environ Toxicol Chem* 16:892-899.

McCoy EC, Hyman J, Rosenkranz HS. 1979. Conversion of Environmental Pollutant to Mutagens by Visible Light. *Biochem Biophys Res Commun* 89:729-734.

McDonald BG, Chapman PM. 2002. PAH Phototoxicity-an Ecologically Irrelevant Phenomenon? *Mar Poll Bull* 44:1321-1326.

McKinney RA, Pruell RJ, Burgess RM. 1999. Ratio of the Concentration of Anthraquinone to Anthracene in Coastal Marine Sediments. *Chemosphere* 38:2415-2430.

Mekenyan OG, Ankley GT, Veith GD, Call DJ. 1994a. QSAR Estimates of Excited States and Photoinduced Acute Toxicity of Polycyclic Aromatic Hydrocarbons. *SAR QSAR Environ Res* 2:237-247.

Mekenyan OG, Ankley GT, Veith GD, Call DJ. 1994b. QSARs for Photoinduced Toxicity: I. Acute Lethality of Polycyclic Aromatic Hydrocarbons to *Daphnia magna*. *Chemosphere* 28:567-582.

Monks TJ, Hanzlik RP, Cohen GM, Ross D, Graham DG. 1992. Quinone Chemistry and Toxicity. *Toxicol Appl Pharmacol* 112:2-16.

Morgan DD, Warshawsky D, Atkinson T. 1977. The Relationship Between Carcinogenic Activities of Polycyclic Aromatic Hydrocarbons and their Singlet, Triplet and Singlet-Triplet Splitting Energies and Phosphorescence Lifetimes. *Photochem Photobiol* 25:31-38.

Mosi AA, Reimer KJ, Eigendorf GK. 1997. Analysis of Polyaromatic Quinones in a Complex Environmental Matrix Using Gas Chromatography Ion Trap Tandem Mass Spectrometry. *Talanta* 44:985-1001.

Mueller SO, Stopper H. 1999. Characterization of the Genotoxicity of Anthraquinones in Mammalian Cells. *Biochim Biophys Acta* 1428:406-414.

Neff JM. 1979. Polycyclic Aromatic Hydrocarbons in the Aquatic Environment. London: Applied Science Publishers Ltd.

Neff JM. 1985. Polycyclic Aromatic Hydrocarbons. In: Rand GM, Petrocelli SR, editors. Fundamentals of Aquatic Toxicology. Toronto, Canada: Hemisphere Publishing Corporation. p 416-454.

Nendza M. 1998. Structure-Activity Relationships in Environmental Sciences. Depledge MH, Sanders B, editors. New York, NY, USA: Chapman and Hall.

Netzeva TI, Aptula AO, Benfenati E, Cronin MTD, Gini G, Lessigiarska I, Maran U, Vracko M, Schuurmann G. 2005. Description of the Electronic Structure of Organic Chemicals Using Semiempirical and Ab Initio Methods for Development of Toxicological QSARs. *J Chem Inf Model* 45:106-114.

Newsted JL, Giesy JP. 1987. Predictive Models for Photoinduced Acute Toxicity of Polycyclic Aromatic Hydrocarbons to *Daphnia magna* Strauss (Cladocera, Crustacea). *Environ Toxicol Chem* 6:445-461.

Nicol S, Dugay J, Hennion M-C. 2001. Determination of Oxygenated Polycyclic Aromatic Compounds in Airborne Particulate Organic Matter Using Gas Chromatography-Tandem Mass Spectrometry. *Chromatographia Suppl* 53:S464-S469.

Niculescu SP, Atkinson A, Hammond G, Lewis M. 2004. Using Fragment Chemistry Data Mining and Probabilistic Neural Networks in Screening Chemicals for Acute Toxicity to the Fathead Minnow. *SAR QSAR Environ Res* 15:293-309.

Nikkila A, Penttinen S, Kukkonen JVK. 1999. UV-B-Induced Toxicity of Pyrene to the Waterflea *Daphnia magna* in Natural Freshwaters. *Ecotoxicol Environ Saf* 46:271-279.

Nikolaou K, Masclet, P. and G. Mouvier. 1984. Sources and Chemical Reactivity of Polynuclear Aromatic Hydrocarbons in the Atmosphere - a Critical Review. *Sci Total Environ* 32:103-132.

Nykamp J, Bols NC, Carlson JC. 2001. Phenanthrenequinone Disrupts Progesterone Production in Rat Luteal Cells. *Reprod Toxicol* 15:393-398.

Oda J, Maeda, I, Mori, T, Yasuhara, A, Saito Y. 1998. The Relative Proportions of Polycyclic Aromatic Hydrocarbons and Oxygenated Derivatives in Accumulated Organic Particulates as Affected by Air Pollution Sources. *Environ Technol* 19:961-976.

Oehme FW. 1979. Toxicology is a Bastard. *Vet Hum Toxicol* 21:164-165.

Olajire AA, Altenburger R, Küster E, Brack W. 2005. Chemical and Ecotoxicological Assessment of Polycyclic Aromatic Hydrocarbon-Contaminated Sediments of the Niger Delta, Southern Nigeria. *Sci Total Environ* 340:123-136.

Oris JT, Giesy JP. 1985. The Photoenhanced Toxicity of Anthracene to Juvenile Sunfish (*Lepomis* Spp.). *Aquat Toxicol* 6:133-146.

Oris JT, Giesy JP. 1986. Photoinduced Toxicity of Anthracene to Juvenile Bluegill Sunfish (*Lepomis macrochirus* Rafinesque): Photoperiod Effects and Predictive Hazard Evaluation. *Environ Toxicol Chem* 5:761-768.

Oris JT, Giesy JP. 1987. The Photo-Induced Toxicity of Polycyclic Aromatic Hydrocarbons to Larvae of the Fathead Minnow (*Pimephales proelas*). *Chemosphere* 16:1395-1404.

OSPAR. 2002. Benzo[rst]pentaphene: www.ospar.org/v_substances/get_page.asp?v1=189559.xls. : OSPAR Commission for the Protection of the Marine Environment of the North-East Atlantic.

Papadoyannis IN, Zotou A, Samanidou VF. 2002. Development of a Solid Phase Extraction Protocol for the Simultaneous Determination of Anthracene and its Oxidation Products in Surface Waters by Reversed-Phase HPLC. *J Liq Chromatogr R T* 25:2635-2653.

Pennak RW. 1989. Freshwater Invertebrates of the United States. New York, NY, USA: John Wiley and Sons.

Penning TM, Burczynski ME, Hung C-F, McCoull KD, Palackal NT, Tsuruda LS. 1999. Dihydrodiol Dehydrogenases and Polycyclic Aromatic Hydrocarbon Activation: Generation of Reactive and Redox Active *o*-Quinones. *Chem Res Toxicol* 12:1-18.

Pitts JN, Vancauwenberghe KA, Grosjean D, Schmid JP, Fitz DR, Belser WL, Knudson GB, Hynds PM. 1978. Atmospheric Reactions of Polycyclic Aromatic-Hydrocarbons - Facile Formation of Mutagenic Nitro-Derivatives. *Science* 202:515-519.

Reckhow KH, Arhonditsis GB, Kenney MA, Hauser L, Tribo J, Wu C, Elcock KJ, Steinberg LJ, Stow CA, McBride SJ. 2005. A Predictive Approach to Nutrient Criteria. *Environ Sci Technol* 39:2913-2919.

Reed MD, Monske ML, Lauer FT, Meserole SP, Born JL, Burchiel SW. 2003. Benzo[a]Pyrene Diones are Produced by Photochemical and Enzymatic Oxidation and Induce Concentration-Dependent Decreases in the Proliferative State of Human Pulmonary Epithelial Cells. *J Toxicol Environ Health A* 66:1189-1205.

Ren L, Zeiler, L.F., Dixon, D.G., Greenberg, B.M. 1996. Photoinduced Effects of Polycyclic Aromatic Hydrocarbons on *Brassica napus* (Canola) during Germination and Early Seedling Development. *Ecotoxicol Environ Saf* 33:73-80.

Schirmer K, Chan AGJ, Greenberg BM, Dixon DG, Bols NC. 1998. Ability of 16 Priority PAHs to be Photocytotoxic to a Cell Line from the Rainbow Trout Gill. *Toxicology* 127:143-155.

Seike K, Murata M, Oikawa S, Hiraku Y, Hirakawa K, Kawanishi S. 2003. Oxidative DNA Damage Induced by Benz[a]anthracene Metabolites via Redox Cycles of Quinone and Unique Non-Quinone. *Chem Res Toxicol* 16:1470-1476.

Shimada H, Oginuma M, Hara A, Imamura Y. 2004. 9,10-Phenanthrenequinone , a Component of Diesel Exhaust Particles, Inhibits the Reduction of 4-Benzoylpyridine and All-*Trans*-Retinal and Mediates Superoxide Formation Through its Redox Cycling in Pig Heart. *Chem Res Toxicol* 17:1145-1150.

Sims P, Grover LL, Saisland A, Pal K, Hewer A. 1974. Metabolic Activation of Benzo[a]pyrene Proceeds by a Diol-Epoxide. *Nature* 252:326-328.

Smith REH, Allen CD, Charlton MN. 2004. Dissolved organic matter and ultraviolet radiation penetration in the Laurentian Great Lakes and tributary waters. *J Great Lakes Res* 30:367-380.

Solomons TWG. 1996. Organic Chemistry. Toronto, ON, Canada: John Wiley & Sons, Inc.

Somers CM, McCarry BE, Malek F, Quinn JS. 2004. Reduction of Particulate Air Pollution Lowers the Risk of Heritable Mutations in Mice. *Science* 304:1008-1010.

Spehar RL, Poucher S, Brooke LT, Hansen DJ, Champlin D, Cox DA. 1999. Comparative Toxicity of Fluoranthene to Freshwater and Saltwater Species Under Fluorescent and Ultraviolet Light. *Arch Environ Contam Toxicol* 37:496-502.

Stephenson GL, Koper N, Atkinson GF, Solomon KR, Scroggins RP. 2000. Use of Nonlinear Regression Techniques for Describing Concentration-Response Relationships of Plant Species Exposed to Contaminated Site Soils. *Environ Toxicol Chem* 19:2968-2981.

Surowiec E, Bartos M. 2002. Identification of the Products of Oxidation of Benzo[a]pyrene. *J Planar Chromat* 15:73-75.

Swartz RC, Ferraro SP, Lamberson JO, Cole FA, Ozretich RJ, Boese BL, Schults DW, Behrenfeld M, Ankley GT. 1997. Photoactivation and Toxicity of Mixtures of

Polycyclic Aromatic Hydrocarbon Compounds in Marine Sediment. *Environ Toxicol Chem* 16:2151-2157.

Taylor BW, Irwin RE. 2004. Linking Economic Activities to the Distribution of Exotic Plants. *Proc Natl Acad Sci U S A* 101:17725-17730.

Thomas RS, Rank DR, Penn SG, Zastrow GM, Hayes KR, Pande K, Glover E, Silander T, Craven MW, Reddy JK and others. 2001. Identification of Toxicologically Predictive Gene Sets Using cDNA Microarrays. *Mol Pharmacol* 60:1189-1194.

Tripuranthakam S, Duxbury CL, Babu TS, Greenberg BM. 1999. Development of a Mitochondrial Respiratory Electron Transport Bioindicator for Assessment of Aromatic Hydrocarbon Toxicity. In: Henshel DS, Black, M.C. and M.C. Harrass, editor. Environmental Toxicology and Risk Assessment: Standardization of Biomarkers for Endocrine Disruption and Environmental Assessment: Eighth Volume, ASTM STP 1364. West Conshohocken, PA: American Society for Testing and Materials.

Trucco RG, Engelhardt FR, Stacey B. 1983. Toxicity, Accumulation and Clearance of Aromatic Hydrocarbons in *Daphnia pulex*. *Environ Poll A* 31:191-202.

Tso PO, Lu P. 1964. Interaction of Nucleic Acids, I. Chemical Linkage of the Carcinogen 3,4-Benzpyrene to DNA Induced By Photoradiation. *Proc Natl Acad Sci U S A* 51:272-80.

Tuppurainen K, Ruuskanen J. 2000. Electronic Eigenvalue (EEVA): A New QSAR/QSPR Descriptor for Electronic Substituent Effects Based on Molecular Orbital Energies. A QSAR Approach to the *Ah* Receptor Binding Affinity of Polychlorinated Biphenyls (PCBs), Dibenzo-*p*-dioxins (PCDDs) and Dibenzofurans (PCDFs). *Chemosphere* 41:843-848.

US EPA. 1998. Method 3550B - Ultrasonic Extraction. SW-846, Test Methods for Evaluating Solids Waste, Physical/Chemical Methods, Fifth Revision. Washington DC , USA: Office of Solid Waste.

US EPA. 2002a. Methods for Measuring the Acute Toxicity of Effluents and Receiving Waters to Freshwater and Marine Organisms. Washington, DC, USA: USEPA Office of Water. Report nr EPA-821-R-02-012.

US EPA. 2002b. National Recommended Water Quality Criteria: 2002. : Office of Water, Office of Science and Technology (4304T), United States Environmental Protection Agency. Report nr EPA-522-R-02-047.

US EPA. 2004. Toxics Release Inventory (TRI) Program Public Data Release; http://www.epa.gov/triinter/tridata/index.htm. : Office of Environmental Information, United States Environmental Protection Agency, Washington, D.C., USA.

Wall DP, Hirsh AE, Fraser HB, Kumm J, Giaever G, Eisen MB, Feldman MW. 2005. Functional Genomic Analysis of the Rates of Protein Evolution. *Proc Natl Acad Sci U S A* 102:5483-5488.

Warne MA, Ebbels TMD, Lindon JC, Nicholson JK. 2003. Semiempirical Molecular-Orbital Properties of Some Polycyclic Aromatic Hydrocarbons and Correlation with Environmental Toxic Equivalency Factors. *Polcycl Aromat Comp* 23:23-47.

Warshawsky D, Cody T, Radike M, Reilman R, Schumann B, LaDow K, Schneider J. 1995. Biotransformation of Benzo[a]pyrene and Other Polycyclic Aromatic Hydrocarbons and Heterocyclic Analogs by Several Green Algae and Other Algal Species Under Gold and White Light. *Chem Biol Interact* 97:131-148.

Weinstein JE, Polk KD. 2001. Phototoxicity of Anthracene and Pyrene to Glochdia of the Freshwater Mussel *Utterbackia imbecillis. Environ Toxicol Chem* 20:2021-2028.

Wernersson A-S, Dave, G. 1997. Phototoxicity Identification by Solid Phase Extraction and Photoinduced Toxicity to *Daphnia magna. Arch Environ Contam Toxicol* 32:268-273.

White JC, Triplett T. 2002. Polycyclic Aromatic Hydrocarbons (PAHs) in the Sediments and Fish of the Mill River, New Haven, Connecticut, USA. *Bull Environ Contam Toxicol* 68:104-110.

White PA. 2002. The Genotoxicity of Priority Polycyclic Aromatic Hydrocarbons in Complex Mixtures. *Mut Res* 515:85-98.

Wiberg KB. 1997. Properties of Some Condensed Aromatic Systems. *J. Org. Chem.* 62:5720-5727.

Wiegman S, Termeer JAG, Verheul T, Kraak MHS, de Voogt P, Admiraal W. 2002. UV Absorbance Dependent Toxicity of Acridine to the Marine Diatom *Phaecodactylum tricornutum. Environ Sci Technol* 36:908-913.

Wright S. 1934. The Method of Path Coefficients. *Ann Math Stat* 5:161-215.

Xia T, Korge P, Weiss JN, Li N, Venkatesen MI, Sioutas C, Nel A. 2004. Quinones and Aromatic Chemical Compounds in Particulate Matter Induce Mitochondrial Dysfunction: Implications for Ultrafine Particle Toxicity. *Environ Health Persp* 112:1347-1358.

Xie F, Koziar S, Lampi MA, Dixon DG, Norwood W, Borgmann U, Greenberg BM. 2005. Assessment of the Toxicity of Mixtures of Copper, 9,10-Phenanthrenequinone and Phenanthrene to *D. magna. Accepted to Environmental Toxicology and Chemistry, May 30, 2005.*

Yaffe D, Cohen Y, Arey J, Grosovsky AJ. 2001. Multimedia Analysis of PAHs and Nitro-PAh Daughter Products in the Los Angeles Basin. *Risk Anal* 21:275-294.

Yan J, Wang L, Fu PP, Yu H. 2004. Photomutagenicity of 16 Polycyclic Aromatic Hydrocarbons from the US EPA Priority List. *Mut Res* 557:99-108.

Yang SK, McCourt DW, Leutz JC, Gelboin HV. 1977. Benzo[a]pyrene Diol Epoxides: Mechanism of Enzymatic Formation and Optically Active Intermediates. *Science* 196:1199-1201.

Yu D, Kazanietz MG, Harbey RG, Penning TM. 2002. Polycyclic Aromatic Hydrocarbon *o*-Quinones Inhibit the Activity of the Catalytic Fragment of Protein Kinase C. *Biochemistry* 41:11888-11894.

Yu H. 2002. Environmental Carcinogenic Polycyclic Aromatic Hydrocarbons: Photochemistry and Phototoxicity. *J Environ Sci Health C* 20:149-183.

Zhu H, Li Y, Trush MA. 1995. Characterization of Benzo[a]pyrene Quinone-Induced Toxicity to Primary Cultured Bone Marrow Stromal Cells from DBA/2 Mice: Potential Role of Mitochondrial Dysfunction. *Toxicol Appl Pharmacol* 130:108-120.